

DTA 49003 DA:NA  
LB 9125106

## GEOLOGY OF THE YUCCA MOUNTAIN SITE AREA

### CONTENTS

Abstract

Introduction

Physiography and geomorphology

    Physiographic setting

        Yucca Mountain

        Crater Flat

        Fortymile Wash

        Other topographic features

    Geomorphology

        Influence of tectonism/Quaternary faulting

        Influence of volcanism

        Influence of climate

Stratigraphy of the volcanic rocks

    Introduction

    General features

    Criteria for differentiating volcanic rock units at Yucca Mountain

        Lithologic and rock-property criteria

        Mineralogic criteria

        Geochemical criteria

        Borehole geophysical-log criteria

Description of rock units

Pre-Cenozoic rocks

Pre-Lithic Ridge volcanic rocks

Lithic Ridge Tuff

Dacitic lava and flow breccia

Crater Flat Group

Tram Tuff of the Crater Flat Group

Bullfrog Tuff of the Crater Flat Group

Prow Pass Tuff

Calico Hills Formation

Paintbrush Group

Topopah Spring Tuff of the Paintbrush Group

Pah Canyon Tuff of the Paintbrush Group

Rhyolites of Black Glass Canyon, Delerium Canyon, and Zig Zag Hill

Yucca Mountain Tuff of the Paintbrush Group

Tiva Canyon Tuff of the Paintbrush Group

Post-Tiva Canyon/pre-Rainier Mesa tuffs and lava flows

Timber Mountain Group

Rainier Mesa Tuff of the Timber Mountain Group

Ammonia Tanks Tuff of the Timber Mountain Group

Younger Basalt

Correlation of lithostratigraphic, hydrologic, and thermo-mechanical units

Quaternary geology

Introduction

General distribution and characteristics of surficial deposits

Trenching activities

Erosion, deposition, and flooding

Landscape response to modern climatic conditions

Landscape response to climate change

Flooding history

Quaternary bedrock erosion rates

Hillslope erosion rates from dated colluvial boulder deposits

Hillslope erosion during the latest Pleistocene-Holocene interval

Erosional history of Fortymile Wash

Potential for future erosion and deposition

Structural geology

Introduction

Block-bounding faults

Paintbrush Canyon fault

Bow Ridge fault

Solitario Canyon and Iron Ridge faults

Fatigue Wash fault

Windy Wash fault

Northern and southern Crater Flat faults

Structural blocks and intrablock faults

Structural block east of Paintbrush Canyon fault

Bow Ridge – Paintbrush Canyon block

Solitario Canyon – Bow Ridge block

Fatigue Wash – Solitario Canyon block

Windy Wash – Fatigue Wash block

Crater Flat – Windy Wash block

Vertical axis rotation

Deformation within fault zones

Geophysical surveys

Fractures

Stratigraphic relations across faults and timing of deformation

Geologic structure of the pre-Cenozoic rocks

Tectonic models

Natural resources

Introduction

Metallic mineral resources

Industrial rocks and minerals

Hydrocarbon and other energy resources

Geothermal resources

Acknowledgements

References

## **FIGURES**



Figure 1. Generalized geologic map showing distribution of major lithostratigraphic units in the Yucca Mountain site area and vicinity.

Figure 2. Map of Yucca Mountain site area showing distribution of principal stratigraphic units, major faults, and locations of geographic features named in text.

Figure 3. Low-oblique aerial photograph looking southeast across Yucca Mountain, with floor of Solitario Canyon in foreground.

Figure 4. View looking south along west-facing scarp of the Windy Wash fault.

Figure 5. Lithostratigraphic zones in the Tiva Canyon and Topopah Spring Tuffs at Yucca Mountain.

Figure 6. Photomicrograph of vitric and densely welded rocks in the crystal-poor member of the Tiva Canyon Tuff.

Figure 7. Graph showing concentrations of titanium and zirconium for core samples from borehole UE-25a#1.

Figure 8. Map showing locations of cross sections and boreholes.

Figure 9. Lithostratigraphy and porosity from cores and geophysical logs and quantitative mineralogy from x-ray diffraction on rock samples from borehole UE-25 UZ#16.

Figure 10. East-west stratigraphic cross section across Yucca Mountain.

Figure 11. North-south stratigraphic cross section across Yucca Mountain.

Figure 12. Generalized surficial geologic map of the Yucca Mountain site area.

Figure 13. Plot showing age distribution of mapped Quaternary units Qa2-Qa5 in Midway Valley and Fortymile Wash.

Figure 14. Generalized cross sections showing evolution of Fortymile Wash.

Figure 15. View looking north toward south slope of Jake Ridge showing debris flows and flow tracks resulting from intense storm activity.

Figure 16. Map showing distribution of faults in Yucca Mountain site area and adjacent areas to south and west.

Figure 17. East-west structure section across Yucca Mountain site area.

Figure 18. Exposure of Paintbrush Canyon fault displacing surficial deposits on west side of Busted Butte.

Figure 19. Map showing location of geophysical surveys in the Yucca Mountain site area.

## **TABLES**

Table 1. Generalized stratigraphic column of Tertiary volcanic rocks in the Yucca Mountain site area.

Table 2. Summary of diagnostic surface and soil characteristics of Quaternary map units at Yucca Mountain.

Table 3. Maximum bedrock erosion rates on Yucca Mountain.

Table 4. Varnish cation ratio age estimates from boulder deposits around Yucca Mountain.

Table 5. Ages of four boulder deposits around Yucca Mountain.

# Geology of the Yucca Mountain site area, southwestern Nevada

**William R. Keefer**

**John W. Whitney**

*U.S. Geological Survey, Box 25046, Federal Center, Denver, Colorado 80225, USA*

**David C. Buesch**

*U.S. Geological Survey, 1180 Town Center Drive, Las Vegas, Nevada 89144, USA*

## **ABSTRACT**

**Yucca Mountain in southwestern Nevada is a prominent, irregularly shaped upland formed by a thick apron of Miocene pyroclastic-flow and fallout tephra deposits, with minor lava flows, that was segmented by through-going, large-displacement normal faults into a series of north-trending, eastwardly tilted structural blocks. The principal volcanic-rock units are the Tiva Canyon and Topopah Spring Tuffs of the Paintbrush Group, which consist of volumetrically large eruptive sequences derived from compositionally distinct magma bodies in the nearby southwestern Nevada volcanic field, and are classic examples of a magmatic zonation characterized by an upper crystal-rich (> 10% crystal fragments) member, a more voluminous lower crystal-poor (< 5% crystal fragments) member, and an intervening thin transition zone. Rocks within the crystal-poor member of the Topopah Spring Tuff, lying some 280 m below the crest of Yucca Mountain, constitute the proposed host rock to be excavated for the storage of high-level radioactive wastes.**

Separation of the tuffaceous rock formations into subunits that allow for detailed mapping and structural interpretations is based on macroscopic features, most importantly the relative abundance of lithophysae and the degree of welding. The latter feature, varying from nonwelded through partly and moderately welded to densely welded, exerts a strong control on matrix porosities and other rock properties that provide essential criteria for distinguishing hydrogeologic and thermal-mechanical units, which are of major interest in evaluating the suitability of Yucca Mountain to host a safe and permanent geologic repository for waste storage.

A thick and varied sequence of surficial deposits mantle large parts of the Yucca Mountain site area. Mapping of these deposits and associated soils in exposures and in the walls of trenches excavated across buried faults provides evidence for multiple surface-rupturing events along all of the major faults during Pleistocene and Holocene times; these paleoseismic studies form the basis for evaluating the potential for future earthquakes and fault displacements. Thermoluminescence and U-series analyses were used to date the surficial materials involved in the Quaternary faulting events.

The rate of erosional downcutting of bedrock on the ridge crests and hillslopes of Yucca Mountain, being of particular concern with respect to the potential for breaching of the proposed underground storage facility, was studied by using rock varnish cation-ratio and  $^{10}\text{Be}$  and  $^{36}\text{Cl}$  cosmogenic dating methods to determine the length of time bedrock outcrops and hillslope boulder deposits were exposed to cosmic rays, which then served as a basis for calculating long-term erosion rates. The results indicate rates ranging from 0.04 to 0.27 cm/k.y., which represent the maximum downcutting along the summit of Yucca Mountain under all climatic conditions that existed there during most of Quaternary time.

Associated studies include the stratigraphy of surficial deposits in Fortymile Wash, the major drainage course in the area, which record a complex history of four to five cut-and-fill cycles within the channel during middle to late Quaternary time. The last 2 to 4 m of incision probably occurred during the last pluvial climatic period, 22 to 18 ka, followed by aggradation to the present time.

Major faults at Yucca Mountain — from east to west, the Paintbrush Canyon, Bow Ridge, Stagecoach Road, Solitario Canyon, Fatigue Wash, Windy Wash, and Northern and Southern Crater Flat Faults — trend predominantly north, are spaced 1 to 5 km apart, have bedrock displacements ranging from 125 m to as much as 500 m, and exhibit Quaternary movements of several centimeters to a few meters. Displacements are predominantly down to the west, and bedrock/alluvium contacts commonly are marked by faultline scarps. The predominant northerly fault trend changes to a more northeasterly trend in adjacent areas south of the site area owing to clockwise vertical-axis rotation. Structural blocks between the block-bounding faults are internally deformed by numerous minor faults, some oriented northwest and exhibiting strike-slip movements.

Investigations to determine the natural resource potential of the Yucca Mountain area — metallic minerals, industrial rocks and minerals, hydrocarbon and other energy resources, and geothermal resources — resulted in findings indicating that a given commodity either (1) is not known to exist in the area, or (2) is present in such low concentrations as to be noneconomic.

**Keywords: Yucca Mountain, geologic repository, high-level radioactive waste, southwestern Nevada volcanic field, volcanic stratigraphy, Quaternary geology, structural blocks, faults**

## **INTRODUCTION**

Geologic and related investigations at Yucca Mountain focus on a rectangular area of some 165 km<sup>2</sup> (65 mi<sup>2</sup>) that covers the central part of the mountain (Fig. 1) and is informally referred to as the "site area" with respect to the proposed geologic repository for high-level radioactive wastes. Geologic mapping at various scales and detailed stratigraphic and structural studies have been conducted there, and in adjacent areas such as contiguous parts of the Nevada Test Site to the east, since the 1960s, and then were pursued with increased effort since the late 1980s as an integral part of a broad, interdisciplinary characterization program designed to comprehensively evaluate the suitability of the site to host a safe and permanent high-level radioactive waste-storage facility (U.S. Department of Energy, 1988). A synthesis of the principal results of these and associated studies, many of which have been published, is presented in this report.

## **PHYSIOGRAPHY AND GEOMORPHOLOGY**

### **Physiographic Setting of Yucca Mountain and Vicinity**

Yucca Mountain, in southwestern Nevada (Fig. 1), lies in the south-central part of the Great Basin that forms the northern subprovince of the Basin and Range physiographic province

(Stuckless and O'Leary, this volume, Fig. 1). More specifically, Yucca Mountain occupies part of the Walker Lane belt, a major structural lineament considered to be a zone of transition between (1) the central and southeastern parts of the Great Basin, characterized by dip-slip normal faulting and typical basin and range topography; and (2) the southwestern Great Basin, typified by dip-slip and strike-slip faulting and irregular topography (Carr, 1984; see O'Leary, this volume). Yucca Mountain itself is situated on the south flank of the southwestern Nevada volcanic field (Fig. 2; also, see Stuckless and O'Leary, this volume, Fig. 9), which consists of a series of volcanic centers from which large volumes of pyroclastic flow and fallout tephra deposits were erupted from about 14.0 to 11.4 Ma (Byers et al., 1976; Sawyer et al., 1994). Accordingly, the mountain and many of the adjacent landforms carry the imprint of the area's extensive volcanic history and its deformational history.

The area surrounding Yucca Mountain can be divided into several clearly defined physiographic elements that combine to produce a variable and diverse terrain typical of the Walker Lane belt (Stewart, 1988; also, see Stuckless and O'Leary, this volume, Fig. 2). Three of these — Yucca Mountain and the flanking landforms to the east and west, Fortymile Wash and Crater Flat, respectively (Fig. 1) — are described below.

### ***Yucca Mountain***

Yucca Mountain is a prominent, irregularly shaped upland, 3 to 8 km wide and about 35 km long, that stretches from near Beatty Wash at the northwest end to near the north edge of the Amargosa Desert at the south end (Stuckless and O'Leary, this volume, Fig. 2). The crest of the mountain reaches elevations of 1,500 to 1,930 m, about 125 to 275 m higher than the floors of adjacent washes and lowlands. The dominantly north-trending pattern of structural blocks



characterizing this prominent upland area is controlled by high-angle block-bounding faults (Scott and Bonk, 1984; Day et al., 1998a; Potter et al., 2004) with vertical displacements of several hundred meters in places. The fault blocks, which consist of volcanic rocks of Miocene age, are tilted eastward, so that the fault-bounded, west-facing slopes are generally high and steep in contrast to the more gentle and commonly deeply dissected east-facing slopes (Fig. 3). The valleys generally are narrow and V-shaped along their upper and middle reaches, but locally contain flat, alluviated floors in their lower reaches. Drainage from the west flank of the mountain flows southward down narrow, fault-controlled canyons and out into Crater Flat; drainage from the east flank flows southeastward down Yucca, Drill Hole, and Dune Washes into Fortymile Wash (Fig. 2).

### ***Crater Flat***

Crater Flat, flanked by Bare Mountain on the west and Yucca Mountain on the east, is a structural basin approximately 24 km long and 6 to 11 km wide (Stuckless and O'Leary, this volume, Fig. 2). The basin has the overall form of a graben (or, more appropriately, a half-graben), its west side having been downdropped several kilometers along the east-dipping Bare Mountain fault and its east side downdropped a few hundred meters along a series of west-dipping normal faults that form the west slope of Yucca Mountain (Carr, 1984; Simonds et al., 1995; Fridrich, 1999). The axial part of the basin floor, covered by alluvial deposits that overlie a thick (as much as 3 km) sequence of Late Cenozoic volcanic rocks, rises gradually from altitudes of about 840 m at the south end to as much as 1,280 m at the foot of Yucca Mountain to the north. Four basaltic vents and their associated lava flows form prominent cones that attain heights ranging from 27 to 140 m above the alluviated surface of the central basin area.

### ***Fortymile Wash***

Fortymile Wash drains the area east and northeast of Yucca Mountain. From its northern headwaters, it flows southward through a steep-sided drainage course some 300 m deep that enters the northeast corner of the site area, continues down the south-sloping piedmont that forms the west end of Jackass Flats, and cuts a nearly linear trench, 150 to 600 m wide and as much as 25 m deep, into the Quaternary alluvial deposits of the piedmont (Fig. 1). This entrenchment gradually decreases downslope until the wash merges with the general level of the piedmont near the northeast margin of the Amargosa Desert basin.

### ***Other Topographic Features***

Three buttes or ridges (Busted Butte and Fran and Alice Ridges) and an alluvial flat (Midway Valley) form prominent topographic features on the east side of Yucca Mountain, and two narrow linear drainage courses (Solitario Canyon and Fatigue Wash) lie to the west. Busted Butte, Fran Ridge, and Alice Ridge (Fig. 2) are faulted bedrock areas rising 110 to 200 m above the surrounding terrain. Midway Valley, lying between these features and the east slope of Yucca Mountain to the west, is an alluviated lowland that slopes gently eastward from an elevation of about 1,220 m in its northwestern part to 1,070 m at a low point between Alice and Fran Ridges. Tributaries to Fortymile Wash head in northwest-trending washes along the east slope of Yucca Mountain, the most prominent of which is Yucca Wash (Fig. 2), and flow eastward across Midway Valley. A number of other washes are incised features toward the south end of Yucca Mountain, the largest being Dune Wash.

Drainages in Solitario Canyon and Fatigue Wash rise in upland areas in the northern part of Yucca Mountain at elevations of approximately 1,425 m and 1,675 m, respectively, and flow southward into northeastern Crater Flat, where elevations are about 1,200 m. The two valleys have been incised some 175 to 275 m into bedrock, and are fault-controlled (Day et al., 1998a). The north end of a third fault-controlled valley, Windy Wash, also extends into the northwestern part of the site area (Fig. 2). The associated faults (with the same names as the valleys) are discussed in the section on "Structural Geology".

## **Geomorphology**

### ***Influence of Tectonism/Quaternary Faulting***

As indicated earlier, Yucca Mountain is characterized by a series of fault blocks bounded by subparallel north-striking, primarily dip-slip faults that transect a broad apron of Miocene volcanic rocks and give rise to linear valleys and ridges such as the crest of Yucca Mountain and the adjoining Solitario Canyon (Fig. 2). Fault scarps, commonly visible along these faults, generally are located between the bedrock footwall and Quaternary colluvium on the hanging wall. Because the exposed volcanic rocks weather slowly, many scarps appear sharp, with fault dips of 55° to 75° (Fig. 4). A pattern of enhanced erosion at the base of some scarps near channels and rills indicates that they have been noticeably enhanced by hillslope erosion and, in essence, are fault-line scarps.

Several of the block-bounding faults show evidence of Quaternary displacements, which (1) influenced depositional patterns of surficial materials on hillslopes and on adjacent valley or basin floors, and (2) in places produced visible scarps in bedrock outcrops and surficial deposits

along some fault traces. However, low rates of offset and long recurrence intervals between successive faulting events on faults in the site area during Quaternary time (slip rates: .002 to .02 mm/yr; recurrence intervals: 20 to >100 k.y.; see Keefer et al., 2004) have resulted in subtle landforms and contributed to the preservation of early and middle Pleistocene deposits on Yucca Mountain hillslopes (Whitney and Harrington, 1993).

A striking feature of Yucca Mountain hillslopes is the lack of well-defined, rounded alluvial fans at the base of the slopes. On the west side of Yucca Mountain, hillslopes are of nearly uniform gradients, decreasing gradually from 32° near ridge tops to about 15° near the base, because of the homogeneous nature of the underlying volcanic tuff at the ridge crest, and because the low rates of uplift have not caused oversteepened slopes or high relief. As a result, the lower slopes of Yucca Mountain appear more like pediments than alluvial fans, which is most evident where lower and middle Pleistocene deposits are truncated and overlain by a veneer (less than 1 m thick) of upper Pleistocene-Holocene alluvium and eolian deposits.

### ***Influence of Volcanism***

Bedrock in the Yucca Mountain site area is composed entirely of volcanic outflow sheets whose caldera sources lay north of the site area. Much of the original morphology of this giant sheet of pyroclastic flows and fallout tephra that covered the area of Yucca Mountain and vicinity is no longer preserved, having been broken and segmented by subsequent faulting. A general southward decrease in elevation may reflect, in part, the regional depositional gradient away from the nearby volcanic centers to the north (Fig. 1). With respect to the volcanic rock sequences now exposed in the site area, differing characteristics between units, particularly the degree of welding, impart varying resistances to erosion, locally creating subdued bench-like

topography (Fig. 3). However, the nonwelded, less resistant units commonly are thin compared to the welded, more resistant units, so the effect of differential erosion is of relatively minor geomorphic importance.

### ***Influence of Climate***

The effects of climate on the evolution of landforms and on patterns of deposition and erosion at Yucca Mountain are discussed in the section on Quaternary Geology. Although the present-day climate is dominated by warm, dry conditions, there is evidence that wetter, cooler conditions existed at times in the past (see S.E. Sharpe, this volume). Such climate changes could take place at some future time.

## **STRATIGRAPHY OF THE VOLCANIC ROCKS**

### **Introduction**

Mid-Tertiary volcanic rocks, consisting mostly of pyroclastic-flow and fallout tephra deposits with minor lava flows, dominate the exposed bedrock formations in the Yucca Mountain site area (Fig. 2). Several published descriptive and interpretive reports (for example, Sawyer et al., 1994; Buesch et al., 1996a) defined what is now generally recognized as the standard hierarchical sequence of named units and subunits composing the principal volcanic rock groups and formations. The detailed order (and descriptions) of both major and minor subdivisions is given in CRWMS M&O (2000, Tables 4.5-1 and 4.5-2); a summary table listing the succession, general lithologies, and thicknesses of major units is presented in Table 1.

## General Features

Division of formations into lithostratigraphic units was initially proposed for the thick tuff sequences in the Yucca Mountain area by Warren et al. (1989). Buesch et al. (1996a) applied this terminology in greater detail after close examination and analysis of many samples collected from outcrops and from borehole cores within the site area. In general, the individual formations represent either volumetrically large eruptive units or a series of products interpreted to have formed from compositionally distinct magma bodies in the southwestern Nevada volcanic field. The Tiva Canyon and Topopah Spring Tuffs of the Paintbrush Group (Table 1), which are the most widespread bedrock units at Yucca Mountain, are classic examples of a compositional zonation characterized by an upper crystal-rich (> than 10% crystal fragments) member and a more voluminous, lower crystal-poor (< 5% crystal fragments) member (Lipman et al., 1966). A transition zone in crystal abundance, typically 5 to 10 m thick, is included as a basal unit of the crystal-rich member (Buesch et al., 1996a). Lipman et al. (1966) attributed the zoning to fractional crystallization such that the upper part of the magma chamber had evolved to a rhyolitic composition that was the first magma erupted and thus formed the crystal-poor basal part of each ash-flow sheet. Eruption from successively deeper parts of the chambers then produced less siliceous ejecta with a higher proportion of crystals, which formed the crystal-rich upper part of an ash-flow sheet with a quartz-latitude composition. Many of the interstratified bedded tuffs and local lava flows that are distinct from overlying and underlying formations (Table 1) probably represent small-volume eruptions.

## **Criteria for Differentiating Volcanic Rock Units at Yucca Mountain**

In the Yucca Mountain area, separation of formations into subunits is based on macroscopic features (for example, degree of welding) of the rocks as they appear in outcrops and borehole cores (Buesch et al., 1996a). Their identification is augmented by quantitative mineralogy (Bish and Chipera, 1986; Chipera et al., 1995), borehole geophysics (Muller and Kibler, 1984; Nelson et al., 1991; Nelson, 1996; CRWMS M&O, 1996), rock properties such as density and porosity (Martin et al., 1994, 1995; Moyer et al., 1996; Flint, 1998), and geochemical composition (Spengler and Peterman, 1991; Peterman and Futa, 1996).

Much of the following discussion focuses on the Tiva Canyon and Topopah Spring Tuffs, because each contains rock sequences that exhibit a range of properties that readily provides a basis for detailed stratigraphic subdivision.

### ***Lithologic and Rock-Property Criteria***

Important lithologic and rock-property criteria for differentiating the volcanic-rock units include (1) variations in grain size and sorting, (2) relative abundance of volcanic glass (vitric compared to devitrified), (3) degree of welding, (4) types and degree of crystallization, (5) relative abundance of lithophysae, (6) amount and types of glass alteration, and (7) fracture characteristics. Many of these rock properties are graphically portrayed in Figure 5 with respect to different zones within the Tiva Canyon and Topopah Spring Tuffs.

The lithologic and rock property criteria listed above, as well as their respective applications toward subdividing formations and members of formations at Yucca Mountain, were discussed in detail by Buesch et al. (1996a). Of these, two are especially important for

distinguishing zones and subzones within the volcanic sequences: (1) the presence or absence of lithophysae, which are features used to define some of the principal zones, particularly within the Tiva Canyon and Topopah Spring Tuffs (Fig. 5), and are closely associated with variously welded units; and (2) the degree of welding (Fig. 6), a property that distinguishes many subzones and also provides a principal means of separating hydrogeologic and thermal-mechanical units based on whether they are nonwelded, partially welded, moderately welded, or densely welded zones (Table 1). Such zones are vertically distributed in a single cooling unit of ash-flow tuff, with nonwelded rocks at the top and bottom of the deposit and increasingly welded rocks toward the center (Smith, 1960a, 1960b; see Fig. 5). Relatively thick deposits, such as the Tiva Canyon and Topopah Spring Tuffs, may have the complete welding range, both laterally and vertically (see below), but thin deposits may lack the more highly welded parts. In general, the degree of welding controls porosity, which ranges from 45 to 65% for nonwelded rocks, 25 to 45% for partially welded rocks, 10 to 25% for moderately welded rocks, and less than 10% for densely welded rocks (Buesch, 2000). The degree of welding is therefore of considerable importance to studies of the hydrogeologic and thermal-mechanical properties of the volcanic rock units in the site area (see Flint, 1998; Ciancia and Heiken, 2006).

### ***Mineralogic Criteria***

Mineralogy also is important in defining lithostratigraphic units in the site area. As shown in Figure 5, Buesch et al. (1996a) observed several crystallization and alteration zones within the Tiva Canyon and Topopah Spring Tuffs. (Note: use of term “zone” in this context is not to be construed as having the same connotation as its use in defining principal formational subdivisions.) The temporal progression of crystallization and alteration in tuffs is well



illustrated by the Topopah Spring Tuff. Following eruption and emplacement, the upper and lower parts of the ash flow cooled rapidly, preserving thin nonwelded vitric margins. Glassy parts between these vitric margins and the central devitrified mass retained enough heat to compact and weld, but not crystallize, and became densely welded vitrophyres within the upper and lower vitric zones. The interior of the cooling mass, some 90% of the total volume, retained sufficient heat to promote crystallization of all the glass, thus forming the devitrified, welded core of the formation. The release of water vapor during the crystallization process led to the crystallization of vapor-phase minerals along early-formed fractures and within pockets formed by gas expansion (lithophysal cavities). Vapor-phase minerals are dominantly feldspars and silica minerals, especially tridymite, some of which was subsequently pseudomorphed by quartz.

Phenocryst content in Yucca Mountain tuffs ranges from less than 1 volume percent to as much as approximately 25% (the highest percentages are in the bedded tuff at the base of the Calico Hills Formation and the upper part of the Bullfrog Tuff); lithic fragments average a few volume percent (Byers et al., 1976; Broxton et al., 1993). Quartz-latic units have consistently high phenocryst abundances, but rhyolitic units have variable abundances. Principal phenocrysts are sanidine, plagioclase, quartz, and biotite, and minor varieties include amphibole, clinopyroxene, and orthopyroxene.

### ***Geochemical Criteria***

Volcanic rocks at Yucca Mountain show systematic variations in their chemical (Lipman et al., 1966) and isotopic compositions (Noble and Hedge, 1969). The most abundant chemical constituents of vitric and devitrified tuffs are  $\text{SiO}_2$  and  $\text{Al}_2\text{O}_3$ . On the basis of the abundances of these two constituents, CRWMS M&O (2000, Fig. 4.5-12) showed that (1) the Calico Hills

Formation, Yucca Mountain Tuff, and crystal-poor members of the Tiva Canyon and Topopah Spring Tuffs are predominantly high-silica rhyolites; (2) tuffs in the Crater Flat Group exhibit a compositional range that is between high- and low-silica rhyolites; (3) the Lithic Ridge and Pah Canyon Tuffs consist of low-silica rhyolites; and (4) the crystal-rich members of the Tiva Canyon and Topopah Spring Tuffs are largely quartz latites. (Sequence of formations is shown in Table 1.)

Analyses of rock samples collected from several different outcrop localities and boreholes show that trace-element concentrations vary systematically with stratigraphic position. Peterman et al. (1993), for example, prepared a graph (Fig. 7) showing concentrations of titanium and zirconium in the sequence of formations cored in borehole UE-25 a#1 (borehole locations shown in Fig. 8). In this borehole, the break between the crystal-rich and crystal-poor members of the Topopah Spring Tuff is clearly evident at a depth of about 160 m (Fig. 7). Similar variations in trace-element concentrations from one borehole to another, as well as to outcrop sections, indicates a general lateral continuity of the volcanic rock units.

Superimposed on the initial composition of the volcanic rocks — that is, glass fragments, lithic inclusions, and phenocrysts — were the variations in mineralogy and chemistry introduced by alteration. Depending on the proportion of secondary minerals precipitated, alteration caused small to large chemical changes in the original rock mass. The initial distribution of vitric and devitrified tuffs (pyroclastic deposits in which high-temperature crystallization changed volcanic glass to a mostly anhydrous mineral assemblage) largely determined the locations of zeolitic and nonzeolitic rocks, respectively, in those parts of Yucca Mountain where the rocks were subjected to zeolitization (CRWMS M&O, 2004, sec. 3.3.5). Both syngenetic and diagenetic alteration were widespread (CRWMS M&O, 2004, sec. 3.3.5). Most syngenetic alteration occurred in and

near devitrified-vitric transition zones, and represents a transition from devitrification to glass dissolution and secondary-mineral precipitation of mostly zeolites, clay, and silica phases. The alteration was caused by a combination of water entrained in an ash flow and infiltrating meteoric water that interacted with the rock and occurred during the very late stages of cooling of the erupted material (Levy and O'Neil, 1989). The volume of rock affected by syngenetic alteration was highly variable, especially because much of the alteration was concentrated along and adjacent to fractures. Alteration in the Topopah Spring Tuff, in the interval from the lower nonlithophysal zone to the top of the nonwelded base of the formation (Fig. 5), is the most widespread and volumetrically abundant example of syngenetic alteration in the unsaturated zone in the site area (CRWMS M&O, 2004, sec. 3.3.5). Common mineral constituents in the altered tuffs include alkali feldspar, smectite, heulandite, and silica minerals. Minor constituents include mordenite, calcite, iron and manganese oxides, and erionite.

The most extensive post-cooling mineralogic and geochemical change affecting the rocks at Yucca Mountain has been the diagenetic zeolitization of nonwelded glassy tuffs. This process involved dissolution of glass shards by ground water at ambient temperatures (e.g., 50°C or lower) and precipitation of clinoptilolite with or without lesser amounts of mordenite, smectite, silica, iron-oxide magnetites and hydroxides, and other minor constituents (CRWMS M&O, 2004, sec. 3.3.5).

### ***Borehole Geophysical-Log Criteria***

Suites of geophysical logs, commonly including caliper, gamma-ray, density, induction, resistivity, and neutron logs, were obtained from several tens of boreholes across the Yucca Mountain site area (Nelson, 1993, 1994, 1996). Because these logs reflect changes in rock

properties, they can be used to correlate lithostratigraphic features — for example, (1) increased welding causes matrix density to increase and porosity to decrease; (2) mineral alteration (from clays and zeolites) causes a decrease in resistivity and an increase in neutron absorption, resulting in a high apparent neutron porosity; (3) differences in magnetic susceptibility and remanence depend on the chemistry of the rock and Earth's magnetic field at the time of eruption and deposition; and (4) devitrification forms highly magnetic minerals that typically increase the magnetic field of the rocks, whereas alteration typically reduces the intensity of many magnetic properties. Figure 9, showing combined geophysical log and core data obtained in borehole UE-25 UZ#16, illustrates correlations that can be made between log responses and various lithologic and mineralogical features within some of the major stratigraphic units.

### **Descriptions of Rock Units**

Formations and intervening bedded tuff units that compose the Tertiary volcanic rock sequence at Yucca Mountain are shown in Table 1, together with thicknesses and brief generalized lithologic descriptions. Also included are columns showing hydrogeologic and thermal-mechanical units that correlate directly with specific stratigraphic units. Subdivisions of each of the formations and their detailed lithologic descriptions are given in CRWMS M&O (2000, Tables 4.5-1 and 4.5-2). Two stratigraphic cross sections, Figures 10 and 11, drawn with the top of the Topopah Spring Tuff as a datum, show the distribution of formations across parts of the Yucca Mountain site area. Bedded tuff units, commonly too thin to plot separately at small scales, are included in the basal parts of the overlying formational units. Descriptions of the bedded tuff units also are included with the overlying formations in the following

discussions. Unless otherwise indicated, stated thicknesses are based on (1) a tabulation of formation tops as identified in some 50 boreholes by R. W. Spengler and D. C. Buesch (U.S. Geological Survey, unpublished data), and (2) a series of isochore maps presented by Bechtel SAIC Company (2002), based largely on the borehole data in item (1). (Note: Borehole depths and measurements typically are recorded in feet, but in the following descriptions they are converted to meters with feet given in parentheses.)

### ***Pre-Cenozoic Rocks***

Pre-Cenozoic rocks, believed to consist primarily of Upper Precambrian and Paleozoic sedimentary strata, underlie the Tertiary volcanic rocks at Yucca Mountain, but little detailed information is available on their thickness and overall lithology. The only direct evidence of their presence within the site area is in borehole UE-25 p#1, which penetrated Paleozoic carbonate rocks in the depth interval 1,244 to 1,805 m (4,081 to 5,922 ft) (Fig. 10). These rocks, almost entirely dolomites, have been correlated with the Lone Mountain Dolomite and Roberts Mountains Formation on the basis of exposures at Bare Mountain to the west (Monsen et al., 1992), and on the presence of Silurian-age conodonts (M.D. Carr et al., 1986). Summary descriptions of pre-Cenozoic rocks in the Yucca Mountain region are given by Stuckless and O'Leary (this volume).

### ***Pre-Lithic Ridge Volcanic Rocks***

The oldest known volcanic rocks in the Yucca Mountain area (> 14 Ma; Sawyer et al., 1994) underlie the Lithic Ridge Tuff. Because they are not exposed at Yucca Mountain, little is known about their extent and stratigraphic relations except locally, where they have been

penetrated in boreholes. In boreholes USW G-1, USW G-2, and USW G-3 (Fig. 11), the sequence consists of bedded tuffaceous deposits, pyroclastic flow deposits, and quartz-latic to rhyolitic lavas and flow breccia (Broxton et al., 1989). Crystal fragments are largely plagioclase, with lesser amounts of sanadine and quartz. Penetrated thicknesses vary from approximately 45 m (148 ft) in USW G-3 to approximately 350 m (1,148 ft) in USW G-2. In borehole UE-25 p#1 (Fig. 10), 180 m (590 ft) of altered tuff lies between the Lithic Ridge Tuff and Paleozoic strata (Muller and Kibler, 1984). Initial compositions of these pre-Lithic Ridge tuffs are poorly known because they are altered to clays, calcite, and chlorite (Spengler et al., 1981; Bish and Vaniman, 1985). These data have been used to determine their alteration history (Bish and Aronson, 1995).

### ***Lithic Ridge Tuff***

The Lithic Ridge Tuff, dated at 14 Ma (Sawyer et al., 1994), is a massive pyroclastic flow deposit (W.J. Carr et al., 1986) ranging in thickness from 185 m (607 ft) at borehole USW G-2 to 304 m (997 ft) in borehole USW G-3 (Fig. 11). The formation is nonwelded to moderately welded, and extensively altered to clay and zeolite minerals. Crystal fragments (quartz, sanadine, plagioclase) average about 10% of the rock, and lithic fragments constitute 5 to 15%. Many slight variations in the degree of welding, crystal-fragment ratios, and lithic-fragment content indicate that several eruptive surges are represented.

### ***Dacitic Lava and Flow Breccia***

Dacitic lava and flow breccia overlie the Lithic Ridge Tuff in deep drill holes in the northern and western parts of the Yucca Mountain site area (Figs. 10 and 11) but are absent

elsewhere. The thickness of the unit is 111 m (365 ft) in borehole USW H-1 (Fig. 8; Rush et al., 1984) and 249 m (817 ft) in borehole H-6 (Fig. 10; Craig et al., 1983). In borehole USW G-1, most of the unit is flow breccia made up of angular to subangular dacite fragments, commonly from 2 to 10 cm long, which are intercalated with lava blocks ranging from 1 m to more than 17 m thick (Spengler et al., 1981). The breccia is autoclastic, indicating that its formation is primarily due to fragmentation of semisolid and solid lava during relatively slow flow. About 8 m of reworked pyroclastic fallout and bedded tuff deposits underlie the flow breccia in borehole USW G-1 (Spengler et al., 1981).

### ***Crater Flat Group***

The Crater Flat Group, dated between 13.5 and 13.0 Ma, consists of three formations of moderate- to large-volume pyroclastic flow deposits — Tram, Bullfrog, and Prow Pass Tuffs (Table 1) — and interstratified bedded tuffs (Sawyer et al., 1994). The group ranges in composition from the high-silica rhyolites characterizing most of the younger Paintbrush Group to the distinctive lower silica rhyolites of the Pah Canyon Tuff of the Paintbrush Group (Bish et al., 2002). The Crater Flat Group is distinguished from other pyroclastic units in the vicinity of Yucca Mountain by the relative abundance of quartz and biotite crystal fragments. In addition, the Prow Pass Tuff and, to a lesser degree, some parts of the Bullfrog Tuff contain distinctive lithic clasts of reddish-brown mudstone. The Tram Tuff overlies dacitic lavas and flow breccias in the northern part of Yucca Mountain, and the Lithic Ridge Tuff in the southern part (Figs. 10 and 11; Broxton et al., 1989).

### ***Tram Tuff of the Crater Flat Group***

Several depositional units have been distinguished within the Tram Tuff on the basis of the abundance and types of pumice and lithic clasts in pyroclastic-flow deposits and rare bedded tuff interbeds. The most easily recognized stratigraphic divisions are the lower lithic-rich unit, which can be locally divided into a lower lithic-poor and an upper lithic-rich set of subunits, and an upper lithic-poor unit. Both lithic-rich and lithic-poor units have been identified and described in several boreholes, including UE-25 p#1, USW G-1, UE-25 b#1, USW G-3, and USW H-1 (Spengler et al., 1981; Maldonado and Koether, 1983). In borehole USW G-2, the upper lithic-poor unit is absent and the lithic-rich unit is well developed (Maldonado and Koether, 1983). Welding is variable, and locally the large concentration of lithic clasts (such as in borehole USW G-2) apparently reduced the degree of welding. In general, the lithic-poor unit is more densely welded than the underlying lithic-rich unit. Crystal fragments include quartz, feldspar, abundant biotite (30–50% of phenocrysts in upper part), and very rare hornblende (?).

Argillic and zeolitic alteration is present in both units of the Tram Tuff. In the lithic-poor unit, the alteration appears to be in two zones separated by the zone of maximum welding. The upper and lower parts of the formation are altered to clinoptilolite  $\pm$  mordenite. In the vicinity of borehole USW G-1, however, analcime appears in the lower part, and in borehole USW G-2 analcime is the dominant zeolite in both the upper and lower parts.

Tram Tuff thicknesses in boreholes range from 104 m to as much as 370 m (340–1,213 ft). A regional isopach map by W.J. Carr et al. (1986) shows the thickness to exceed 400 m (1,310 ft) in the northern part of Crater Flat to the west.

The lower lithic-rich unit overlies a complex sequence of altered and weathered pyroclastic fallout deposits and minor pyroclastic-flow deposits (e.g., see Diehl and Chornack 1990). With respect to the seven boreholes plotted in Figures 10 and 11, these pre-Tram Tuff bedded tuffs



(included in the Tram Tuff interval) range in thickness from 0 in borehole UE-25 p#1 to 21 m (68 ft) in borehole USW G-2.

### ***Bullfrog Tuff of the Crater Flat Group***

Descriptions of the Bullfrog Tuff, which is exposed only in limited outcrops in the northwest corner of the site area, are based primarily on studies of core from boreholes USW G-1 and USW G-4 (Spengler et al., 1981; Spengler and Chornack, 1984). The formation is composed of two pyroclastic-flow deposits, both of which are simple cooling units; they are separated by an interval of pumiceous fallout. Borehole thicknesses range from 67 to 188 m (221–618 ft). Regionally, W.J. Carr et al. (1986) show the formation to be as much as 400 m (1,310 ft) thick in an area of maximum deposition in the southern part of Crater Flat.

The upper pyroclastic-flow unit is variably welded and altered to zeolites and(or) clay. The lower unit is moderately welded in its central part, and the intervening pumiceous deposit is partly to moderately welded. Pumice clasts constitute as much as 20 to 25% of the rock; crystal fragments include quartz, feldspar, biotite, and minor pyroxene.

The pre-Bullfrog Tuff bedded tuff unit (included in the Bullfrog Tuff interval) consists primarily of weathered pyroclastic-flow deposits interbedded with thin zones of fallout tephra. Diehl and Chornack (1990) correlated five marker horizons through the sequence between boreholes USW G-1, USW G-2, and USW G-3. Thicknesses of the unit in the seven boreholes in Figures 10 and 11 range from 6 to 11 m (20 to 37 ft). In addition to an intervening bedded tuff, the Bullfrog Tuff can be differentiated from the overlying Prow Pass Tuff on the basis of crystal assemblages and bulk chemistry (Moyer and Geslin, 1995). The Bullfrog, for example,

contains abundant biotite and rare pyroxene, whereas the Prow Pass contains altered orthopyroxene and biotite in about equal amounts.

### ***Prow Pass Tuff of the Crater Flat Group***

The Prow Pass Tuff consists of four variably welded pyroclastic-flow deposits formed by eruptions from an unidentified source between 13.0 and 13.25 Ma (Sawyer et al., 1994). Descriptions and unit thicknesses (except for the pre-Prow Pass Tuff bedded tuff) given below are summarized from Moyer and Geslin (1995), based in large part on studies of core samples from boreholes USW G-1, USW G-2, USW GU-3, USW G-4, USW UZ-14, UE-25 a#1, UE-25 c#1 (and nearby c#2 and c#3), and UE-25 UZ#16, and from observations of exposures at The Prow (Fig. 2).

The basal bedded tuff unit (pre-Prow Pass Tuff bedded tuff), less than 1 m to about 3.5 m (3 to 11 ft) thick in the boreholes shown in Figures 10 and 11 (included in the Prow Pass Tuff interval), consists of welded and zeolitically altered tuffaceous deposits.

The lowermost pyroclastic-flow deposit of the Prow Pass Tuff (designated unit 1 by Moyer and Geslin, 1995), with an aggregate thickness of 25 to 70 m (82 to 230 ft), consists of three subunits separated on the basis of their lithic clast content. The subunits generally are similar, with zeolitically altered matrices. The next overlying unit (unit 2) is a sequence of pyroclastic-flow deposits that have not been subdivided because they lack distinguishing characteristics. Locally preserved ash horizons and abrupt changes in the amounts and sizes of pumice and lithic clasts, however, indicate at least three flow deposits in most boreholes studied. The aggregate thickness ranges from about 3 to 34 m (10 to 112 ft). Six subunits defined by changes in the degree of welding or the intensity of vapor-phase alteration characterize the third flow deposit

(unit 3). Its thickness ranges from 40 m (131 ft) to nearly 80 m (262 ft). The top unit of the Prow Pass Tuff (unit 4), which ranges from 4 m (13 ft) to as much as 20.5 m (67 ft) thick in cored boreholes, can be divided into three irregularly distributed subunits differentiated by changes in the average diameter and percentage of pumice clasts that decrease stratigraphically upward.

Among its characteristics, the Prow Pass Tuff is distinguished by the presence of altered orthopyroxene in addition to biotite as crystal fragments and by distinctive, fine-grained, oxidized lithic inclusions of red mudstone. In contrast, the overlying Calico Hills Formation contains different amounts of crystal fragments and proportions of quartz in the crystal assemblage. The basal bedded tuff and sandstone units of the Calico Hills serve as consistent stratigraphic markers in several boreholes (Diehl and Chornack, 1990).

### ***Calico Hills Formation***

The Calico Hills Formation and the underlying bedded tuffs form one of the most potentially important barriers to the migration of exchangeable cations at Yucca Mountain. Despite its great heterogeneity, the formation has a consistently high matrix porosity (average 28 to 35%; see Moyer and Geslin, 1995), which indicates an important role for matrix flow of ground water. Other properties, particularly permeability, are extremely variable and strongly dependent on mineralogy; permeability decreases by about two orders of magnitude, and sorption by cation exchange increases as much as five orders of magnitude, in the transition from vitric to zeolitic rocks within the formation.

The Calico Hills Formation is a complex series of rhyolite tuffs and lavas that resulted from an episode of volcanism approximately 12.9 Ma (Sawyer et al., 1994). Five pyroclastic units,

overlying a bedded tuff unit and, locally, a basal sandstone unit, were distinguished in the Yucca Mountain site area by Moyer and Geslin (1995). The formation is 250 m (820 ft) thick in borehole G-2 toward the northern part of the site area (Figs. 8 and 11) and thins southward to 11 m (37 ft) in borehole H-3 (Fig. 8). The following descriptions are summarized from Moyer and Geslin (1995), whose studies were based on examinations of cores and observations of outcrops in the same boreholes and surface locality as those listed above for the Prow Pass Tuff.

The basal volcanoclastic sandstone unit of the Calico Hills Formation is interbedded with rare reworked pyroclastic-flow deposits; thicknesses of the unit range from 0 to 5.5 m (0 to 18 ft). The overlying bedded tuff (labeled pre-Calico Hills Formation bedded tuff in Table 1), 9 to 39 m (30 to 128 ft) thick, is composed primarily of pyroclastic-fallout deposits. Each of the five pyroclastic units forming the bulk of the formation consists of one or more pyroclastic-flow deposits separated by locally preserved fallout horizons. Ash-fall and ash-flow deposits beneath the repository block give way to lava flows to the north and east.

X-ray diffraction of drill-core samples by Caporuscio et al. (1982), Bish and Vaniman (1985), and Bish and Chipera (1986) and of outcrop samples by Broxton et al. (1993) showed an abundance of authigenic zeolites in all units of the Calico Hills Formation. The pyroclastic units have extremely high clinoptilolite and mordenite contents (40 to 80%; Caporuscio et al., 1982; Vaniman et al., 1984; Bish and Vaniman, 1985; Bish and Chipera, 1986) that contrast with the somewhat lower zeolite content of the bedded tuffs and basal sandstone (Moyer and Geslin, 1995). Mapping of the distribution of zeolites shows that (1) they are more widely present in the bedded tuffs than in the pyroclastic units, and (2) zeolite mineralization is pervasive in the northern part of Yucca Mountain but absent in some southern locations. In the vicinities of boreholes USW GU-3 and USW H-4, for example, the entire formation is vitric (Moyer and

Geslin, 1995). The presence of zeolitized zones within the Calico Hills, and within other formations such as the Prow Pass Tuff, has important implications with respect to paleohydrologic interpretations and the potential development of natural barriers to contaminant movement by ground water (e.g., see CRWMS M&O, 1998).

The complex series of rhyolite tuffs and lavas in the Calico Hills Formation grades laterally from completely zeolitized to unaltered vitric rock from east to west across the site area. Crystal fragments, which compose as much as 7 to 12% of some units, predominantly are quartz, feldspar, and biotite, with trace magnetite and accessory clinopyroxene, ilmenite, allanite, and zircon. Lithic clasts make up as much as 40% of the rocks, but the proportion is more commonly in the 15 to 20% range. The formation is distinguished from the Topopah Spring Tuff by differences in mineralogy and chemical composition; lithostratigraphic units of the former have crystal assemblages with a higher proportion of quartz and higher concentrations Ca and Ba than units of the latter.

### ***Paintbrush Group***

The Paintbrush Group consists of four formations, each primarily composed of pyroclastic-flow deposits interstratified with small-volume pyroclastic-flow and fallout-tephra deposits, and, locally, lava flows and secondary volcanoclastic deposits from eolian and fluvial processes (Buesch et al. 1996a). In ascending order, the formations include the Topopah Spring, Pah Canyon, Yucca Mountain, and Tiva Canyon Tuffs; they are dated at 12.8 to 12.7 Ma (Sawyer et al., 1994). This group is one of the most widespread and voluminous caldera-related assemblages in the southwestern Nevada volcanic field (Sawyer et al., 1994). The Topopah Spring Tuff forms the host rock for the proposed repository, therefore it is one of the most

intensely studied formations at Yucca Mountain. Locations of eruptive centers for the Topopah Spring and Pah Canyon Tuffs are uncertain, but the Claim Canyon caldera (Fig. 1) is the identified source of the Tiva Canyon Tuff and possibly the Yucca Mountain Tuff (Byers et al., 1976; Sawyer et al., 1994).

The Paintbrush Group is dominated volumetrically by the Topopah Spring and Tiva Canyon Tuffs. The Yucca Mountain and Pah Canyon Tuffs are minor units but are of potential hydrologic importance because of their high matrix porosity compared to the Tiva Canyon and Topopah Spring, which are largely densely welded with low matrix porosity. The welded tuffs also have higher fracture abundance and connectivity, providing stratified contrasts in unsaturated hydrologic properties in the Paintbrush Group rocks above the proposed repository block.

Descriptions of the formations within the Paintbrush Group are generalized from detailed studies of outcrops and borehole cores by Buesch et al. (1996a), supplemented by core descriptions obtained from Geslin et al. (1995); Geslin and Moyer (1995); and Moyer et al. (1995). Divisions of the Tiva Canyon and Topopah Spring Tuffs into members, zones, subzones, and intervals (Buesch et al., 1996a) indicates that both formations are simple cooling units within the site area (Lipman et al., 1966). The interaction among depositional, welding, crystallization, and fracturing processes produces unit contacts that range from sharp to gradational. Depositional contacts, such as the bases of pyroclastic-flow and fallout deposits and redeposited material, are examples of sharp contacts. The tops of these deposits typically are sharp, but may be gradational where there is evidence of reworking or pedogenesis. The transition from nonwelded to densely welded tuff typically is gradational, such as near the base of the Topopah Spring Tuff in boreholes USW GU-3 and USW WT-2. Contacts of several lithostratigraphic

units correspond with hydrogeologic and thermal-mechanical unit boundaries throughout Yucca Mountain (Table 1).

### ***Topopah Spring Tuff of the Paintbrush Group***

The Topopah Spring Tuff includes the host rock units for the proposed radioactive waste repository. As such, its characteristics are of direct importance to repository design, unsaturated-zone hydrologic flow and radionuclide transport, and total-system performance assessment. A complete description of the Topopah Spring Tuff is presented in Buesch et al. (1996a).

The Topopah Spring Tuff is 149 to 369 m (488–1,209 ft) thick as identified in boreholes in the Yucca Mountain site area. The formation is divided into a lower crystal-poor member and an upper crystal-rich member. Vitric rocks form zones at the top and bottom of the formation, and alternating lithophysal and nonlithophysal zones characterize the remaining parts of the two members (Fig. 5). Further subdivision primarily is based on the degree of welding, crystal content and assemblage, and size and abundance of pumice and lithic clasts.

The Topopah Spring Tuff is compositionally zoned with an upward chemical change from high-silica rhyolite in the crystal-poor member to quartz latite (also referred to as quartz trachyte) in the crystal-rich member (Lipman et al., 1966; Sawyer et al., 1994). The lower part of the formation is one of the most chemically homogeneous rock types in the site area (Bish et al., 2002). The homogeneity of the major-element chemistry also extends to trace elements. Somewhat greater chemical variability is seen in the quartz latites of the crystal-rich member.

The crystal-poor member, characterized by 3% (or less) felsic crystal fragments composed mainly of sanadine and plagioclase with traces of quartz and mafic minerals, is divided into vitric rocks of the vitric zone near the base and (in ascending order) devitrified rocks of the lower

nonlithophysal, lower lithophysal, middle nonlithophysal, and upper lithophysal zones (Fig. 5; Buesch et al., 1996a). The latter four zones form the host rock for the proposed repository. The vitric zone is divided primarily on the basis of degrees of welding, which range upward from a nonwelded to partially welded subzone at the base, through a moderately welded subzone, to a densely welded subzone at the top. The vitric, densely welded subzone, commonly referred to as the vitrophyre, is identified as an important subunit within the Topopah Spring welded thermal-mechanical unit (Table 1).

Within the devitrified, rhyolitic part of the Topopah Spring Tuff, crystal fragments are minor constituents (less than 5%) of the rock and the remainder consists of fine-grained devitrification minerals. These devitrification products are principally feldspars plus a variable combination of the silica polymorphs tridymite, cristobalite, and quartz. Abundance of quartz is a useful stratigraphic marker within the devitrified, rhyolitic Topopah Spring Tuff, but quartz crystal fragments nevertheless are much less abundant (less than 0.5%) than groundmass quartz (approximately 20%) throughout this interval. The silica polymorph distributions are particularly important because of their thermal stability, dissolution properties, and other properties that can create inhalation hazards.

A transitional zone, commonly referred to as the vitric-zeolitic transition that is composed of partly devitrified vitrophyre, extends downward from the base of the lower nonlithophysal zone into the crystal-poor vitric zone through a stratigraphic interval ranging from about 3 to 30 m (10 to 100 ft) in thickness. In many parts of Yucca Mountain, the moderately welded and nonwelded subzones at the base of the crystal-poor vitric zone are overprinted by zeolite alteration zones (Buesch et al., 1996a). Accordingly, a vitric-zeolitic boundary can be drawn that varies within a narrow range of stratigraphic positions, but generally coincides closely with the



contact between the moderately welded subzone and the overlying densely welded subzone (Buesch and Spengler, 1999). This boundary is further defined as the contact between the Topopah Spring welded hydrogeologic unit and the underlying Calico Hills nonwelded hydrogeologic unit (Table 1).

The crystal-rich member of the Topopah Spring Tuff is characterized by 10 to 15% crystal fragments (sanadine and plagioclase, traces of quartz, biotite, pyroxene, and hornblende), with a crystal-transition subzone at the base where crystal abundance increases upward from 3 to 10%. The member is divided into lithophysal, nonlithophysal, and vitric zones (Fig. 5). Rocks in the lower two zones are devitrified, and the division is based on the presence or absence of lithophysae. The vitric zone at the top of the member is distinguished by preservation of the volcanic glass to form rocks with a vitreous luster that typically grade upward from densely welded to nonwelded. This zone is relatively impermeable, which impedes the downward flow of ground water in the unsaturated zone.

The tuffaceous rock unit (pre-Topopah Spring Tuff bedded tuff) that lies between the Topopah Spring Tuff and the Calico Hills Formation is 0 to 17 m (0 to 55 ft) thick in the boreholes plotted in Figures 10 and 11; it is included in the Topopah Spring interval.

### ***Pah Canyon Tuff of the Paintbrush Group***

The Pah Canyon Tuff is a simple cooling unit (Christiansen, 1979) consisting of multiple flow units that are composed of low-silica rhyolites (Vaniman et al., 1996). The formation reaches a thickness of 72 m (237 ft) in borehole G-2 and thins southward to zero in the vicinity of borehole USW UZ#16 (Fig. 8; Moyer et al., 1996). The formation varies from nonwelded to moderately welded, and, throughout much of the site area, vitric pumice clasts are preserved in a

nondeformed matrix that was either sintered or was lithified by vapor-phase mineralization. Crystal fragments in the matrix and in large pumice clasts constitute 5 to 10% of the rock, with a greater proportion of feldspars relative to mafic minerals (biotite and clinopyroxene). Lithic clasts of devitrified rhyolite (as much as 5% of the rock) are common, and clasts of porphyritic obsidian are in some horizons. Shards are either poorly preserved clear glass or form devitrified material. The high water saturation of porous nonwelded units in the Pah Canyon, as well as in the overlying Yucca Mountain Tuff, leads to a relatively high degree of alteration where there is an underlying barrier to transmission. Because of the relatively impermeable upper vitrophyre of the underlying Topopah Spring Tuff, the alteration of the Pah Canyon Tuff (typically to smectite) generally is more extensive than that of the overlying Yucca Mountain Tuff. Therefore, despite its minor volume, the Pah Canyon Tuff has an important effect on reactions between unsaturated-zone water and the host tuffs.

The pre-Pah Canyon Tuff bedded tuff, 3 to 10 m thick (10 to 32 ft) in the boreholes plotted in Figures 10 and 11 (included in the Pah Canyon Tuff interval), consists of moderately well sorted pumiceous tephra with thin layers of lithic-rich fallout and very fine-grained ash at the base.

### ***Rhyolites of Black Glass Canyon, Delirium Canyon, and Zig Zag Hill***

Relatively minor amounts of rhyolite lava flows and related tephra deposits crop out locally in the northern part of the Yucca Mountain site area (Day et al., 1998a). The rhyolite of Zig Zag Hill is exposed in one small outcrop in the vicinity of The Prow in the northwest corner of the area (Fig. 2), where it forms a thin unit (thickness 10 m or less) between the Pah Canyon Tuff and the pre-Yucca Mountain Tuff bedded tuff (Table 1). The Delirium Canyon and Black Glass

Canyon units are in limited outcrops in the northeast and north-central parts of the site area. Lava flows in the Delirium Canyon are as much as 250 m (820 ft) thick, and ash-flow tuffs are as much as 100 m (328 ft) thick (Table 1); the combined unit is considered to be equivalent to parts of the Rhyolite of Zig Zag Hill and the pre-Yucca Mountain Tuff bedded tuff (Table 1; Day et al., 1998a). The Rhyolite of Black Glass Canyon, 2 to 14 m (6.5 to 46 ft) thick, lies stratigraphically between the Yucca Mountain Tuff and the pre-Yucca Mountain Tuff bedded tuff (Table 1; Day et al., 1998a). Crystal fragments in the lavas and tephra consist of 5 to 10% sanidine and plagioclase and less than 1% hornblende, biotite, and sphene.

#### ***Yucca Mountain Tuff of the Paintbrush Group***

The Yucca Mountain Tuff is a simple cooling unit that is nonwelded throughout much of the Yucca Mountain area, but is partially to densely welded where it thickens in the northern and western parts. Although typically vitric in most locations in the central part, the tuff is increasingly devitrified where thickest. The formation is as much as 55 m (180 ft) thick in parts of Yucca Mountain, but thins to zero southward (Table 1). It is nonlithophysal throughout Yucca Mountain, but contains lithophysae where densely welded in northern Crater Flat. Although chemically similar to the high-silica rhyolites of the Tiva Canyon and Topopah Spring Tuffs, it contains plagioclase and sanidine crystal fragments, which is characteristic of the rhyolitic parts of the Topopah Spring but not those of the Tiva Canyon that contain only sanidine phenocrysts.

The pre-Yucca Mountain Tuff bedded tuff consists of pumiceous, vitric, nonwelded pyroclastic-flow deposits. In the boreholes shown in Figures 10 and 11, the unit, which is

included in the Yucca Mountain Tuff interval, ranges from less than 1 m to as much as 46 m (<3 to 150 ft) in thickness (Table 1).

### ***Tiva Canyon Tuff of the Paintbrush Group***

The Tiva Canyon Tuff is a large-volume, regionally extensive, compositionally zoned (from rhyolite to quartz latite) tuff sequence (Table 1) that forms most of the rocks exposed at the surface in the Yucca Mountain site area (Day et al., 1998a). Thicknesses of those parts of the formation penetrated in boreholes or observed in outcrops range from less than 50 m to as much as 175 m (165 to 575 ft). Separation of the formation into a lower crystal-poor member and an upper crystal-rich member, and into zones within each of these members, is based on criteria similar to those discussed above for the Topopah Spring Tuff.

The rhyolitic crystal-poor member is divided into five zones: in ascending order, these are the vitric, lower nonlithophysal, lower lithophysal, middle nonlithophysal, and upper lithophysal zones (Fig. 5; Buesch et al., 1996a). Further division into subzones is based on vitric versus devitrified rocks, degree of welding (Fig. 6), differences in pumice clasts, presence or absence of lithophysae, and fracture morphology. The lowest part of the member consists of densely welded to nonwelded high-silica rhyolitic glass. Only about 5% of the rock is composed of crystal fragments (sanadine with traces of hornblende, biotite, and sphene). The crystal-poor member and overlying crystal-rich member are separated by a thin transitional subzone in which there is an upward increase in crystal content and an increase in the proportion of mafic relative to felsic crystal fragments.

The quartz-latitic crystal-rich member, which consists primarily of devitrified nonlithophysal material, locally contains lithophysae near the base; it is capped by a thin (less

than 1 m thick) vitric zone that is preserved only locally and has been eroded from most of Yucca Mountain. Crystal fragments, predominantly sanadine and plagioclase with trace amounts of quartz, biotite, pyroxene, hornblende, and sphene, constitute 10 to 15% of the rock. The crystal-rich nonlithophysal zone is divided into four subzones based upon such depositional features as abundance of crystal fragments and pumice. Much of this zone has undergone corrosion and alteration, which has substantially increased its porosity compared to the overlying and underlying rocks.

The pre-Tiva Canyon bedded tuff is characterized by thin beds of fallout tephra deposits interbedded with thin oxidized, weathered zones (Diehl and Chornack, 1990). Thicknesses of the unit penetrated in the seven boreholes plotted in Figures 10 and 11 (shown as part of the Tiva Canyon Tuff interval) range from less than 1 m to 3 m (<3 to 10 ft).

#### ***Post-Tiva Canyon/pre-Rainier Mesa Tuffs and Lava Flows***

Several rhyolite lava flows and fallout tephra deposits are in the upper part of the Paintbrush Group in the vicinity of Yucca Mountain (Buesch et al., 1996a; see Fig. 2). These units, lying between the top of the Tiva Canyon Tuff and the base of the pre-Rainier Mesa bedded tuff, include (in ascending order) the post-Tiva Canyon Tuff bedded tuff, rhyolite of Vent Pass, tuff unit "X", and rhyolite of Comb Peak (Table 1). The rhyolitic lavas and ash-flow tuffs of the Vent Pass unit are exposed in the north-central part of the site area where thicknesses are as much as 150 m (490 ft) (Day et al., 1998a). Lavas and tuffs of the Rhyolite of Comb Peak form extensive outcrops in the large area of bedrock in the northeast part of the site area, north of Midway Valley and Yucca Wash (Fig. 2). These rocks aggregate maximum thicknesses of nearly 130 m (426 ft) (Table 1; Day et al., 1998a).

A 6- to 23-m-thick (20 to 75 ft) lithic-rich pyroclastic-flow deposit (Table 1), which was penetrated in several boreholes on the west side of Midway Valley near Exile Hill (such as borehole UE-25 RF#3, Fig. 8) and is exposed in the excavation for the north portal of the Exploratory Studies Facility (ESF) (Swan et al., 2001; see Fig. 16), was referred to informally as tuff unit "X" by Carr (1992). The unit is a pumiceous, nonwelded, in part zeolitic ash flow that was tentatively correlated with the Rhyolite of Comb Peak (Table 1) by Buesch et al. (1996a). Additional descriptions based on core studies from boreholes on the west side of Exile Hill were given by Geslin et al. (1995).

The post-Tiva Canyon Tuff bedded tuff is a tuffaceous rock unit commonly consisting of numerous depositional sequences separated by possible paleosols (Buesch et al., 1996a). Thicknesses in several boreholes near Exile Hill range from less than 2 to 4.5 m (<7-15 ft) (Table 1; Carr, 1992; Geslin et al., 1995).

### ***Timber Mountain Group***

The Timber Mountain Group includes all quartz-bearing pyroclastic-flow and fallout-tephra deposits erupted about 11.5 Ma from the Timber Mountain caldera complex, the south edge of which lies just north of the area shown in Figure 1 (Byers et al., 1976; Sawyer et al. 1994). The complex consists of two overlapping, resurgent calderas: an older caldera formed by the eruption of the Rainier Mesa Tuff, and a younger, nested caldera formed by the eruption of the Ammonia Tanks Tuff (Table 1; Minor et al., 1993; Sawyer et al., 1994).

### ***Rainier Mesa Tuff of the Timber Mountain Group***

The Rainier Mesa Tuff is a compositionally zoned compound cooling unit consisting of high-silica rhyolite tuff overlain by a considerably thinner quartz latite tuff (Table 1) that is restricted to the vicinity of the Timber Mountain caldera (Byers et al., 1976). The formation is not present across much of Yucca Mountain, but is locally exposed on the downthrown blocks of large faults in valleys toward the south end of the mountain (Day et al., 1998a; see Fig. 2). It is also exposed in the extreme northwest corner of the site area and was penetrated in a few boreholes on the east side. Based on examination of cores from boreholes UE-25 NRG#2, #2B, #2C, and #2D (UE-25 NRG#2 is shown in Fig. 8; the other boreholes are nearby), the Rainier Mesa Tuff consists of a nonlithified to lithified and partially welded pyroclastic-flow deposit generally less than 30 m (98 ft) thick (Geslin and Moyer, 1995; Geslin et al., 1995). A maximum thickness of 240 m (787 ft) was observed in the southwestern part of Crater Flat (Fridrich, 1999). Pumice clasts compose 10 to 25% of the rocks, crystal fragments 10 to 20% (quartz, plagioclase, sanadine, biotite), and lithic clasts 1 to 5%.

The pre-Rainier Mesa Tuff bedded tuff consists of nonlithified fallout-tephra and pyroclastic-flow deposits (Table 1; Geslin and Moyer, 1995; Geslin et al., 1995). The sequence occupies intervals of about 17 m (55 ft) in boreholes UE-25 NRG#2C and UE-25 NRG#2D, and is characterized by moderately well-sorted white pumice lapilli and volcanic lithic clasts.

#### ***Ammonia Tanks Tuff of the Timber Mountain Group***

The Ammonia Tanks Tuff (Table 1) is not present across Yucca Mountain, but is exposed in the southern part of Crater Flat and was penetrated by one borehole in the Crater Flat area (Fridrich, 1999). There, the formation consists of welded to nonwelded rhyolite tuff, with highly variable thicknesses (maximum as much as 215 m [705 ft]).

### ***Younger Basalt***

The youngest volcanic rocks in the Yucca Mountain site area (not included in Table 1) are represented by thin basalt dikes that were intruded along some minor faults near the head of Solitario Canyon (Day et al., 1998a). The dikes consist of fine-grained olivine-bearing basalt, locally with scoria and altered glass, which were dated at 10 Ma (Crow et al., 1995). Basalt also forms scoria cones, thin lava flows, and flow breccias in Crater Flat to the west (Fig. 1), where they have been studied by Crowe et al. (1995) and Heizler et al. (1999).

### **Correlation of Lithostratigraphic, Hydrogeologic, and Thermal-Mechanical Units**

Three primary stratigraphic systems have been developed to investigate the distribution of lithostratigraphic, hydrogeologic, and thermal-mechanical units at Yucca Mountain. Common to all these systems are the properties of bulk-rock density, grain density, and porosity. Changes in these rock properties result in commensurate changes in many of the associated hydrogeologic and thermal-mechanical properties that define units whose boundaries coincide with a specific stratigraphic contact. (See Ciancia and Heiken (2006) for discussion of geotechnical properties of tuffs at Yucca Mountain.)

As shown in Table 1, lithostratigraphic units within the Tertiary volcanic rock sequence are grouped into five major hydrogeologic units — in descending order, unconsolidated surficial materials, Tiva Canyon welded unit, Paintbrush Tuff nonwelded unit, Topopah Spring welded unit, and Calico Hills nonwelded unit — that were defined principally on the basis of major variations in the degree of welding (Montazer and Wilson, 1984). Hydrogeologic properties of



these units were presented by Flint (1998) and will not be discussed here, except to make specific mention of the Paintbrush Tuff nonwelded hydrogeologic unit (PTn), which is of special interest to stratigraphic and hydrologic studies in the site area. The distribution and characteristics of this unit are discussed in detail by Moyer et al. (1996) and Buesch and Spengler (1999).

The PTn occupies the stratigraphic interval between the top of the vitric zone in the upper part of the crystal-rich member of the Topopah Spring Tuff upward to the base of the densely welded rocks of the vitric zone in the lower part of the crystal-poor member of the Tiva Canyon Tuff (Table 1; see Buesch et al., 1996a). Because of its high porosity (average about 47%; CRWMS M&O, 2000, Table 5-4), the PTn is considered to form a potential permeability boundary affecting the flow of ground water above the repository block (Flint, 1998).

Stratigraphic units with distinct thermal and mechanical properties within the volcanic rock sequence at Yucca Mountain were identified by Ortiz et al. (1985). As with the hydrogeologic units, the boundaries of thermal-mechanical units (Table 1) are based on changes in macroscopic features that define stratigraphic units and permit the preliminary correlation of laboratory measurements with specific lithostratigraphic units (Buesch et al., 1996a). Analytical data indicate that most thermal-mechanical unit boundaries roughly correspond to (1) lithostratigraphic contacts that mark the transition from vitric, moderately welded rocks to densely welded subzones; or (2) the contact between the vitric, moderately welded rocks and devitrified rocks. Additional criteria are based on the percentage of lithophysae.

## **QUATERNARY GEOLOGY**

## Introduction

Surficial geologic mapping and chronostratigraphic studies of surface and near-surface deposits, soils, and geomorphic surfaces in the Yucca Mountain site area have resulted in the recognition and differentiation of several principal surficial units, which are composed mostly of alluvium and colluvium with minor amounts of eolian and debris-flow sediments that mantle hillslopes and cover the floors of valleys and washes. Figure 12 shows the general distribution of Quaternary deposits in the site area, based on the 1:50,000-scale regional compilation by Potter et al. (2002a). The small scale of the map (Fig. 12) necessitated the combining of various units and also did not permit the plotting of units that had only limited extent in some areas.

Early studies of Quaternary stratigraphy in the vicinity of Yucca Mountain, particularly those in the area of the Nevada Test Site to the east, by Hoover and Morrison (1980), Hoover et al. (1981), Swadley et al. (1984), and Hoover (1989), resulted in the general recognition of three major units ranging in age from Pliocene (?) and early Pleistocene to late Pleistocene and Holocene. Swadley et al. (1984) mapped these units in Midway Valley (Fig. 2), but no detailed mapping that further subdivided the surficial sequence was published in that area until Taylor (1986) distinguished six different units in the fluvial-terrace and alluvial-fan deposits along Yucca and Fortymile Washes, as well as in a small area in the northernmost part of Midway Valley, with a strong emphasis on variations in surface characteristics and soil development.

In more recent studies, the Quaternary stratigraphic sequence in the Yucca Mountain site area has been separated into eight individual units (designated, in ascending order, as QT0, Qa1-Qa7; Table 2), based principally on the mapping of alluvial deposits and overlying geomorphic surfaces and on the logging of some 30 soil pits by Wesling et al. (1992) and Swan et al. (2001)

in Midway Valley. The principal criteria used for subdivision include (1) relative stratigraphic and geomorphic position, (2) lithologic characteristics, (3) soil-profile development, (4) degree of desert pavement development, (5) amount and degree of desert varnish accumulation, and (6) degree of preservation of original bar-and-swale topography.

Sedimentologic properties of the various alluvial units are similar. In general, fluvial deposits are predominantly sandy gravel with interbedded gravelly sand and sand; facies include relatively coarse-grained channel bars and intervening finer grained swales. Gravel size ranges from pebble to boulder, and clasts generally are subangular to subrounded. In addition to the predominantly volcanic-rock detritus forming the deposits, there are varying amounts of pedogenic calcite and opal. A summary of diagnostic surface and soil characteristics for the various surficial units is presented in Table 2.

The relative ages of the deposits, soils, and geomorphic surfaces around Yucca Mountain are well established. Numerical age control, however, is limited, but the dating of several samples collected from mapped units Qa2 through Qa5 at various localities in Midway Valley and Fortymile Wash supports their assigned relative stratigraphic positions. A statistical analysis by S. K. Pezzopane (U.S. Geological Survey, written communication, 2001) of the results obtained from (1) U-series disequilibrium dating of silica- and carbonate-rich materials in soils, and (2) thermoluminescence dating of the silt-size fractions in fluvial and eolian deposits, indicate the following ages: unit Qa2, middle Pleistocene; Qa3, middle (?) to late Pleistocene; Qa4, late Pleistocene; and Qa5, latest Pleistocene to early Holocene (see Whitney et al., 2004c). Age ranges are graphically portrayed in Figure 13. The shaded areas are interpreted to represent the main periods of deposition and soil development, or both; for unit Qa3, there appears to have been two distinct depositional cycles. Dates extending beyond the shaded areas could be caused

by miscorrelation of the sampled deposits, or they could, in fact, represent valid extensions of the age boundaries, thus indicating that it may not be possible to establish absolute temporal boundaries between successive units.

With regard to unit Qa1, there is evidence from eolian deposits at Busted Butte (Figs. 2 and 12; see Menges et al., 2004) that it is associated with a period of deposition as old as the Bishop Ash (Izett et al., 1988), which is dated at 760 ka (Sarna-Wojcicki et al., 1993) and therefore considered to be of early to middle Pleistocene in age. Accordingly, the age of unit QT0 is assumed to be greater than 760 ka, possibly as old as Pliocene. Unit Qa6, assumed to be younger than unit Qa5, is assigned a middle to late Holocene age, and unit Qa7 is the deposit presently accumulating along the modern stream courses.

### **General Distribution and Characteristics of Surficial Deposits**

Unit QT0 consists of a single terrace remnant at the north end of Alice Ridge (Fig. 2), forming a prominent bench 46 m above the modern channel of Yucca Wash. Thickness of the unit appears to be only a few meters, and an early Quaternary to possibly Pliocene age is evident from its highly dissected and eroded nature and its rounded landform morphology. No soil data were collected from the QT0 surface.

Unit Qa1 is preserved at the surface on the Yucca Wash alluvial fan; the fan surface has been dissected by younger drainages and is preserved as slightly rounded interfluves. The unit also is present on the west flank of Yucca Mountain and in northeastern Crater Flat. Locally, the desert pavement associated with the Qa1 surface is well developed, but in most areas it has been

extensively degraded. No original bar-and-swale morphology is preserved on the surface.

Strongly developed soils are 1.5 to 2.0 m (5 to 6.6 ft) thick.

Unit Qa2 is recognized primarily as thin elongated patches of alluvium in northern Midway Valley, where it is inset in unit Qa1 (Wesling et al., 1992). The unit has a well-developed desert pavement that contains darkly varnished clasts (Table 2). The original bar-and-swale morphology has been reduced to the height of the larger clasts on the surface. Where exposed in soil pits, thicknesses range from 2.5 (8 ft) to more than 3.5 m (11.5 ft). Soils are strongly developed, with Av and Bkq horizons formed in eolian sediments capping the deposit.

Unit Qa3 is present as large remnant alluvial-fan surfaces and as fluvial terraces. It is one of the dominant Quaternary map units in the Yucca Mountain site area, and underlies the main Fortymile Wash terrace (Fig. 14). A well-developed desert pavement containing darkly varnished clasts characterizes the Qa3 surface (Table 2). The original bar-and-swale morphology has been reduced to the height of individual clasts (some exceeding 30-cm diameter) above the surface. Thickness of the unit averages about 2 to 2.5 m (6.5 to 8.2 ft) and locally exceeds 3.3 m (10.8 ft) in soil pits and along the Fortymile Wash terraces. Clay films and a strong blocky structure are characteristic of the argillic soil horizons that also commonly have accumulations of secondary silica and carbonate.

Unit Qa4 consists of small, inset fluvial terrace and alluvial fan remnants on the east side of Yucca Mountain. The desert pavement on the surface ranges from loosely to tightly interlocking and is noticeably less well developed than pavements formed on the older fluvial surfaces. Bar-and-swale relief mostly has been reduced to clast height above the surface. Thickness of the unit averages about 1 m (3.3 ft) and does not exceed 2 m (6.5 ft) where observed in soil pits. The

strongly developed Qa4 soil is characterized by a reddened argillic horizon and accumulations of carbonate and silica.

Unit Qa5 covers parts of alluvial fans and forms inset terraces along drainages. The desert pavement is loosely packed and poorly formed, and surface clasts have minor accumulations of rock varnish. Qa5 surfaces display well-developed bar-and-swale morphology, the amount of relief being related to landscape position and sediment sources; coarsest grained bars are in the proximal fan regions. Smaller, lower, partly buried bars lie on distal fans, where the intervening swales are partly filled by fine-grained eolian silts and sands. In soil-pit and trench exposures, the average thickness of Qa5 is approximately 1 m (3.3 ft), and the maximum observed thickness is about 2.5 m (8.2 ft). Soils are weakly developed, being strongest in swales and weakest on bars.

Unit Qa6 is present along the active washes as low floodplains less than 1 m (3.3 ft) above the active channels and as vegetated bars. No desert pavement has developed, and surface clasts are unvarnished and unweathered. Relief on the Qa6 surface is primarily the result of preservation of original bar-and-swale morphology. Natural outcrops and manmade exposures indicate that the total thickness of the unit does not exceed 2 m (6.5 ft). Soil development is limited to minimal oxidation of the deposit and sparse accumulation of carbonate, which is more concentrated toward the upper 10 cm (4 in) of the deposit, although the matrix typically contains widely disseminated carbonate.

Unit Qa7 consists of deposits along active channels and adjacent floodplains. No desert pavement has formed on the surface, and no desert varnish occurs on clasts except that which may be on clasts reworked from older surfaces. Clasts are unweathered, and the original depositional bar-and-swale relief is unaltered. The total exposed thickness of Qa7 does not

exceed 2 m (6.5 ft). No in situ pedogenic alterations were observed, but the matrix contains reworked, disseminated carbonate.

Colluvial and debris-flow deposits are undifferentiated as surficial map units because of their limited areal extent and the limited exposure of all but the youngest deposits. Such deposits generally consist of gravelly silty sands and silty fine- to medium-gravel with pebble to small cobble clasts. They are poorly sorted and nonbedded to crudely bedded. Thicknesses are generally less than 2 to 3 m (6.5 to 10 ft) as observed in trench and soil-pit exposures. Most of the colluvial deposits on hillslopes exhibit surface characteristics of units Qa5 and Qa6 (latest Pleistocene to late Holocene), but the deposits having surface characteristics similar to unit Qa4 surfaces (late Pleistocene) commonly are near the toe of the hillslope.

Two types of eolian sediment were observed in the Yucca Mountain site area: (1) reworked eolian deposits within sand ramps surrounding Busted Butte and along the southeastern margin of Midway Valley (Figs. 2 and 12), and (2) thin accumulations of silt and fine sand in the A and B horizons of most surface soils and relict accumulations within some buried soils. Sand ramps at Busted Butte and in southeastern Midway Valley are composed of a stacked sequence of eolian-colluvial units that have textures of pebbly, silty, fine- to medium-grained sand interbedded with sandy pebble to cobble gravel. Gravel clasts are angular to subangular and commonly less than 5 cm (2 in) in diameter, but some clasts are as large as 50 cm (20 in) in diameter. Maximum thickness of the sand-ramp deposits exceeds 15 m (49 ft). A weakly to moderately interlocking desert pavement covers most of the surfaces. Typically, one or more buried soils are within the deposits.

The presence of Bishop Ash (Izett et al., 1988) in lower sand-ramp deposits at Busted Butte (Whitney et al., 1985; Menges et al., 1994, 2004) and at other localities near Yucca Mountain

(Hoover, 1989) indicates that those landforms began forming within the region prior to about 760 ka (age of Bishop Ash). At Busted Butte, some of the buried soils have been dated as middle to late Pleistocene (Menges et al., 1994, 2004). Multiple buried soils above the Bishop tephra indicate that accumulation of the sand ramps is episodic and punctuated by periods of surface stabilization and soil formation. Numerical ages of  $73\pm 9$  ka and  $38\pm 6$  ka from two successive units in the upper 3 m of the deposits in a trench in southern Midway Valley possibly indicate the ages of two of the more recent depositional episodes, and another date of  $6\pm 1$  ka from a sample of the A soil horizon is indicative of continuing accumulation of eolian sediments during the Holocene (Menges et al., 2004).

A few to several tens of centimeters of eolian silt and fine sand have accumulated on most alluvial geomorphic surfaces in the Yucca Mountain site area and have been incorporated into soil profiles formed on those surfaces. These eolian accumulations are not mapped separately because of their relatively thin nature. Models of desert pavement and soil formation show the importance of eolian accumulations as a source for the fine earth fraction, carbonate, and soluble salts that occur in otherwise clean sandy gravel deposits in arid regions (Birkeland, 1984; McFadden et al., 1987; McFadden and Weldon, 1987; McDonald and McFadden, 1994).

Pedogenic carbonate with subordinate opaline silica (calcrete) is present as slope-parallel deposits and as remobilized fracture fillings. The deposits generally are poorly indurated and fine grained. Ooids and pellets are locally abundant, and preserved fossils are of roots (Stuckless et al., 1998) rather than aquatic animals.

### **Trenching Activities**



Information on the stratigraphic relations among surficial deposits was augmented considerably by the large-scale mapping and detailed descriptions of vertical sequences that were freshly exposed in trenches excavated across those faults suspected of being active during Quaternary time. Within the site area, some 50 trenches were emplaced across such faults (Whitney et al., 2004b) primarily for the purpose of determining the extent of Quaternary tectonic activity with respect to (1) the number, amount of displacement, and age of individual surface-rupturing events causing earthquakes; (2) fault slip rates; and (3) recurrence intervals between successive events on a given fault. Results of the detailed Quaternary fault studies are given in Keefer et al. (2004) and brief summaries are presented in the Structural Geology section.

### **Erosion, Deposition, and Flooding**

Studies of past and modern geomorphic processes at Yucca Mountain primarily were designed to estimate the long-term average rates of erosion on the ridge crests and hillslopes of the mountain, thereby to determine the potential for erosional breaching of the proposed underground facility for the storage of high-level radioactive wastes. Flow characteristics within Fortymile Wash are of particular importance because of the concern over whether potential dissolution products from the stored wastes could be entrained by flow within the lower reaches of this drainage system and subsequently become incorporated within the flow of the Amargosa River southwest of Yucca Mountain (Fig. 1).

### ***Landscape Response to Modern Climatic Conditions***

In the dry, semiarid climatic regime of the Yucca Mountain area, precipitation and runoff that produces streamflow in Fortymile Wash generally occurs only during infrequent but intense local thunderstorms that produce flash floods and cause extensive hillslope erosion and rapid deposition of coarse debris on alluvial fans and in stream channels. One such event occurred on July 21-22, 1984, when rainfall of about 85 mm (3.35 in) caused a series of debris flows on the south slope of Jake Ridge (Fig. 15), in the northeastern part of the site area (Fig. 2). Coe et al. (1997) reported that (1) 7,040 m<sup>3</sup> of debris were stripped from the hillslope and redistributed over an area of 49,132 m<sup>2</sup>, which included a tributary of Fortymile Wash and a part of the wash itself; and (2) maximum depth of hillslope erosion was 1.8 m. The runoff in Fortymile Wash infiltrates the stream channel at high rates downstream past Yucca Mountain to distal reaches of its alluvial fan (Osterkamp et al., 1994). As a consequence of progressive downstream channel losses and flow attenuation within the wash, channel capacity decreases along the approximately 24-km-stretch that extends south and southwest from its northern reaches to the northeast edge of Amargosa Valley (Fig. 1). Along this section of Fortymile Wash, large-scale sediment deposition has transformed the entrenched channel into a broadly braided alluvial fan.

Eolian processes of sand movement and dust deposition are presently active around Yucca Mountain. Modern dust deposition in southern Nevada ranges from 4.3 to 5.7 grams/m<sup>2</sup>/year (Reheis and Kihl, 1995). Annual dust flux increases with mean annual temperature but appears to more closely reflect changes in annual precipitation (relative drought conditions) rather than temperature. Playa and alluvial sources produce about the same amount of dust per unit area; however, the total volume of dust produced is much larger from alluvial sources. The mineralogic and major oxide composition of dust samples indicates that sand and some silt is locally derived and deposited, whereas clay and some silt can be derived from distant sources.

Modern and Holocene dust has been accumulating below desert pavements and on hillslopes in the site area.

### ***Landscape Response to Climate Change***

In contrast to the present warm and dry semiarid conditions, cooler and wetter conditions existed at times in the Yucca Mountain region during the Quaternary (Forester et al., 1999). The climatic changes followed a cycle consisting of four general phases — interpluvial (present conditions), interpluvial to pluvial transition, pluvial, and pluvial to interpluvial transition. Primary characteristics for each of these phases are briefly summarized below to indicate changes in geomorphic processes that may occur in response to changing climatic conditions in future years at Yucca Mountain.

1. Interpluvial phase. Under warm and dry conditions, there is low vegetation density and little or no grassland. Infrequent hillslope stripping results in local aggradation and fan building. Main valleys aggrade slowly or remain essentially stable. Fine-grained eolian material accumulates on geomorphic surfaces and hillslopes. Sporadic large sediment yield from hillslopes continues until most colluvium is removed, and hillslopes begin to stabilize.
2. Interpluvial to pluvial transition phase. As temperature cools and precipitation increases during each season, there is greater vegetation density, hillslopes stabilize, and hillslope-sediment yield decreases. Hillslope deposition is renewed as the removal of colluvium is retarded by vegetation, and there is increased trapping of eolian and other sediments on the hillslopes. The increased retention of surficial materials on

hillslopes, combined with greater precipitation, causes a change from aggradation to incision in sections of trunk streams that are above stable base levels.

3. Pluvial phase. Under wetter and cooler conditions, landscape stability is reached through physical weathering of the bedrock, a covering of bouldery colluvium forms on the hillslopes, and there is denser vegetation growth that inhibits erosion.
4. Pluvial to interpluvial transition phase. During the transition to warmer, drier conditions, vegetation becomes less dense, hillslopes destabilize, and sediment yield increases primarily through debris-flow transport of the previously weathered material to the valley floors. Debris-flow stripping occurs during infrequent high-intensity storms, resulting in alluvial-fan building and valley aggradation. Eolian activity may increase.

### ***Flooding History***

Glancy (1994) discussed geologic evidence for prehistoric flooding in Coyote Wash, a branch of Drill Hole Wash located between Dead Yucca Ridge and Live Yucca Ridge on the east side of Yucca Mountain (Fig. 2). Trenches excavated across and along the modern-day wash channel, which splits headward into two forks, exposed sediments indicative of multiple flood events, including debris flows. Glancy (1994) concluded that moderately indurated sediments overlying the bedrock and underlying the stream terraces adjacent to the channel probably were deposited during the late Pleistocene or early Holocene (older than 10 ka), and that nonindurated sediments overlying the older sediments were probably of Holocene age (less than 10 ka). Using surficial boulders near the trenches, Glancy (1994) estimated the magnitude of the flood that deposited them during the Holocene. Assuming the flood was water-dominated (Newtonian

fluid) and that all of the boulders were emplaced by the same flood, a peak discharge of 2,400 ft<sup>3</sup>/s was estimated to have occurred in the north fork of Coyote Wash. The combined flows of the north and south forks could result in a peak flow as large as 5,000 ft<sup>3</sup>/s. [Note: Stream-flow and flow-velocity measurements typically are recorded in English units rather than metric units.]

A flood that occurred on February 24, 1969, is believed to have been, overall, the most severe flood in the Amargosa River drainage basin during recent times. The peak flow on that date in Fortymile Wash, at a point just downstream from the Yucca Mountain road crossing (located 3.4 km north and 1.3 km west of the southeast corner of the site area), was estimated by Squires and Young (1984) at about 20,000 ft<sup>3</sup>/s on the basis of channel geometry and residual evidence discovered during a flood-prediction study. This estimate was independently supported by a witness who described the flow as “wall-to-wall” water, about 4 ft deep, across the 800- to 900-ft-wide flood plain at the bottom of the incised channel. At an average depth of 4 ft, the cross-sectional flow area would be on the order of 3,200 to 3,600 ft<sup>2</sup>. Assuming a peak flow of 20,000 ft<sup>3</sup>/s, the resultant average velocity would have been about 5.5 to 6.25 ft/s, depending on cross-sectional area. For comparison, average runoff velocities recorded at a gaging station located near borehole UE-25 J-13 (Fig. 8), 0.8 km south of the Yucca Mountain road crossing, during March 1995 (peak flow of 3,000 ft<sup>3</sup>/s; see CRWMS M&O, 2000, Table 7.1-1) and February 1998 (peak flow of 200 ft<sup>3</sup>/s) were 7 to 8 ft/s and 3 ft/s, respectively.

Fortymile Wash flowed on March 3, 1983, as a result of a regional rainstorm that may have melted some snowpack at the higher basin altitudes (Pabst et al., 1993); the flow peaked at 570 ft<sup>3</sup>/s, as recorded by the gaging station near borehole UE-25 J-13 (Fig. 8). Fortymile Wash also flowed three times in the summer of 1984 in response to convective rainstorms during a prolonged and unusually intensive monsoon-storm season. Magnitudes of the three flows

(July 21-22, July 22, and August 19, 1984) at the recording station near borehole UE-25 J-13 were 1,860, ~ 150, and ~ 850 ft<sup>3</sup>/s, respectively (Pabst et al., 1993).

Fortymile Wash did not flow again within the site area for almost 11 years following the 1984 summer storms. It next flowed for 10 to 12 hours on March 11, 1995, in upper-basin reaches as the result of a regional rainstorm and probably was amplified by rainfall-induced snowmelt from highlands north of Yucca Mountain (Beck and Glancy, 1995); peak flow of 3,000 ft<sup>3</sup>/s was recorded at the gaging station near borehole UE-25 J-13. Stretches of the Amargosa River also flowed for 10 to 12 hours on the same day, marking this runoff event as the first documented storm wherein Fortymile Wash and the Amargosa River flowed simultaneously throughout their main-stem-channel reaches into Death Valley. A similarly caused runoff with a peak flow of 200 ft<sup>3</sup>/s in Fortymile Wash occurred on February 22-23, 1998 (Tanko and Glancy, 2001), at which time there was also flow in the Amargosa River into Death Valley. In summary, Fortymile Wash flowed six times during the 15 years from March 1983 through February 1998, and streamflow data indicated that most of the flows probably continued downstream to Death Valley.

### ***Bedrock Erosion Rates during the Quaternary***

A cosmogenic dating technique, primarily involving measurement of the concentrations on bedrock surfaces of <sup>10</sup>Be, was used to calculate the maximum erosion rate of exposures on ridge crests in the Yucca Mountain site area (see Faure, 1986). The dating method assumes that erosion had proceeded at a gradual and constant rate.

Quartz separates from seven samples of tuffaceous rocks of the Tiva Canyon Tuff exposed on Antler Ridge and an adjacent ridge to the south (Fig. 2) were analyzed for <sup>10</sup>Be (Table 3),

resulting in a calculated maximum possible erosion rate for these bedrock outcrops of 0.04 to 0.27 cm/k.y. This rate (1) integrates all erosion occurring on the summit of Yucca Mountain under all climatic conditions that have existed in the area during most (if not all) of the Quaternary; (2) indicates a remarkable erosional stability for this landscape; and (3) compares well with the long-term average erosion rate in hillslope colluvium on the middle to lower hillslopes at Yucca Mountain (U.S. Department of Energy, 1993). The average erosion rate for the seven bedrock analyses on Yucca Mountain is equal to 1.38 m/m.y., which is almost as low as rock erosion rates of <1m/m.y. measured in Australia (Bierman and Caffee, 2002) and is at the low end of erosion rates of 1.4-20 m/m.y. measured on granite landforms in the Alabama Hills in California (Nichols et al., 2006).

#### ***Hillslope Erosion Rates from Dated Colluvial Boulder Deposits***

The surface-exposure ages of relict boulder deposits on Yucca Mountain and nearby hillslopes were dated (see below) to calculate the long-term rate of removal of unconsolidated material on the middle and lower hillslopes of Yucca Mountain. In addition, the depth of erosion in 50-m-wide zones on both sides of a deposit, including channel incision, was measured (Whitney and Harrington, 1993). The paleotopographic hillslope surface at each locality was assumed to be represented by the top of the boulder deposit on that hillslope. Because (1) the present relief across the middle hillslopes is low (maximum 2 m), and (2) stripping of hillslopes by debris flows is the dominant process presently moving material down these hillslopes, the modern relief on these hillslopes probably represents a maximum for much of the late Quaternary.

Boulder deposits, with boulders 0.3 to 2 m in diameter, range from wide continuous mantles to isolated narrow bands bounded by gullies. Eleven such deposits were sampled (Whitney and Harrington, 1993) for cation-ratio dating (Table 4) — six on the flanks of Yucca Mountain, three on the southwest hillslope of Skull Mountain (20 km to the east), one on the northeast slope of Little Skull Mountain (10 km to the southeast, Fig. 3), and one on the east slope of Buckboard Mesa (25 km north-northeast of Yucca Wash). The erosion rate was calculated based on the amount of erosion on the hillslope since the boulder deposit formed, divided by the surface-exposure age of the deposit. Both the rock-varnish cation ratio and the in-situ  $^{36}\text{Cl}$  cosmogenic-nuclide dating methods (Harrington and Whitney, 1987; Whitney and Harrington, 1993; Gosse et al., 1996) were applied (see CRWMS M&O, 2000, section 7.4.2.2, for a detailed discussion on rock-varnish and cosmogenic dating of these deposits). The estimated varnish cation-ratio ages of the analyzed samples range from 100 ka (80 to 140 ka) to 1,020 ka (730 to 1,430 ka), as shown in Table 4, and ages of several of the sampled deposits by cosmogenic dating are given in Table 5. The long-term erosion rates of stripping of unconsolidated material from Yucca Mountain hillslopes were calculated to be less than 0.5 cm/k.y. (average about 0.2 cm/k.y., based on a range of 0.02 to 0.6 cm/k.y.; Whitney and Harrington, 1993).

### ***Hillslope Erosion during the Latest Pleistocene-Holocene Interval***

The climatic cycles recorded within the valley alluvium in Fortymile Wash and Midway Valley indicate a general landscape stability, punctuated by short pulses of either hillslope stripping or valley incision. The presence of relict boulder deposits that cover parts of most



hillsides provides evidence that hillslope stripping was incomplete even through several climate cycles.

The time interval during which alluvial unit Qa5 (latest Pleistocene-Holocene, about 18 to 2 ka; see Fig. 13) was deposited in Midway Valley and Fortymile Wash can be used to derive semiquantitative boundary values for the amount of erosion then occurring on Yucca Mountain hillslopes. This 16-k.y. period encompasses the last pluvial to interpluvial transition, a time of climatic transition to semiarid conditions favorable for erosional stripping of hillslope sediment. The estimated mean depth of unconsolidated material removed from these hillslopes to form alluvial unit Qa5 in Midway Valley (Forester et al., 1999) is 27 cm. If this mean depth is assumed to have been eroded during these 16 k.y., a rate of 1.7 cm/k.y. for erosion of unconsolidated hillslope material is indicated, although it should be noted that this rate does not incorporate either the eolian-sediment addition to the hillslopes or the sediment that moved through Midway Valley and into Fortymile Wash. Based on an analysis of alluvial deposits in Fortymile Wash, Forester et al. (1999) estimated the depth of erosion of bedrock during the last 15 k.y. to be about 18 cm, which indicates a rate of 1.2 cm/k.y. These relatively short-term erosional rates are larger than the long-term (middle and late Quaternary) rates calculated for Yucca Mountain hillslopes (0.2 cm/k.y.) and bedrock ridges (0.04 to 0.27 cm/k.y.) (see above).

In the 10 k.y. prior to the deposition of unit Qa5, the climate was wetter, hillslopes were more densely vegetated, and little material was being removed from the surrounding hillslopes. The erosion rate for the complete climatic cycle from 28 to 2 ka for the Yucca Mountain hillslopes therefore was 1.04 cm/k.y. for unconsolidated material and 0.7 cm/k.y. for hillslope bedrock.

### ***Erosional History of Fortymile Wash***

Fortymile Wash, the principal tributary of the Amargosa River lying within the site area (Fig. 2), flows through the 25-km-long Fortymile Canyon, and continues southward for about another 20 km along the east side of Yucca Mountain before entering the eastern part of the Amargosa Valley (inset map, Fig. 1). Between the mouth of the canyon and the Amargosa Desert, the stream channel is entrenched as much as 25 m in alluvial fill. The depth of incision decreases over a 6-km stretch, where the channel becomes the head of a long fan that crosses the Amargosa Valley. Analysis of the Fortymile Canyon sedimentary provenance and altitude distribution of volcanic rocks (Lundstrom and Warren, 1994) indicates that the canyon was formed during the late Miocene or Pliocene, sometime before 3 Ma. A relict gravel deposit exposed in Fortymile Wash contains a different lithology than the Quaternary gravel fills, probably indicating that the present drainage captured a formerly northward-flowing drainage along the moat of the Timber Mountain caldera, north of the site area, sometime between 9 and 3 Ma.

Surficial deposits within and flanking Fortymile Wash record a complex history of aggradation and channel incision, as shown diagrammatically in two cross sections: (1) the northern one (Fig. 14A) located at a point between Alice Ridge west of the wash (Fig. 2) and the western toe of what is termed the Calico Fan across the wash to the east at the east edge of the site area; and (2) the southern one (Fig. 14B) located near the Yucca Mountain road crossing, which is 4 km north and 1.3 km west of the southeast corner of the site area (locations of sections shown in Fig. 8). Multiple episodes of downcutting are evident from a comparison of the different stratigraphic sequences on the east and west walls of the wash, as shown on the two cross sections. At the Yucca Mountain road crossing (Fig. 14B), there are four gravelly alluvial

units on the west wall, each capped by a soil representative of pluvial conditions when vegetation was dense and the stream channel was not being aggraded. The buried soils on the west wall are missing from the east wall, indicating that the alluvial fill on the east side of the wash wall is older than the 50- to 100-ka soils at the top of the fill, but younger than the 300- to 500-ka buried soil exposed in the west wall. Farther north, at the Calico fan site, the 170-ka buried soil on the west side is missing on the east wall (Fig. 14; note: these older ages are based on U-series analyses). Exposed in gullies in the east wall are upper Tertiary gravels and middle Pleistocene eolian deposits that are overlain by unit Qa3 alluvium, providing evidence of at least two episodes of downcutting that predate unit Qa3. If the 170-ka age on the buried soil in the west wall is valid, then a major incision and erosion of the older alluvium took place during the climatic time of oxygen isotope stage (OIS) 6 of the global climate record (derived from marine cores; see Imbrie et al., 1984), the wettest climatic episode at the end of the middle Pleistocene.

The alluvium of unit Qa3 (Fig. 14) that underlies the main Fortymile Wash stream terrace was subsequently deposited during the interglacial OIS 5e-5a, and it has developed a soil that is primarily of OIS 4 age.

The most recent incision of Fortymile Wash (Lundstrom et al., 1996) probably took place during the latter part of the pluvial episode, OIS 4 (about 116 to 60 ka; Winograd et al., 1988), from about 116 to 60 ka, and the early part of OIS 3 (about 55 to 40 ka). Within 2 m of the present channel of Fortymile Wash are remnants of a strath terrace with a thin alluvial deposit mapped as unit Qa4 at the Yucca Mountain road crossing (Fig. 14B). This terrace likely represents a pause in the downcutting of Fortymile Wash during the relatively short interglacial climate represented by OIS 3. The last 2 to 4 m of incision probably occurred during the last pluvial climate at Yucca Mountain, 22 to 18 ka. Aggradation has taken place in the channel and

on the lower Fortymile Wash alluvial fan, represented by unit Qa5 deposits, during the Pleistocene-Holocene transition and continuing through the Holocene to the present.

Based solely on thermoluminescence-dating of silt in sand-dominated horizons in soils capping the alluvial units in the west wall of Fortymile Wash and the belief that the oldest dated deposit is less than 150 ka, Lundstrom et al. (1998) advanced the interpretation that 13 m of aggradation occurred in the wash from 140 to 50 ka, followed by about 20 m of incision between 36 and 24 ka. This interpretation, however, does not account for the presence of buried soils in the west wall that are not present on the east wall (Fig. 14B), which is an important stratigraphic relation that indicates a much longer period (perhaps as much as 500 k.y.) of sediment accumulation along the wash.

In summary, a comprehensive interpretation of Fortymile Wash using all buried soils and the U-series dates obtained from the central wash reveals a complex history of four to five cut-and-fill cycles spanning the middle to late Quaternary. The incision in the wash occurred over a limited vertical range in elevation of not more than several tens of meters. Furthermore, the wash did not cut and fill the same channel each time, but instead migrated laterally across the Fortymile Wash fan. Thus, the channel during the middle and late Quaternary was incised during pluvial periods; then, during the transition to interpluvial climates, when hillslopes were most actively stripped, the wash aggraded and migrated laterally prior to the next cutting cycle.

### ***Potential for Future Erosion and Deposition***

Most streams draining the east slope of Yucca Mountain cross Midway Valley and flow into Fortymile Wash (Fig. 3). Although the true base level for these tributary valleys is Fortymile Wash, the effective base level is the floor of Midway Valley that is presently

undergoing aggradation because of the existing interpluvial, warm and dry climate. Since at least the beginning of the Holocene, local storms have activated debris-flow stripping of the hillslopes around Midway Valley (e.g., see Fig. 15) resulting in a rising base level as sediments accumulated on the valley floor. If a period of incision were to ensue as a result of a change in climate to one of greater effective moisture, the main drainage courses in Midway Valley would ultimately start to incise the valley floor, then erode headward causing downcutting in the tributary valleys and removal of channel-fill deposits. If wetter climatic conditions continued for a long enough period of time, all of the alluvium in these valleys would be moved to the floor of the valley.

An exposure of the fill in Coyote Wash demonstrates that such a complete emptying of the alluvium in the tributary valleys did not occur during the last glacial cycle (Glancy, 1994). Relict Pleistocene fill documents the incomplete stripping of the valley alluvium during the last two climatic cycles. The climate change to a regime favoring sediment removal that began approximately 28 ka did not last long enough to allow complete sediment removal from these tributary valleys. Since approximately 15 to 18 ka, when the climate began to become drier, these valleys have been aggraded. The incomplete removal of hillslope and valley alluvium in the tributary valleys during the 10,000–13,000 “wet” years of the last climate cycle indicates that more than 10 k.y. is needed to remove alluvium from these valleys, assuming that the climate for that time interval was favorable for erosion. Based on Coyote Wash data, it would require substantially more than 10 k.y. to effectively remove the alluvium and to begin actively eroding the bedrock floors of the washes. Because evidence shows that aggradation and degradation cycles respond to regional climatic changes, there is no indication, based on an analysis of future climates in the Yucca Mountain region (see Sharpe, this volume), that another period of

downcutting of more than a few meters will occur in Fortymile Wash and its tributaries within the next 10 k.y.

Another important factor to consider, relative to future incision of Fortymile Wash and its tributaries, is that the effective base level for Fortymile Wash is the broad expanse of the surface of Amargosa Valley alluvium. No substantial incision within the present valley of Fortymile Wash is possible unless a major incision, or deep headcut, occurs far downstream in the present Amargosa Valley, migrates some 95 km (60 mi) or more upstream through the present fill of Amargosa Valley, and continues headward through the present alluvial fan of Fortymile Wash. Headcutting across the Amargosa Valley over the next 10 k.y. is unlikely, not only because of the long distance involved, but also because no evidence of earlier Quaternary valley incision has been observed along the Amargosa River.

## **STRUCTURAL GEOLOGY**

### **Introduction**

The structural geology of Yucca Mountain and vicinity is dominated by a series of north-striking normal faults along which Tertiary volcanic rocks were tilted eastward and displaced hundreds of meters (predominantly down-to-the-west), primarily during a period of extensional deformation in middle to late Miocene time. These through-going faults divided the site area into several structural blocks, each of which is further deformed by minor intrablock faults (Figs. 16 and 17). The complex pattern of faulting is shown in detail on two bedrock geologic maps based on extensive field investigations conducted largely in 1996 and 1997 as an integral part of

the Yucca Mountain site characterization program (U.S. Department of Energy, 1988). The two maps are: (1) a 1:24,000-scale map by Day et al. (1998a) covering the 165 km<sup>2</sup> (65 mi<sup>2</sup>) of the site area (Figs. 1 and 2), and (2) a 1:6,000-scale map by Day et al. (1998b) covering 41 km<sup>2</sup> (15.7 mi<sup>2</sup>) of the central part of the site area that includes the proposed repository block itself. At these scales, it was possible to map individually many of the stratigraphic subdivisions (zones, some subzones, and bedded tuff units) within various volcanic formations and to record faults generally with displacements as little as 5 m at the 1:24,000 scale and as little as 1.5 m at the 1:6,000 scale. The site-area map by Day et al. (1998a) incorporated the work of Dickerson and Drake (1998; map scale 1:6,000) in the northeastern part of the site area. Detailed results of the 1996-1997 geologic mapping program are discussed by Potter et al. (2004).

The studies by Day et al. (1998a, 1998b) benefited substantially from earlier mapping and structural interpretations of areas within and around the site area by Christiansen and Lipman (1965), Lipman and McKay (1965), and Scott and Bonk (1984). The latter map, at a scale of 1:12,000 and considered to be largely reconnaissance in nature, was particularly useful in that numerous zones within the Tiva Canyon and Topopah Spring Tuffs were defined and mapped, resulting in the delineation of minor faults not previously recognized. Regional map compilations by Frizzell and Shulters (1990) and Potter et al. (2002a) place the geology of Yucca Mountain in a regional setting.

In addition to the maps mentioned above, Simonds et al. (1995) compiled a 1:24,000-scale fault map that incorporated all of the then known information on Quaternary to recent fault activity in the Yucca Mountain site area, which served as a guide for the subsequent trenching and detailed studies of newly exposed surficial-deposit sequences to determine the extent, magnitude, and ages of Quaternary deformational events. Studies of the structural and

stratigraphic relations exposed in the trench excavations are described in a series of published reports (Keefer et al., 2004).

Detailed maps and descriptions of faults and fracture systems encountered in the ESF and Cross Drift (CD) locations shown in Fig. 16) have been presented in several reports, including Beason et al. (1996), Albin et al. (1997), and Mongano et al. (1999). Summary data from these reports are incorporated in discussions of the subsurface characteristics of selected features exposed in the ESF and Cross Drift.

### **Block-Bounding Faults**

Block-bounding faults are spaced 1 to 5 km apart and include, from east to west within the site area, the Paintbrush Canyon, Bow Ridge, Solitario Canyon, Fatigue Wash, and Windy Wash faults (Fig. 16). The Crater Flat faults lying west of the site area are also included in this discussion of block-bounding faults because they form the west boundary of the structural block that occupies the northwesternmost corner of the site area. Fault descriptions are summarized primarily from (1) bedrock geologic maps of Day et al. (1998a, 1998b) and Dickerson and Drake (1998); (2) a compilation of fault data by Simonds et al. (1995); (3) a regional geologic map compiled by Potter et al. (2002a); (4) detailed descriptions of structural features by Potter et al. (2004); and (5) a series of reports describing results of the mapping of trenches to determine the history of Quaternary deformation along the major faults in and adjacent to the site area (Keefer et al., 2004).

Displacements along block-bounding faults are mainly dip-slip (down-to-the-west), with subordinate strike-slip or oblique-slip components of movement exhibited by some faults.



Seismic reflection data have been interpreted to indicate that the faults penetrate and offset the Tertiary-Paleozoic contact beneath Yucca Mountain (Brocher et al., 1998). Strain is transferred between block-bounding faults along relay faults that intersect the block-bounding faults at oblique angles and provide an intrablock kinematic link between some of the bounding structures (Day et al., 1998a; Potter et al., 2004). Fault scarps visible along many fault traces dip from 50° to 80° to the west (Fig. 4).

### ***Paintbrush Canyon Fault***

The Paintbrush Canyon fault is the major block-bounding fault between Midway Valley to the west and a line of small ridges (Busted Butte, Fran and Alice Ridges) to the east (Figs. 2, 16, and 17). The fault is exposed for a distance of approximately 5 km in bedrock forming highlands north of Yucca Wash (Fig. 2), where it is shown by Dickerson and Drake (1998) as a west-dipping (56°–76°) normal fault. In that area, Paintbrush Group rhyolite lava flows are downdropped against rocks of the Topopah Spring and Pah Canyon Tuffs and the Calico Hills Formation, and the fault trace is marked by a discontinuous, west-dipping fault scarp 0.3 to 4.0 m in height.

The Paintbrush Canyon fault extends to the south beneath the alluvium of Midway Valley for some 5 km before strands are exposed for about 1 km in bedrock along the west side of Fran Ridge. A major splay trends southwest from a point toward the north end of Fran Ridge, circles around the west side of San Juan Hill and joins the main trace toward the south end of Fran Ridge (Fig. 2). From there northward the fault length is 11 km. However, it may continue southward for another 8 km to a possible intersection with the Stagecoach Road fault beyond the south edge of the site area (Fig. 16), in which case the total fault length may be as much as 19

km (Potter et al., 2002a). The Stagecoach Road fault forms that part of the east boundary of the Solitario Canyon-Bow Ridge structural block that lies south of the site area (Fig. 16).

Estimates of the amount of bedrock displacement on the Paintbrush Canyon fault range from 210 m in the northern segment (Dickerson and Drake, 1998) to as much as 500 m along other segments (Scott and Bonk, 1984; Potter et al., 2004). The fault also shows evidence of multiple surface-rupturing events during the Quaternary, causing offsets of 5.5 to 8.0 m in surficial deposits as measured in trenches and at natural exposures located near Alice Ridge, Busted Butte, and in the southern part of Midway Valley (Menges et al., 2004). At the Busted Butte locality a series of sand-ramp and colluvial deposits resting on Bishop Ash (dated at 760 ka) are offset (Fig. 18), providing a continuous record of fault movement since early middle Pleistocene time.

### ***Bow Ridge Fault***

The Bow Ridge fault is well exposed along a 200-m-long segment on the west side of Exile Hill (Fig. 2), where the Rainier Mesa Tuff is faulted down against the crystal-rich and crystal-poor members of the Tiva Canyon Tuff along a low fault-line bedrock escarpment (Day et al., 1998a). From there north, it extends beneath surficial deposits to the north side of Yucca Wash, a distance of about 4 km, and continues for another 1.5 km to the north edge of the site area, cutting bedrock composed mostly of rhyolite lavas and the Pah Canyon Tuff of the Paintbrush Group (Potter et al., 2002a). South of Exile Hill, the Bow Ridge fault is shown by Day et al. (1998a) to extend southward beneath surficial deposits for about 3.25 km to a point where it is exposed in bedrock (Tiva Canyon Tuff is displaced) for a short distance along the west side of Bow Ridge (Fig. 2). From there, the fault trace is projected to the southeast beneath alluvium for

another 2.5 km to a possible intersection with the Paintbrush Canyon fault (Fig. 16), making a total length of about 11.5 km.

Bedrock is displaced about 125 m down to the west along the Bow Ridge fault at the west side of Exile Hill (Scott and Bonk, 1984). The fault dips  $75^{\circ}$  to  $80^{\circ}$  W. (Simonds et al. 1995) and net displacement is left-oblique. It was intersected 200 m inside the North Ramp of the ESF, where it was observed to strike north-south and dip  $75^{\circ}$  W., and to downdrop the Pre-Rainier Mesa Tuff bedded tuff against units of the Tiva Canyon Tuff; down-to-the-west dip-slip stratigraphic separation is approximately 128 m along a 2.7-m-wide brecciated fault zone (Beason et al., 1996). A north-trending fault with down-to-the-east dip-slip offset of 7 m in a 5-m-wide fractured and brecciated zone was intersected some 235 m farther west in the ESF. This feature is believed to be antithetic to, and to terminate against, the Bow Ridge fault at depth and appears to correlate with a strand mapped at the surface in the hanging wall block (Figs. 16, 17; see Day et al., 1998a). Exposures in trenches that were excavated across projections of the Bow Ridge fault beneath surficial deposits at the Exile Hill locality, notably trench 14D described by Menges et al. (1997), reveal small-displacement Pleistocene faulting events with a total offset of 0.5 to 1.22 m (Menges et al., 2004).

### ***Solitario Canyon and Iron Ridge Faults***

The longest continuously exposed fault trace in the site area is associated with the Solitario Canyon fault, which forms the west boundary of the central part of Yucca Mountain that contains the proposed repository block. The segment within the site area is 15 km long (Fig. 2), and to the south it continues for at least another 3 km to where it is shown to have a possible connection with the Southern Windy Wash fault system (Fig. 16; Potter et al., 2002a). There are numerous

associated fault splays, particularly toward the south end (Day et al., 1998a; Scott and Bonk, 1984).

The Solitario Canyon fault is well expressed along the east side of Solitario Canyon where, for much of its length, it forms a prominent fault-line scarp as much as 5 m in height along the bedrock-alluvium contact at the base of a large topographic bedrock escarpment (Fig. 2). Bedrock faults split off the main fault trace near the mouth of Solitario Canyon, and one connects to the southeast with a prominent, west-facing, fault-line scarp as much as 15 m high at the base of a prominent bedrock escarpment. This splay, referred to as the Iron Ridge fault by Scott (1992), extends southeast and south for 8 km and appears to intersect the Stagecoach Road fault south of the site area (Fig. 16; Potter et al., 2002a).

Along the central segment of the Solitario Canyon fault, where two main strands were mapped by Day et al. (1998a; see Fig. 16), units of the Tiva Canyon Tuff in the hanging wall of the eastern strand were downfaulted against rocks of the Topopah Spring Tuff that form all but the upper slopes of the steep west flank of Yucca Mountain (Fig. 2). The down-to-the-west displacement is shown to be 450 m along a fault zone dipping about 65° W. by Day et al. (1998a, cross section B-B'); some left-oblique slip also is indicated by slickensides displayed locally on fault scarps. The western fault strand is covered by surficial deposits for most of its extent. Farther south the faulting involves units of the Topopah Spring, and the down-to-the-west displacement is less owing to the transfer of strain to fault splays. Along the northernmost 3-km-segment within the site area, the movement is reversed, with an east-side-down displacement of bedrock of only about 50 m; hence, the Solitario Canyon fault demonstrates a scissors geometry.

A cross drift extending southwestward from near the west end of the northern section of the ESF intersects the central section of the Solitario Canyon fault (see Fig. 16). Only the eastern

strand was reached in the boring, at which point the fault plane is defined by an 8- to 12-cm-thick zone of fault gouge separating rocks in the upper part of the crystal-poor member of the Topopah Spring Tuff in the hanging wall (west side) from rocks in the lower part of that member in the footwall; the down-to-the-west displacement is about 260 m (Mongano et al., 1999). The fault plane strikes N.18°W., and dips 62°W.; slickenside rakes average 40°. Wide zones (30 to 40 m) of brecciation and fracturing are in both the hanging wall and footwall blocks, being most intense in the latter.

The Iron Ridge fault is a major splay trending south-southeast off the main trace of the Solitario Canyon fault (Figs. 2, 16). It has an average dip of 68° W. where observed at the surface, with down-to-the-west offset. Along the northern trace of the Iron Ridge fault, rocks in the uppermost Tiva Canyon Tuff are downdropped against the middle part of the Topopah Spring Tuff, a down-to-the-west displacement of approximately 100 m. Farther south, the amount of displacement increases to about 300 m (Day et al., 1998b).

The Solitario Canyon fault was trenched at 11 locations along the fault trace, with most trenches being sited where the fault extends beneath surficial deposits. Mapping of several of the excavations recorded evidence of multiple middle to late Quaternary surface-rupturing events (Ramelli et al., 2004), with the total amount of displacement ranging from 1.7 to 2.5 m at various sites. One trench was excavated across the Iron Ridge fault, and at least one Quaternary faulting event occurred there with a possible displacement of about 2 m.

### ***Fatigue Wash Fault***

The Fatigue Wash fault (Fig. 2) is mapped as a nearly continuous 9-km-long, south-southwest-trending fault along Fatigue Wash (Day et al., 1998a). Except locally, where it forms

a fault-line scarp at the base of bedrock escarpments (mainly Yucca Mountain and Pah Canyon Tuffs, and basal units of the Tiva Canyon Tuff) on the east side of the wash, the fault is buried by surficial deposits (Fig. 2). From the mouth of Fatigue Wash, the fault is shown by Potter et al. (2002a) to continue south for a distance of another 8 km to a possible intersection with splays off the Southern Windy Wash fault (Fig. 16) south of the site area (also, see Simonds et al., 1995).

The amount of down-to-the-west displacement of bedrock toward the north end of the Fatigue Wash fault zone is about 100 m, but where it emerges from Fatigue Wash to the south, displacement is about 400 m (Day et al., 1998a, cross section B-B'; see Fig. 17). Average dip of the fault plane is 70° W. (Simonds et al., 1995), and slickenside lineations indicate a moderate amount of left-slip movement.

Studies of surficial deposits exposed in trench excavations across the south-central segment of the Fatigue Wash fault, and measurements of scarp profiles near the trenches, provide evidence that five or more paleoearthquakes occurred on the fault since middle Pleistocene time (Coe et al., 2004). The amount of displacement of the Quaternary units ranges from 1 to 3 m.

### ***Windy Wash Fault***

The Windy Wash fault is expressed as a prominent fault-line scarp on the east side of Windy Wash (Fig. 4). It is traceable nearly continuously from the south rim of the Claim Canyon caldera (Fig. 1), one of the eruptive centers in the southwestern Nevada volcanic field (Christiansen and Lipman, 1965), to the southeast edge of Crater Flat, a distance of about 25 km. It is a complex fault system consisting of two main sections, referred to as the Northern Windy Wash and Southern Windy Wash faults (Fig. 16), with down-to-the-west displacements; the two faults are separated by a 4- to 5-km-long discontinuous zone of east-facing scarps (Simonds et

al., 1995). Only about a 5.5-km-long segment of the Northern Windy Wash fault is in the northwest corner of the site area, where it is marked by a west-dipping fault-line scarp at the base of a bedrock escarpment formed largely by units of the Topopah Spring Tuff on the footwall and Yucca Mountain and Tiva Canyon Tuffs on the hanging wall (Fig. 2; Day et al., 1998a). The amount of down-to-the-west displacement of bedrock along this well-exposed segment, on a fault plane with an average west dip of about 65°, is more than 500 m.

Trenches were excavated only across the north end of the Southern Windy Wash fault, the mapping of which provided evidence of as many as eight surface-rupturing events during middle to late Quaternary time that resulted in a total net displacement of 3.7 m in the surficial deposits (Whitney et al., 2004a). With regard to the 5.5-km-long segment of the Northern Windy Wash fault in the northwest corner of the site area, Simonds et al. (1995) showed a nearly continuous scarp along the bedrock-alluvium contact that is interpreted to be indicative of probable Quaternary movement.

### ***Northern and Southern Crater Flat Faults***

The Northern and Southern Crater Flat faults lie entirely west of the site area (Fig. 16), but are included here because they form the west boundary of the Windy Wash-Crater Flat structural block to be discussed later. These two faults compose a complex fault system that can be traced discontinuously for a total length of as much as 20 km (Menges and Whitney, 2004) along the east side of Crater Flat, although the relations between the main north and south sections are obscured by surficial deposits in intervening areas. Individual exposures of the fault traces generally are less than 1 km long, with some being as much as 2 km in length. The fault traces are marked in places by small discontinuous bedrock scarps, subtle scarps and lineaments in

alluvium, and short bedrock-alluvium contacts. A 3.5-km-long segment of the southern fault is marked by a linear contact between Pliocene basalt on the east and Quaternary alluvium on the west that locally produces a west-facing scarp (Simonds et al., 1995). Trenches were excavated across both sections of the fault system, showing evidence of at least three Quaternary faulting events that displaced surficial deposits about 0.75 m on the Southern Crater Flat fault (Taylor, 2004) and four to five Quaternary events that displaced surficial deposits 1.2 m on the Northern Crater Flat fault (Coe, 2004). The amount of bedrock displacement could not be determined.

### **Structural Blocks and Intrablock Faults**

The six structural blocks delineated by the block-bounding faults within the Yucca Mountain site area range in width from 1 to 5 km (Fig. 16). Average dip of the tilted volcanic rock units within individual blocks is about 10° E. (Fig. 17), with increasing dips (to as much as 30°) near the east sides of the hanging wall blocks. Each of the blocks is segmented by numerous faults with mostly north to northwest trends. Like the block-bounding faults, displacements are mainly dip-slip, down-to-the-west, but there are some with down-to-the-east offsets that define shallow intervening graben structures (Potter et al., 2004). Notable exceptions are the northwest-trending, largely strike-slip (right lateral) faults in Drill Hole, Pagany, and Sever Washes in the north-central part of the site area (Fig. 16). Principal intrablock features within individual structural blocks are discussed briefly in the following sections.

#### ***Structural Block East of the Paintbrush Canyon Fault***



Geologic relations across much of the eastern part of the site area, east of the Paintbrush Canyon fault, are poorly known because of the thick blanket of alluvium in Fortymile Wash and over the western part of Jackass Flats (Potter et al., 2002a; see Figs. 1 and 12). However, bedrock exposures on Busted Butte and Fran and Alice Ridges, as well as in the highlands north of Yucca Wash and on both sides of Fortymile Canyon, indicate that a discrete structural block occupies this part of the site area. As yet there is insufficient evidence for defining an eastern block boundary. The easternmost down-to-the-west normal fault mapped in the northeastern part of the site area is inferred by Potter et al. (2002a) to extend south following Fortymile Wash to a point near the north end of Busted Butte, based in part on differences in the attitude of rock units on opposite sides of Fortymile Canyon and in part on the projection of stratal dips in the Topopah Spring Tuff on Fran Ridge with respect to the top of that formation in borehole UE-25 J-13 just east of the wash (see Figs. 8 and 10). Such a fault is shown in Figure 16, but its existence has not been confirmed nor can it be labeled a block-bounding fault on the basis of the available evidence.

Areas of exposed bedrock within the structural block are cut by minor faults. Those faults in the highlands in the northern part are down-to-the-west normal faults involving various units of the Paintbrush Group and the Calico Hills Formation. On Busted Butte and Fran Ridge (Fig. 2), they are mostly splays off the Paintbrush Canyon fault, producing displacements in rocks of the Paintbrush Group and locally forming north-trending zones 0.5 to 1 km wide. One such fault with down-to-the-west displacement trends north-south through the center of Busted Butte and another, termed the Busted Butte fault (Fig. 16), cuts across the east side with down-to-the-east displacement (Day et al., 1998a).

### ***Bow Ridge-Paintbrush Canyon Block***

The Bow Ridge-Paintbrush Canyon structural block is characterized by bedrock areas in both the northern and southern parts separated by a large expanse of surficial deposits in Midway Valley. Several north- to northwest-trending normal faults, most with down-to-the-west displacements, were mapped in rhyolite lavas of the Paintbrush Group in the area that lies between the Bow Ridge and Paintbrush Canyon faults north of Yucca Wash (Dickerson and Drake, 1998). At the south end of the block, south of Midway Valley, a few minor faults outlining some small graben structures were mapped in rocks of the Tiva Canyon Tuff exposed on Bow Ridge. One of these is the Midway Valley fault (Fig. 16), which was shown by Day et al. (1998a) to extend north from the Bow Ridge exposures as a concealed fault beneath alluvium for 8 km before reaching the faulted outcrops north of Midway Valley. Bedrock displacements (normal, down to the west) are shown by Scott and Bonk (1984) and Day et al. (1998a) to be 100 m and 30 m, respectively. Results of geophysical surveys further support the presence of the Midway Valley fault, as well as other north-trending faults beneath the alluvium of the valley floor (Ponce, 1993; Ponce and Langenheim, 1994; Swan et al., 2001).

The Exile Hill fault (Fig. 17) is a minor down-to-the-east, north-trending normal fault along the east side of Exile Hill (Swan et al., 2001); it is shown by Day et al. (1998a) to merge southward with the Midway Valley fault and northward with the eastern strand of the Bow Ridge fault. An exposure in the excavation at the east end of the north portal of the ESF (Fig. 16) shows the bedrock unit referred to as Tuff unit "X" (see Table 1) to be downfaulted against the crystal-rich member of the Tiva Canyon Tuff; estimated displacement is 15 to 30 m (Swan et al., 2001). Two other minor faults cut bedrock on Exile Hill; these trend northwest with dip-slip to oblique-slip displacements of 10 m or less, and are classed as relay structures by Day et al.

(1998a), linking the Bow Ridge and Exile Hill faults. The southeast-trending part of the Bow Ridge fault also is considered to be a relay structure between the main north-trending section of that fault with the Paintbrush Canyon fault to the southeast.

None of the intrablock faults in the Bow Ridge-Paintbrush Canyon structural block show evidence of Quaternary activity in trenches excavated in surficial deposits across inferred fault trends (Swan et al., 2001).

### ***Solitario Canyon-Bow Ridge Block***

The structural block bounded on the west by the Solitario Canyon fault and on the east by the Bow Ridge fault (and in part by the Paintbrush Canyon fault) is areally the largest block in the Yucca Mountain site area, ranging from about 2 to 5 km in width (Fig. 16). Because it also hosts the proposed waste repository, structural features within the block are of special interest and importance to site characterization. Numerous faults with varying orientations and displacement directions were mapped by Day et al. (1998a) and described by Potter et al. (2004). Among the more prominent of these is the Iron Ridge fault (Fig 16), which is a major splay of the Solitario Canyon fault that was described earlier. In essence, the Iron Ridge fault, with displacements of 180 to 245 m, bounds the east side of a subblock within the major block.

The Ghost Dance fault, which trends north-south 150 to 200 m east of the north-south-oriented main drift of the ESF (Fig. 16), was mapped in considerable detail by Day et al. (1998b). The fault extends south from about 0.25 km south of Drill Hole Wash to Broken Limb Ridge, a distance of 2.5 km (Fig. 2). Farther south, the fault bifurcates, striking to the southwest into the Abandoned Wash fault (Scott and Bonk, 1984) and to the southeast toward (but not into) the Dune Wash fault (Fig. 16). Down-to-the-west displacements along the Ghost Dance fault in

surface exposures range from a maximum of 27 m in the central part between Split Wash and Broken Limb Ridge (Fig. 2), where the brecciated zone between splays is as much as 150 m wide, to a minimum of 3 m along segments to the south (Day et al., 1998b).

The Ghost Dance fault does not extend far enough north to be encountered in the northern section of the ESF (Day et al., 1998a). However, a shear with a thin (1- to 10-cm- thick) gouge zone and less than 0.1-m offset was mapped along the projected north strike of the fault by Mongano et al. (1999). However, the fault was intersected toward the south end of the north-south-oriented main drift of the ESF (Fig. 16), where the fault was observed to strike N.25°E. with a vertical dip and to have only 1.2 m of down-to-the-west offset in rocks of the crystal-poor member of the Topopah Spring Tuff (Albin et al., 1997). The fault was also exposed in alcoves excavated off the main drift of the ESF, where it displays displacements ranging from 6 m to about 25 m along fault-damage zones 0.6 to 1.0 m wide (Taylor et al., 1998). The Ghost Dance fault was trenched at several locations, but studies of the excavations recorded no evidence of Quaternary movements (Taylor et al., 2004).

The Sundance fault (Fig. 16) is mapped as a 750-m-long, 70-m-wide brecciated zone of small discontinuous faults trending northwest from Live Yucca Ridge to Dead Yucca Ridge (Fig. 2; Potter et al., 1999). The fault, with down-to-the-east bedrock displacement ranging from 6 to 11 m, terminates west of the trace of the Ghost Dance fault (Day et al., 1998b). It was intersected in both the main drift of the ESF and in the CD (Fig. 16). In the main drift, the fault appears to have several meters of down-to-the-west offset within a 20-cm-thick gouge zone (Mongano et al., 1999); this observed offset is opposite to that observed at the surface. In the Cross Drift, the Sundance fault likewise appears to have down-to-the-west-displacement of a few

meters (Mongano et al., 1999). Like the Ghost Dance fault, there is no evidence to indicate that Quaternary activity took place along the Sundance fault.

From where it branches off the Ghost Dance fault, the Abandoned Wash fault continues southwest and south for about 5 km (Fig. 16). It is exposed in bedrock (Tiva Canyon Tuff) along its northern trace but is buried by alluvium to the south. The fault displays as much as 24 m of down-to-the-west displacement marked by a fault scarp dipping 81°W. (Dickerson and Drake, 2004). In contrast, the southeast-trending Dune Wash fault (Fig. 16) is concealed beneath surficial deposits of Dune Wash for most of its indicated length of 5 km, being exposed only at the north end where bedrock (Tiva Canyon Tuff) is displaced about 50 m down to the west. To the west, the East Ridge fault (Fig. 16), with as much as 145 m of down-to-the-east displacement, defines the west side of a feature referred to as the Dune Wash graben (Day et al., 1998a). This prominent downfaulted feature may terminate south against the southern extension of the Paintbrush Canyon fault, but the relations are obscured by surficial deposits.

Sever, Pagany, and Drill Hole Washes are prominent northwest-trending drainages in the northern part of the Solitario Canyon-Bow Ridge structural block that appear to be controlled by northwest-striking faults (Fig. 16). The faults were identified on the basis of geophysical investigations, bedrock mapping, and examination of drill cores from Drill Hole Wash (Scott et al., 1984). A similar fault also was inferred to project beneath the Quaternary alluvial deposits of Yucca Wash (Fig. 2) by Scott (1992), but more extensive geologic and geophysical investigations have not confirmed its existence (Langenheim and Ponce, 1994; Dickerson and Drake, 1998; Day et al., 1998a). The Sever Wash and Pagany Wash faults (Fig. 16) are exposed in bedrock and locally have produced small bedrock scarps. The Drill Hole Wash fault (Fig. 16) also is concealed by Quaternary alluvium, but two faults encountered in the northern section of

the ESF were correlated with the Drill Hole Wash fault zone (Beason et al., 1996).

Approximately 4 m of vertical separation was observed on these features, and horizontal slickensides also indicate strike-slip movement, but the total amount of displacement could not be determined. Quaternary alluvial terraces on the floors of the washes do not appear to be displaced by the northwest-trending faults; a trench excavated across the Pagany Wash fault exposed faulted bedrock on the trench floor, but the overlying bedrock regolith and colluvial units are not displaced (Taylor et al., 2004).

The northwest-trending faults are steeply dipping and thought to be strike-slip faults because fault-plane surfaces locally contain slickenside lineations that are nearly horizontal, and vertical displacements generally are less than 5 to 10 m (Scott et al., 1984). The Sever Wash and Pagany Wash faults show slickenside orientations and Riedel shears that indicate right-lateral slip; the amount of displacement was estimated to be about 40 m on each fault by Scott et al. (1984). These two faults are each about 4 km long; both appear to terminate against the Solitario Canyon fault to the west and, although concealed, are postulated to terminate against a down-to-the-east north-trending fault lying a short distance west of the Bow Ridge fault (Fig. 16; Day et al., 1998b). The Drill Hole Wash fault also is about 4 km long and also may terminate against the same north-trending fault.

A closely spaced series of normal faults form an asymmetric graben-like feature that trends north from Boundary Ridge across the toes of Antler and Live Yucca Ridges (Fig. 2); some are shown between the Ghost Dance and Bow Ridge faults on the cross section in Figure 17. Cumulative offset ranges to as much as 30 m. Such fault clusters were referred to as “imbricate fault zones” by Scott (1990), and were considered by him to be characteristic of the more intense deformation that took place along the east side of some structural blocks where dips of

compaction foliations become steeper. However, the term “imbricate fault zone” was not used for descriptive purposes by Day et al. (1998a, 1998b), who interpreted the steep foliation dips to be caused by rotation of blocks in a tectonic breccia zone rather than by fault displacements.

### ***Fatigue Wash-Solitario Canyon Block***

The prominent feature in the Fatigue Wash-Solitario Canyon structural block is the east-dipping sequence of volcanic rocks that make up Jet Ridge (Fig. 2). Several normal faults, mostly with small offsets in the Tiva Canyon, Yucca Mountain, and Pah Canyon Tuffs, are in the northern part of the block (Fig. 16). The most extensive is a northwest-trending feature about 2.5 km long with down-to-the-east displacement exhibited mainly in rocks of the Yucca Mountain Tuff. A number of faults also cut bedrock (Tiva Canyon Tuff) farther south along the east slope of Jet Ridge, including the 4.5-km-long, north-northeast-trending intrablock Boomerang Point normal fault (Fig. 16). North- to northwest-trending, down-to-the-west normal faults at the south ends of both Jet Ridge and Boomerang Point were considered by Day et al. (1998a) to be relay faults linking the Fatigue Wash and Boomerang Point faults and the Boomerang Point and Solitario Canyon faults, respectively (Fig. 16). Structural relations farther south in this structural block are obscured by surficial deposits.

### ***Windy Wash-Fatigue Wash Block***

West Ridge and Fatigue Wash (to the east) occupy that part of the Windy Wash-Fatigue Wash structural block lying within the western part of the Yucca Mountain site area (Figs. 2 and 16). Intrablock structures are mainly small displacement normal faults in the northern and central parts of West Ridge. A cluster of closely spaced, northwest-trending relay faults

terminate against the Northern Windy Wash fault to the west and the Fatigue Wash fault to the east (Fig. 16; Day et al. 1998a). Displacements are both down to the southwest and down to the northeast, with a cumulative offset of about 60 m down to the southwest. The structural block terminates just south of the southwest corner of the site area, at the apparent junction between the two bounding faults (Fig. 16).

### ***Crater Flat-Windy Wash Block***

Only the northeastern part of the Crater Flat-Windy Wash structural block lies within the site area (Fig. 16). A few north-trending normal faults in bedrock are present in that area, with one fault showing Yucca Mountain Tuff in the hanging wall downdropped (west side down) against ash-flow tuffs of the Calico Hills Formation in the footwall (Day et al., 1998a). Much of the block elsewhere along the east margin of Crater Flat is covered by surficial deposits, so little of the structure can be directly observed. Locations of faults shown on the 1:50,000-scale map compilation by Potter et al. (2002a) are based primarily on interpretation of geophysical surveys within Crater Flat proper.

### **Vertical Axis Rotation**

An important characteristic of the existing fault patterns at and near Yucca Mountain is a noticeable change from the predominant northerly fault trends within the site area proper to more northeasterly trends in adjacent areas toward the south end of the mountain (Fridrich et al., 1999; Rosenbaum et al., 1991; see Fig. 16). This relation is attributed to a progressive north to south increase in post-12.7 Ma vertical-axis rotation clockwise from 0° in the area near The Prow (Fig.



2) to about 30° in an area about 10 km south of the site area. It is interpreted to be the result of (1) right-lateral deformation within the Walker Lane structural belt (see O'Leary, this volume, for location) by Fridrich et al. (1999) and Rosenbaum et al. (1991), or (2) differential displacement on normal faults that shallow with depth (i.e., listric faults) by Stamatakos and Ferrill (1998). Within the site area itself, vertical rotation ranges from 0° at The Prow to 5° at the latitude of Busted Butte (Fig. 2). Commensurate with the north-to-south increase in the clockwise vertical-axis rotation is a general southward increase in displacements along block-bounding faults. This increase in displacement is supported by Potter et al. (2004), who reported that the magnitude of east-west extension was 8% across north-central Yucca Mountain, 10.5% across the southern part of the site area, and 12% in the area still farther south. In intrablock areas, the transition from a less-extended terrane in the northern part of Yucca Mountain to a more-extended terrane farther south generally is expressed by the appearances of numerous closely spaced minor normal faults that coalesce and gain displacement to the south and of wider, fault-bounded half grabens.

### **Deformation within Fault Zones**

Because faults represent zones of poor rock quality resulting in potential hydrologic pathways, or as impediments to flow in some cases, deformation along the faults bordering the proposed repository area has been studied extensively. Map patterns demonstrate that tectonic mixing of various Paintbrush Group lithologies has occurred within the most intensely deformed parts of block-bounding fault systems. This is most apparent in the Solitario Canyon fault system (Scott and Bonk, 1984; Day et al., 1998b). In this wide (as much as 400 m) system,

lenses from stratigraphically diverse parts of the Tiva Canyon Tuff are juxtaposed. Slices of Topopah Spring Tuff are also mixed, and in some areas lenses from more than one Paintbrush Group formation are tectonically juxtaposed (Day et al., 1998b). Tectonic mixing is also apparent along the Northern Windy Wash fault system west of The Prow, along the Bow Ridge fault system in the saddle between Bow Ridge and Boundary Ridge, and in the Paintbrush Canyon fault system along the west flank of Fran Ridge (see Figs. 2 and 16; Potter et al., 2004). Individual fault strands within these tectonically mixed zones are brecciated; in some cases the fault-bounded lenses are internally brecciated.

In addition to tectonic mixing, there are areas where coherent blocks of Tiva Canyon Tuff, as much as 250 m wide, dip to the west, opposite to the prevailing easterly dips of the major structural blocks (Day et al., 1998b). Locally, anticlines with axes subparallel to the fault zone are present within individual fault slices and in the immediate footwall of the Solitario Canyon fault. These folds are likely produced by local transpression that folded and rotated volcanic strata. Mapped fold hinges may actually be small-displacement, brittle fault zones lying at shallow structural levels. Small thrust faults are mapped within the Solitario Canyon fault system and in the hanging wall of the Bow Ridge fault near the south portal of the ESF (Day et al., 1998b). The anastomosing pattern of faults that characterizes these fault systems also produced individual fault splays that cut into both the hanging wall and footwall.

As indicated earlier, the eastern (main) strand of the Solitario Canyon fault was encountered in the west end of the Cross Drift (Fig. 16), where about 260 m of down-to-the-west offset placed the lower nonlithophysal zone of the Topopah Spring Tuff in the footwall against the upper lithophysal zone of the Topopah Spring Tuff in the hanging wall. However, the tectonic mixing described above also is observed within the fault zone at depth in the Cross

Drift, where there is a breccia composed of clasts of the overlying lower nonlithophysal zone of the Tiva Canyon Tuff. Footwall deformation (mostly brecciation) is fairly extensive in the area of the drift, extending approximately 50 m east of the main fault.

## **Geophysical Surveys**

Several geophysical methods, including seismic reflection, gravity, and magnetic surveys, were used in attempts to characterize the subsurface geologic structure within the Yucca Mountain site area (Fig. 19). Such surveys, however, have met with varying degrees of success. Seismic reflection profiling, for example, which was conducted along most of the lines shown in Figure 19, is difficult because the propagation of seismic energy is greatly inhibited by the fracturing and lithologic heterogeneities that characterize much of the thick sequences of volcanic rocks. Gravity data also were obtained along most of the survey lines and were used primarily to interpret regional structure and to assist in locating faults and determining their general displacements in local areas. Ground magnetic surveys and aeromagnetic data were mainly used to infer fault locations and offsets, especially where the relatively magnetic Topopah Spring Tuff was involved in the faulting. Attempts were made to detect and characterize buried faults and geologic heterogeneities by using the magnetotelluric method, but this method was limited unless supplemented by other geophysical techniques.

The results of geophysical surveys in the site area are reported in numerous publications, including Fitterman (1982), Senterfit et al. (1982), Smith and Ross (1982), Pankrantz (1982), McGovern (1983), U.S. Geological Survey (1984), Frischknecht and Raab (1984), Reynolds and Associates (1985), Ponce (1993), Ponce and Langenheim (1994), Feighner et al. (1996), Majer et

al. (1996), Brocher et al. (1998), CRWMS M&O (1998; 2000), and Swan et al. (2001). Some of the reported findings from these sources are summarized below.

Data from the generally east-trending, 32-km-long seismic reflection survey across Crater Flat, Yucca Mountain, Midway Valley, and Fortymile Wash (lines REG-2 and REG-3, Fig. 19) were interpreted to reflect a series of west-dipping normal faults that project through the volcanic rocks and displace the Tertiary volcanic-rock/pre-Tertiary sedimentary-rock contact at depth (Brocher et al., 1998). Suggestions that this contact is formed by an active detachment fault beneath Yucca Mountain (for example, Scott, 1990; Hamilton, 1988) are therefore inconsistent with the seismic reflection data.

Ponce (1993) and Ponce and Langenheim (1994) conducted gravity and magnetic surveys (Fig. 19) in Midway Valley, from which anomalies were identified that were interpreted to be faults concealed by the thick alluvial deposits covering the central part of the valley. One of the anomalies was presumed to be associated with the Midway Valley fault, with the data indicating a vertical displacement of several tens of meters in the underlying bedrock. Ponce and Langenheim (1994) also interpreted data from ground magnetic surveys to indicate that north-trending faults could be traced continuously across Yucca Wash, thus casting doubt on the existence of a northwest-trending fault along the floor of the wash that had been postulated by earlier investigators (for example, Scott and Bonk, 1984).

Because a primary question to be addressed in the site area is the amount, style, depth, and continuity of faulting in the repository block itself, various geophysical methods were compared to evaluate their effectiveness in imaging both a block-bounding fault (Bow Ridge fault) and a prominent intrablock fault (Ghost Dance fault). In the case of the Bow Ridge fault, only the ground-based gravity and aeromagnetic surveys yielded reliable results. The gravity data show a

distinct gravity low on the hanging wall of this block-bounding fault where bedrock is buried by less dense surficial deposits. The aeromagnetic data show a high on the footwall side and a low on the hanging wall side, a relation that is interpreted as a signature of displacement of the relatively magnetic Topopah Spring Tuff. Seismic reflection surveys produced unreliable results.

Ground-based magnetic and magnetotelluric profiling worked well for detecting the Ghost Dance fault, whereas ground-based gravity and standard high-resolution seismic reflection surveys (those with 6- to 12-m station spacings) did not record significant anomalies. The ground-based magnetic data indicate a characteristic magnetic low, typically about 100 m wide, on the footwall of the fault, and the magnetotelluric data show a clear change in resistivity for the fault. On very high resolution seismic reflection lines (station spacing 1 to 2 m), displacement of reflections was apparent across the Ghost Dance fault, thus enabling individual splays to be mapped in places.

The general conclusion was that standard geophysical techniques used at Yucca Mountain are best suited for detection of faults with at least tens of meters of offset (CRWMS M&O, 2000, p. 4.6-32).

## **Fractures**

Combined three-dimensional studies of fractures in natural and cleared exposures, boreholes, and underground excavations (ESF and Cross Drift) led to important conclusions regarding their distribution and characteristics in the Yucca Mountain site area. Attributes of fracture systems within the principal formations that are most closely associated with the

proposed repository — Tiva Canyon and Topopah Spring Tuffs, Calico Hills Formation, and Prow Pass Tuff, as well as some of the major units within the PTn hydrogeologic unit — and the study methods used, are described in considerable detail in CRWMS M&O (1998). The data presented in that report were used to characterize fracture systems in support of (1) surface infiltration model development (Flint and Flint, 1994), (2) numerical simulations of discrete fracture networks (Anna and Wallman, 1997), (3) calculations of bulk-rock permeability for use in equivalent continuum models of the unsaturated zone (Schenker et al., 1995; Arnold et al., 1995), (4) studies bearing on the mechanical stability of the proposed repository, and (5) investigations to determine the paleostress history of Yucca Mountain. Some of the general relations that were observed between fracture patterns and lithology and of fracturing in fault zones are summarized briefly below, based on CRWMS M&O (1998).

Fracture characteristics in the pyroclastic flows in the Yucca Mountain site area are controlled primarily by variations in the degree of welding and secondarily by lithophysal development, alteration, and pumice content. Such controls affected fracture spacing, fracture type, number of fracture sets, continuity of individual fractures within each lithostratigraphic unit, and the connectivity of fractures within the network as a whole. Fracture networks commonly act as preexisting lines of weakness in the rock mass, having originated as cooling joints that formed as tensional openings in response to contraction during cooling of the volcanic rock mass; subsequent extensional strain could then be accommodated through distributed slip along the preexisting joint sets. The presence of thin breccia zones along such joints, and observable slip lineations along their surfaces, are indicative of joint reactivation. Tectonic fractures are also common in the volcanic rocks, having been developed independently of the cooling joint sets in response to regional or local stresses, and are recognized as discontinuities

across which simple openings (face separations) of less than 10 cm of displacement have occurred in contrast to reactivated joints.

Because fracturing in zones adjacent to fault planes exerts an important influence on hydrologic flow pathways, many fracture studies focused on the frequency and characteristics of fractures near some of the faults close to the repository block, particularly of fracture sets exposed in the ESF and Cross Drift (e.g., see Mongano et al. 1999). Although the amount of fracturing associated with faults depends, in part, on the lithologic units involved, the width of a fracture zone in the immediate vicinity of a fault generally correlates with the amount of fault offset. Intrablock faults with small amounts of displacement (1 to 5 m) have fracture zones 1 to 2 m wide, whereas block-bounding faults with tens of meters of offset have zones ranging in widths as much as 6 to 10 m.

Studies of the Ghost Dance fault, which transects the proposed repository area (Fig. 16), have concentrated on fracture patterns exposed in an excavation for the USW UZ-7a drillpad (location in Fig. 8) and on a cleared pavement on the south flank of Antler Ridge (Fig. 2). One generalization is that the total amount of rock damage and fracturing is greater in the hanging wall than in the footwall. At the USW UZ-7a locality, for example, the intervening rock between the west-dipping main fault and a secondary east-dipping fault 42 m to the west, in the hanging wall, is intensely broken and consists of a complex network of short-length fractures, whereas rocks (lower part of lower lithophysal zone of the Tiva Canyon Tuff) in the footwall east of the main fault trace are noticeably less fractured. At the Antler Ridge locality, there are 13 to 20 m of cumulative down-to-the-west displacement across several splays of the Ghost Dance fault distributed over a map width of 100 to 150 m (Day et al., 1998a). The fracture network in various units of the Tiva Canyon Tuff within or proximal to the fault zone is

dominated by closely spaced, steeply dipping fractures, many of which show minor offsets, that may be the result of their proximity to the fault, although, alternatively, they may be more closely related to the cluster of closely spaced faults mapped farther east toward the toe of Antler Ridge (Day et al., 1998b). In the case of the Sundance fault, it occupies a well-defined single strand in places where cooling joints are poorly developed in the crystal-rich member of the Tiva Canyon, but where there is a greater abundance of cooling joints the displacement is distributed across a broader zone (Potter et al., 1999).

### **Stratigraphic Relations across Faults and Timing of Deformation**

Stratigraphic relations and geologic map patterns across block-bounding and intrablock faults in the Yucca Mountain site area show evidence of episodic movement during the depositional period (12.8 to 12.7 Ma) of the Paintbrush Group (Potter et al., 2004). Several examples of such evidence are discussed in detail in CRWMS M&O (2000, p. 4.6-12 to 4.6-15), a few of which are summarized below:

1. Near the mouth of Solitario Canyon, the stratigraphic interval of the pre-Pah Canyon bedded tuffs and the Pah Canyon Tuff thins across a prominent splay of the Solitario Canyon fault, from a thickness of 7 m on the hanging wall to 2 m on the footwall; as observed by Day et al. (1998a), the top of the Topopah Spring Tuff is offset 13 m whereas the bases of the Yucca Mountain and Tiva Canyon Tuffs are offset only 3 m.
2. At a locality near The Prow (Fig. 2), pre-Yucca Mountain Tuff bedded tuffs thicken abruptly across the north end of the Fatigue Wash fault. Along a parallel fault 150 m to the west, a 45-m-thick rhyolite flow between the Pah Canyon Tuff and the pre-Yucca



Mountain Tuff bedded tuffs in the hanging wall is absent in the footwall, indicating that at least 45 m of displacement occurred after deposition of the Pah Canyon.

3. Growth faulting along the Ghost Dance fault during deposition of the crystal-rich member of the Topopah Spring Tuff and overlying bedded tuffs at the base of the Tiva Canyon Tuff is indicated by a 30-m decrease in the thickness of the upper lithophysal zone of the Topopah Spring observed on a lithologic log of borehole USW UZ-7a, which penetrates the fault. Combined with a 15-m offset of the Tiva Canyon Tuff observed during surface mapping, the relations are interpreted by Day et al. (1998b) to indicate that (1) about 15 m of post-Topopah Spring, pre-Tiva Canyon displacement occurred followed by an additional offset of 15 m after deposition of the Tiva Canyon; and (2) a small amount of fault-related topography existed prior to Tiva Canyon time.
4. Numerous minor faults (splays of the Busted Butte fault, Fig. 16) on the west side of Fran Ridge (Fig. 2) and the north end of Busted Butte displace the top of the Topopah Spring Tuff and the pre-Pah Canyon bedded tuffs 1 to 10 m, but the pre-Tiva Canyon Tuff bedded tuff unit and the base of the Tiva Canyon are unfaulted.

In addition to episodic deformation during the deposition of various units within the Paintbrush Group, there was an episode of faulting and tilting of strata between deposition of the Tiva Canyon Tuff and that of the Timber Mountain Group rocks. Near the mouth of Solitario Canyon, for example, a complex of small faults splaying off the main trace of the Solitario Canyon fault and displacing Paintbrush Group tuffs is overlapped by unfaulted Rainier Mesa Tuff (Fig. 2; Day et al., 1998a). Fridrich et al. (1999) interpreted stratal dips in the site area to indicate that (1) the Tiva Canyon Tuff was tilted 10° to 20° to the east and southeast prior to the deposition of the Rainier Mesa (11.6 Ma), (2) less than 5° of eastward tilting occurred 11.6 to

10.5 Ma, and (3) less than 5° of eastward tilting occurred after 10.5 Ma. Scott (1990), using compaction foliations, suggested that there is more than 10° of discordance between the Rainier Mesa and Tiva Canyon Tuffs west and northwest of Busted Butte. In much of the site area, however, mapping by Day et al. (1998a) indicated that the Rainier Mesa Tuff was displaced by faulting and tilted nearly the same amount as the Tiva Canyon Tuff.

As indicated in descriptions of the block-bounding faults, deformation also continued through Quaternary time (Keefer et al., 2004).

### **Geologic Structure of the Pre-Cenozoic Rocks**

Little can be said about the structural geology of the Paleozoic and Precambrian rocks that lie beneath Yucca Mountain. They are not exposed in the site area and have been penetrated in only one borehole (borehole UE-25 p#1; see Fig. 10). Based on exposures in other areas, such as Bare Mountain 12 km to the west of Yucca Mountain (Monsen et al. 1992) and Calico Hills 3 km to the east (Potter et al. 2002a), the pre-Cenozoic rocks of the region were highly deformed at some time prior to the deposition of the Tertiary volcanic rocks. Robinson (1985) presented a geologic map of the Proterozoic and Paleozoic rocks of the Yucca Mountain region on which he showed an inferred distribution of Paleozoic strata (Silurian to Mississippian) as directly underlying the volcanic rocks and, for the most part, occupying a broad syncline. Compilations by Sweetkind et al. (2001) and Potter et al. (2002b) show the deep subsurface structure of an extensive region in southwestern Nevada and adjacent parts of California, based largely on the projection of features from structures mapped in exposed areas and on interpretations of available geophysical and borehole information. One of the structures inferred to have involved

the Paleozoic rocks beneath Yucca Mountain is an east-west trending, south-vergent thrust fault block (labeled CP thrust fault by Cole, 1997) that was projected to extend from the CP Hills, some 25 km east of Yucca Mountain, westward to connect with a similarly oriented thrust fault mapped in Lower Paleozoic rocks at Bare Mountain (labeled Panama thrust fault by Potter et al., 2002b). Its actual existence can neither be proved nor disproved, but if present it does not appear to have affected the structural patterns observed in the Tertiary volcanic rocks, or to have given rise to any known seismic activity.

### ***Tectonic Models for Yucca Mountain***

Various tectonic models that have been proposed for Yucca Mountain are the subject of a chapter in this volume by D.W. O'Leary. Accordingly, the subject will not be discussed further here, except to note that, in terms of structural style and deformational history, Yucca Mountain is closely linked to Crater Flat basin to the west (Fig. 1). In view of that relation, Fridrich (1999) proposed that these two features form a single and distinct graben-like structural domain — the Crater Flat domain.

## **NATURAL RESOURCES**

### **Introduction**

Identification and evaluation of the natural resources in the Yucca Mountain area have been the subject of several reports prepared as part of the site characterization program. A detailed discussion of resources potential is given in CRWMS M&O (2001); other reports include: (1)

Castor et al. (1999) for metallic minerals; (2) Castor and Lock (1995) for industrial rocks and minerals; (3) Barker (1994), Grow et al. (1994), Cashman and Trexler (1995), Trexler et al. (1996), Castor et al. (1999), and French (2000) for hydrocarbon and other energy resources; and (4) Flynn et al. (1996) for geothermal resources. Summary discussions on the various resources, given below, primarily are based largely on one or another of these reports.

### **Metallic Mineral Resources**

Nevada is well known for production of several metallic resources, including gold, silver, copper, mercury, and uranium (Nevada Bureau of Mines and Geology, 1997). Similarly, the region surrounding Yucca Mountain contains deposits or potentially economic resources of these metallic minerals (Castor et al., 1999). Geologic conditions within the site area generally are similar to those in nearby mineralized areas. However, although episodes of alteration and mineralization followed the deposition of the Paintbrush Group tuffaceous rocks in areas a few kilometers away, it appears that the hydrothermal activity resulting in mineral deposits elsewhere did not extend into the Yucca Mountain area. This conclusion is based on studies of the mineralogy, petrography, and alteration of numerous rock samples, geophysical data, remote sensing imagery, and results of chemical analyses, which, combined, show no direct evidence for economic mineralization. Detailed descriptions and interpretations of the studies and tests that were conducted in the site area are presented by Castor et al. (1999), who found that the small, largely trace amounts of the minerals that were detected (for example, tin, gold, and uranium) were far below the concentrations or the volumes required for any economic consideration.

## **Industrial Rocks and Minerals**

The Yucca Mountain region contains many deposits of industrial rocks and minerals (Castor and Lock, 1995). Borite, clay minerals, fluorite, and zeolite have been identified in samples from Yucca Mountain; building stone, construction aggregate, limestone, pumice, silica, and vitrophyre/perlite also are present. Based on such factors as quality and quantity of the resource, accessibility, and competition from alternate, more readily available sources of supply elsewhere in the region, none of these commodities are considered to be of economic importance (CRWMS M&O, 2001).

## **Hydrocarbon and other Energy Resources**

There are few data for determining the extent to which the essential elements for the generation and accumulation of oil and gas – source rocks, favorable maturation history, reservoir rocks, and sealing and trapping conditions – are developed in the Yucca Mountain area. Only one borehole (UE-25 p#1, Figs. 8, 10) was drilled deep enough to penetrate rocks below the Tertiary volcanic sequence; these pre-Tertiary rocks were identified as strata representing the Lone Mountain Dolomite and Roberts Mountains Formation of Silurian age. No oil shows or residue were reported from an examination of the borehole cores (Carr et al., 1986). To date (2006), no significant volumes of oil or gas have been found in southern Nevada or adjacent California and Arizona.

French (2000), in an assessment of the hydrocarbon potential of the Yucca Mountain area, concluded that, although the basic elements of a viable petroleum system are present,

comparisons with known producing fields in the region indicate that (1) the volume of potential source rock is limited, and (2) one of the important seals of the region (an unconformity at the base of valley-fill sediments in some producing areas) is not well developed. Based on these and other factors, French (2000) and Grow et al. (1994) interpreted the geologic conditions at Yucca Mountain to indicate a low potential for the generation and accumulation of oil and gas.

Other energy resources — tar sands, oil shale, and coal — are not known to exist in the rocks underlying Yucca Mountain, not having been detected in any of the boreholes drilled in the area or recognized in outcrops in nearby areas (see Castor et al., 1999).

### **Geothermal Resources**

Flynn et al. (1996), citing geological, geophysical, and geochemical findings, chemical geothermometry, and the very low measured thermal gradient, concluded that there is no potential for geothermal development in the area. This is supported by temperatures measured in springs south of latitude 38°30' in Nevada, which are uniformly less than 41°C (Garside and Schilling, 1979).

## ACKNOWLEDGMENTS

The synthesis of geologic information presented here is based on a large volume of basic data that was collected and analyzed by scores of investigators involved in the Yucca Mountain Site Characterization program. Although individual contributions forming the basis for much of the descriptive, interpretive, and illustrative content of this report are appropriately cited, we wish to acknowledge certain individual scientists who played key roles in the conduct of field and laboratory studies that were fundamental to developing the structural and stratigraphic framework of the Yucca Mountain site area. Unless otherwise indicated, named individuals are U.S. Geological Survey personnel.

W.C. Day led a team, including R.P. Dickerson (Pacific Western Technology, Inc.), R.M. Drake, III, C.J. Potter, and D.S. Sweetkind, that produced bedrock geologic maps showing in considerable detail major and minor faults and other structural features, many of which had not been recognized previously. As indicated in our report, virtually all of the discussions of bedrock structure and the distribution and displacements of bedrock stratigraphic units are based on the maps, cross sections, and descriptions published by these investigators. A review of a preliminary draft of our report by W.C. Day is also gratefully acknowledged.

R.W. Spengler was a leading member of the group, including J.K. Geslin and T.C. Moyer (Science Applications International Corp.), that was instrumental in defining and describing lithostratigraphic units within the thick volcanic-rock sequences that form Yucca Mountain. Their studies were fundamental to the characterization and distribution of the physical and chemical properties of the rocks that compose and surround the proposed repository block.

Personnel of the Los Alamos National Laboratory, including D.L. Bish, D.E. Broxton, B.A. Carlos, S.J. Chipera, S.S. Levy, and D.T. Vaniman, also contributed basic mineralogical and geochemical data. R.W. Spengler was involved in a major effort to accurately identify lithostratigraphic contacts in boreholes that provided much of the data on rock thicknesses and essential information for the 3-D modeling of the site area.

J.A. Coe, S.C. Lundstrom, C.M. Menges, A.R. Ramelli (Nevada Bureau of Mines and Geology), E.M. Taylor, J.R. Wesling (Geomatrix Consultants, Inc.), and J.C. Yount were principal investigators in the detailed study of Quaternary surficial deposits and the mapping of trench excavations across buried faults that provided evidence of the magnitude and ages of Quaternary faulting events. Ages of sediments and soils were determined principally by J.B. Paces (U-series analyses) and S.A. Mahan (thermoluminescence analyses).



## REFERENCES CITED

- Albin, A.L., Singleton, W.L., Moyer, T.C., Lee, A.C., Lung, R.C., Eatmon, G.L.W., and Barr, D.L., 1997, Geology of the Main Drift — Station 28+00 to 55+00, Exploratory Studies Facility, Yucca Mountain Project, Yucca Mountain, Nevada: Summary Report by the U.S. Bureau of Reclamation to the U.S. Department of Energy, Yucca Mountain Project Data Tracking Number GS970208314224.005, 312 p., 6 plates.
- Anna, L.O., and Wallman, P., 1997, Characterizing the fracture network at Yucca Mountain, Nevada, Part 2, Numerical simulation of flow in a three-dimensional discrete fracture network, *in* Hoak, T.E., Klatwitter, A.L., and Blomquist, P.K., eds., Fractured reservoirs: Characterization and modeling: Rocky Mountain Association of Geologists, Characterization and Modeling Guidebook-1997.
- Arnold, B.W., Altman, S.J., Robey, T.H., Barnard, R.W., and Brown, T.J., 1995, Unsaturated-zone fast-path flow calculations for Yucca Mountain groundwater travel time analysis: Sandia National Laboratories SAND 95-0857.
- Barker, C.E., 1994, Thermal and petroleum generation history of the Mississippian Eleana Formation and Tertiary source rocks, Yucca Mountain area, southern Nye County, Nevada: U.S. Geological Survey Open-File Report 94-161, 26 p.

Beason, S.C., Turlington, G.A., Lung, R.C., Eatman, G.L.W., Ryter, D., and Barr, D.L., 1996, Geology of the North Ramp — Station 0+60 to 4+00, Exploratory Studies Facility, Yucca Mountain Project, Yucca Mountain, Nevada: Summary Report by the U.S. Bureau of Reclamation to the U.S. Department of Energy, Yucca Mountain Project Data Tracking Number GS960908314224.019, 174 p., 15 plates.

Bechtel SAIC Company, 2002, Geologic framework model: Bechtel SAIC Company MDL-NBS-GS-000002, Rev. 01.

Beck, D.A., and Glancy, P.A., 1995, Overview of runoff of March 11, 1995, in Fortymile Wash and Amargosa River, southern Nevada: U.S. Geological Survey Fact Sheet FS-210-95.

Bierman, P.C., and Caffee, M.C., 2002, Cosmogenic exposure and erosion history of ancient Australian bedrock landforms: Geological Society of America Bulletin, v. 114, p. 787-803.

Birkeland, P.W., 1984, Soils and geomorphology: Oxford University Press, New York, New York, 372 p.

Bish, D.L., and Aronson, J.L., 1993, Paleogeothermal and paleohydrologic conditions in silica tuff from Yucca Mountain, Nevada: Clays and Clay Minerals, v. 41, p. 148–161, Pergamon Press, Long Island City, New York.

Bish, D.L., Carey, J.W., Carlos, S.J., Chipera, S.J., Guthrie, G.D., Jr., Levy, S.S., Vaniman, D.T., and WoldeGabriel, G., 2002, Summary and synthesis report on mineralogy and petrology Studies for the Yucca Mountain Site Characterization Project: Los Alamos National Laboratory Report LA-UR-02-7840, 1,300 p.

Bish, D.L., and Chipera, S.J., 1986, Mineralogy of drill holes J-13, UE-25A#1, and USW G-1 at Yucca Mountain, Nevada: Los Alamos National Laboratory LA-10764-MS.

Bish, D.L., and Vaniman, D.T., 1985, Mineralogic summary of Yucca Mountain, Nevada: Los Alamos National Laboratory LA-10543-MS.

Brocher, T.M., Hunter, W.C., and Langenheim, V.E., 1998, Implications of seismic reflection and potential field geophysical data on the structural framework of the Yucca Mountain – Crater Flat region, Nevada: Geological Society of America Bulletin, v. 110, p. 947–971.

Broxton, D.E., Byers, F.M., Jr., and Warren, R.G., 1989, Petrography and phenocryst chemistry of volcanic units at Yucca Mountain, Nevada: Los Alamos National Laboratories LA-11503-MS.

Broxton, D.E., Chipera, S.J., Byers, F.M., Jr., and Rautman, C.A., 1993, Geologic evaluation of six nonwelded tuff sites in the vicinity of Yucca Mountain, Nevada for a surface-based test facility for the Yucca Mountain project: Los Alamos National Laboratory LA-12542-MS.

Buesch, D.C., 2000, Application of theoretical relations of density, porosity, and composition in volcanic rocks from Yucca Mountain, Nevada: Geological Society of America Abstracts with Programs, v. 32, p. A-89.

Buesch, D.C., and Spengler, R.W., 1999, Stratigraphic framework of the North Ramp area of the Exploratory Studies Facility, Yucca Mountain, *in* Rousseau, J.P., Kwicklis, E.M., and Gillies, D.C., eds., Hydrology of the unsaturated zone, North Ramp area of the Exploratory Studies Facility, Yucca Mountain, Nevada: U.S. Geological Survey Water-Resources Investigations Report 98-4050, p. 17–44.

Buesch, D.C., Spengler, R.W., Moyer, T.C., and Geslin, J.K., 1996a, Proposed stratigraphic nomenclature and macroscopic identification of lithostratigraphic units of the Paintbrush Group exposed at Yucca Mountain, Nevada: U.S. Geological Survey Open-File Report 94-469.

Buesch, D.C., Spengler, R.W., Nelson, P.H., and Flint, L.E., 1996b, Correlation of lithologic features, hydrogeologic properties and borehole geophysical logs at Yucca Mountain, Nevada: Geological Society of America Abstracts with Programs, v. 28, p. A-521.

Byers, F.M., Jr., Carr, W.J., Orkild, P.P., Quinlivan, W.D., and Sargent, K.A., 1976, Volcanic suites and related cauldrons of Timber Mountain – Oasis Valley caldera complex, southern Nevada: U.S. Geological Survey Professional Paper 919.

Caporuscio, F., Vaniman, D., Bish, D., Broxton, D., Arney, B., Heikeu, G., Byers, F., Gooley, R., and Semarge, E., 1982, Petrologic studies of drill cores USW-G2 and UE25b-1H, Yucca Mountain, Nevada: Los Alamos National Laboratory LA-9255-MS.

Carr, M.D., Waddell, S.J., Vick, G.S., Stock, J.M., Monsen, S.A., Harris, A.G., Cork, B.W., and Byers, F.M., Jr., 1986, Geology of drill core UE25p#1: A test hole into pre-Tertiary rocks near Yucca Mountain, southern Nevada: U.S. Geological Survey Open-File Report 86-175.

Carr, W.J., 1984, Regional structural setting of Yucca Mountain, southwestern Nevada, and Late Cenozoic rates of tectonic activity in part of southwestern Great Basin, Nevada and California: U.S. Geological Survey Open-File Report 84-854.

Carr, W.J., 1992, Structural model for western Midway Valley based on RF drillhole data and bedrock outcrops, *in* Gibson, J., Swan, F., Wesling, J., Bullard, T., Perman, R., Angell, M., and DiSilvestro, L., Summary and evaluation of existing geological and geophysical data near prospective surface facilities in Midway Valley, Yucca Mountain project, Nye County, Nevada: Sandia National Laboratories SAND90-2491, Appendix A.

Carr, W.J., Byers, F.M., Jr., and Orkild, P.P., 1986, Stratigraphic and volcano-tectonic relations of Crater Flat Tuff and some older volcanic units, Nye County, Nevada: U.S. Geological Survey Professional Paper 1323.

Cashman, P.H., and Trexler, J.H., Jr., 1995, Task 8: Evaluation of hydrocarbon potential, *in* Evaluation of the geologic relations and seismotectonic stability of the Yucca Mountain area, Nevada nuclear waste site investigation: Mackay School of Mines Progress Report 30, University of Nevada, Reno, Nevada.

Castor, S.B., Garside, L.J., Tingley, J.V., LaPointe, D.D., Desilets, M.O., Hsu, L-C., Goldstrand, P.M., Lugaski, T.P., and Ross, H.P., 1999, Assessment of metallic and mined energy resources in the Yucca Mountain Conceptual Controlled Area, Nye County, Nevada: Nevada Bureau of Mines and Geology Open-File Report 99-13, Reno, Nevada.

Castor, S.B., and Lock, D.E., 1995, Assessment of industrial minerals and rocks in the controlled area: Nevada Bureau of Mines and Geology, Reno, Nevada, Yucca Mountain Project Data Tracking Number MO 950000000006.002.

Chipera, S.J., Vaniman, D.T., Carlos, B.A., and Bish, D.L., 1995, Mineralogic variation in drill core UE-25 UZ#16, Yucca Mountain, Nevada: Los Alamos National Laboratory LA-12810-MS.

Christiansen, R.L., 1979, Cooling units and composite sheets in relation to caldera structure: Geological Society of America Special Paper 180, p. 29–42.

Christiansen, R.L., and Lipman, P.W., 1965, Geologic map of the Topopah Spring NW quadrangle, Nye County, Nevada: U.S. Geological Survey Geologic Quadrangle Map GQ 444, scale 1:24,000.

Ciancia, Mala, and Heiken, Grant, 2006, Geotechnical properties of tuffs at Yucca Mountain, Nevada, *in* Heiken, Grant, ed., Tuffs — Their properties, uses, hydrology, and resources: Geological Society of America Special Paper 408, p. 33-89.

Coe, J.A., 2004, Quaternary faulting on the Northern Crater Flat fault, *in* Keefer, W.R., Whitney, J.W., and Taylor, G.M., eds., Quaternary paleoseismology and stratigraphy of the Yucca Mountain area, Nevada: U.S. Geological Survey Professional Paper 1689, p. 145–154.

Coe, J.A., Glancy, P.A., and Whitney, J.W., 1997, Volumetric analysis and hydrologic characterization of a modern debris flow near Yucca Mountain, Nevada: *Geomorphology*, v. 20, p. 11–28.

Coe, J.A., Oswald, J., Vadurro, G., and Lundstrom, S.C., 2004, Quaternary faulting on the Fatigue Wash fault, *in* Keefer, W.R., Whitney, J.W., and Taylor, E.M., eds., Quaternary paleoseismology and stratigraphy of the Yucca Mountain area, Nevada: U.S. Geological Survey Professional Paper 1689, p. 111–124.

Cole, J.C., 1997, Major structural controls on the distribution of pre-Tertiary rocks, Nevada Test Site vicinity, southern Nevada: U.S. Geological Survey Open-File Report 97-533.

Craig, R.W., Reed, R.L., and Spengler, R.W., 1983, Geohydrologic data for test well USW H-6, Yucca Mountain area, Nye County, Nevada: U.S. Geological Survey Open-File Report 83-856.

Crowe, B., Perry, F., Geissman, J., McFadden, L., Wells, S., Murrell, M., Poths, J., Valentine, G., Bowker, L., and Finnegan, K., 1995, Status of volcanism studies for the Yucca Mountain site characterization project: Los Alamos National Laboratory LA-12908-MS.

CRWMS M&O (Civilian Radioactive Waste Management System Management and Operation Contractor), 1996, Borehole geophysics, *in* Synthesis of borehole and surface geophysical studies at Yucca Mountain, Nevada and vicinity: CRWMS & M&O, Las Vegas, Nevada, Report BAAA00000-01717-0200-00015, Rev 00, Volume II.

CRWMS M&O, 1998, Yucca Mountain site description: CRWMS M&O, Las Vegas, Nevada, Report B00000000-01717-5700-00019, Rev 01.

CRWMS M&O, 2000, Yucca Mountain site description: CRWMS M&O, Las Vegas, Nevada, Report TDR-CRW-GS-000001, Rev 01.

CRWMS M&O, 2001, Natural resources assessment: CRWMS M&O, Las Vegas, Nevada, Report ANL-NBS-GS-000001, Rev 00.



CRWMS M&O, 2004, Yucca Mountain Site Description: CRWMS M&O, Las Vegas, Nevada, Report TOR-CRW-GS-000001, Rev 02, ICN 001.

Day, W.C., Dickerson, R.P., Potter, C.J., Sweetkind, D.S., San Juan, C.A., Drake, R.M., II, and Fridrich, C.J., 1998a, Bedrock geologic map of the Yucca Mountain area, Nye County, Nevada: U.S. Geological Survey Geologic Investigations Series Map I-2627, scale 1:24,000.

Day, W.C., Potter, C.J., Sweetkind, D.C., Dickerson, R.P., and San Juan, C.A., 1998b, Bedrock geologic map of the central block area, Yucca Mountain area, Nye County, Nevada; U.S. Geological Survey Geologic Investigations Series I-2601, scale 1:6,000.

Dickerson, R.P., and Drake, R.M., II, 1998, Geologic map of the Paintbrush Canyon area, Yucca Mountain, Nevada: U.S. Geological Survey Open-File Report 97-783, scale 1:6,000.

Dickerson, R.P., and Drake, R.M., II, 2004, Geologic map of south-central Yucca Mountain, Nye County, Nevada: U.S. Geological Survey Miscellaneous Field Studies Map MF-2422, scale 1:6,000. Map can be printed/downloaded at: <http://pubs.usgs.gov/mf2004/mf-2422/>

Diehl, S.F., and Chornack, M.P., 1990, Stratigraphic correlation and petrography of the bedded tuffs, Yucca Mountain, Nye County, Nevada: U.S. Geological Survey Open-File Report 89-3.

Faure, G., 1986, Principles of isotope geology: John Wiley and Sons, New York, New York, 2<sup>nd</sup> edition.

Feighner, M., Johnson, L., Lee, K., Daley, T., Karageorgi, E., Parker, P., Smith, T., Williams, K., Romero, A., and McEvelly, T., 1996, Results and interpretation of multiple geophysical surveys at Yucca Mountain, Nevada: Lawrence Berkeley National Laboratory LBL-38200, 139 p.

Fitterman, D.V., 1982, Magnetometric resistivity survey near Fortymile Wash, Nevada Test Site, Nevada: U.S. Geological Survey Open-File Report 82-401.

Flint, A.L., and Flint, L.E., 1994, Spatial distribution of potential near surface moisture flux at Yucca Mountain, *in* High Level Radioactive Waste Management: Proceedings of the Fifth Annual International Conference, Las Vegas, Nevada, May 22-26, 1994, American Nuclear Society, La Grange, Illinois, v. 4, p. 2352–2358.

Flint, L.E., 1998, Characterization of hydrogeologic units using matrix properties, Yucca Mountain, Nevada: U.S. Geological Survey Water-Resources Investigations Report 97-4243.

- Flynn, T., Buchanan, P., Trexler, D., Shevenell, L., and Garside, L., 1996, Geothermal resource assessment of the Yucca Mountain area, Nye County, Nevada: University and Community College System of Nevada, DI # BA0000000-03255-5705-00002.
- Forester, R.M., Bradbury, J.P., Carter, C., Elvidge-Tuma, A.B., Hemphill, M.L., Lundstrom, S.C., Mahan, S.A., Marshall, B.D., Neymark, L.S., Paces, J.B., Sharpe, S.E., Whelan, J.F., and Wigand, P.E., 1999, The climate and hydrologic history of southern Nevada during the Late Quaternary: U.S. Geological Survey Open-File Report 98-635.
- French, D.E., 2000, Hydrocarbon assessment of the Yucca Mountain vicinity, Nye County, Nevada: Nevada Bureau of Mines and Geology Open-File Report 2000-2.
- Fridrich, C.J., 1999, Tectonic evolution of the Crater Flat Basin, Yucca Mountain region, Nevada, *in* Wright, L.A., and Troxel, B.W., eds., Cenozoic basins of the Death Valley region: Geological Society of America Special Paper 333, p. 169–195.
- Fridrich, C.J., Whitney, J.W., Hudson, M.R., and Crowe, B.M., 1999, Space-time patterns of late Cenozoic extension, vertical axis rotation, and volcanism in Crater Flat basin, southwest Nevada: Geological Society of America Special Paper 333, p. 197-212.
- Frischknecht, F.C., and Raab, P.V., 1984, Time-domain electromagnetic sounds at the Nevada Test Site, Nevada: *Geophysics*, v. 49, p. 981–992.

Frizzell, V.A., Jr., and Shulters, Jacqueline, 1990, Geologic map of the Nevada Test Site, southern Nevada: U.S. Geological Survey Miscellaneous Investigations Series Map I-2046, scale 1:100,000.

Garside, L.J., and Schilling, J.H., 1979, Thermal waters of Nevada: Nevada Bureau of Mines and Geology Bulletin 91, p. 163.

Geslin, J.K., and Moyer, T.C., 1995, Summary of lithologic logging of new and existing boreholes at Yucca Mountain, Nevada, March 1994 to June 1994: U.S. Geological Survey Open-File Report 94-451.

Geslin, J.K., Moyer, T.C., and Buesch, D.C., 1995, Summary of lithologic logging of new and existing boreholes at Yucca Mountain, Nevada, August 1993 to February 1994: U.S. Geological Survey Open-File Report 94-342.

Gile, L.H., Peterson, F.F., and Grossman, R.B., 1966, Morphological and genetic sequences of carbonate accumulation in desert soils: *Soil Science*, v. 101, p. 347-360.

Glancy, P.A., 1994, Evidence of prehistoric flooding and the potential for future extreme flooding at Coyote Wash, Yucca Mountain, Nye County, Nevada: U.S. Geological Survey Open-File Report 92-458.

Gosse, J.C., Harrington, C.D., and Whitney, J.W., 1996, Application of in situ cosmogenic nuclides in the site characterization of Yucca Mountain, Nevada: Material Research Society Symposium Proceedings, v. 412, p. 799-806.

Grow, J.A., Barker, C.E., and Harris, A.G., 1994, Oil and gas exploration near Yucca Mountain, Nevada, *in* High Level Radioactive Waste Management: Proceedings of the Fifth Annual International Conference, Las Vegas, Nevada, May 22-26, 1994, American Nuclear Society, LaGrange, Illinois, v. 3, p. 1298–1315.

Hamilton, W.B., 1988, Detachment faulting in the Death Valley region, California and Nevada, *in* Carr, M.D., and Yount, J.C., eds., Geologic and hydrologic investigations of a potential nuclear waste disposal site at Yucca Mountain, southern Nevada: U.S. Geological Survey Bulletin 1790, p. 51–85.

Harrington, C.D., and Whitney, J.W., 1987, Scanning electron microscope method for rock-varnish dating: Geological Society of America, *Geology*, v. 15, p. 967–970.

Heizler, M.T., Perry, F.V., Crowe, B.M., Peters, Lisa, and Appelt, R., 1999, The age of the Lathrop Wells volcanic center; an  $^{40}\text{Ar}/^{39}\text{Ar}$  dating investigation: *Journal of Geophysical Research*, v. 104, no. B1, p. 767-804.

Hoover, D.L., 1989, Preliminary description of Quaternary and late Pliocene surficial deposits at Yucca Mountain and vicinity, Nye County, Nevada: U.S. Geological Survey Open-File Report 89-359.

Hoover, D.L., and Morrison, J.N., 1980, Geology of the Syncline Ridge area related to nuclear waste disposal, Nevada Test Site, Nye County, Nevada: U.S. Geological Survey Open-File Report 80-942.

Hoover, D.L., Swadley, WC, and Gordon, A.J., 1981, Correlation characteristics of surficial deposits with a description of surficial stratigraphy in the Nevada Test Site region: U.S. Geological Survey Open-File Report 81-512.

Hopkins, D.M., 1975, Time-stratigraphic nomenclature for the Holocene epoch: *Geoderma*, v. 14, p. 2.

Hudson, M.R., Minor, S.A., and Fridrich, C.J., 1996, The distribution, timing, and character of steep-axis rotations in a broad zone of dextral shear in southwestern Nevada: *Geological Society of America Abstracts with Programs*, v. 28, p. A-451.

Imbrie, J., Hays, J.D., Martinson, D.G., McIntyre, A., Mix, A.C., Morley, J.J., Pisias, N.G., Prell, W.L., Shackleton, N.J., 1984, The orbital theory of Pleistocene climate: Support from a revised chronology of the marine  $\delta^{18}\text{O}$  record, *in* Berger, A., Imbrie, J., Hays, J., Kukla,

- G., and Saltzman, B., eds., *Milankovitch and Climate, Part I*: Reidel Publishing Company, Netherlands, p. 269–305.
- Izett, G.A., Obradovich, J.D., and Mehnert, H.H., 1988, The Bishop Ash Bed (middle Pleistocene) and some older (Pliocene and Pleistocene) chemically and mineralogically similar ash beds in California, Nevada, and Utah: U.S. Geological Survey Bulletin 1675, 37 p.
- Keefer, W.R., Whitney, J.W., and Taylor, E.M., eds., 2004, Quaternary paleoseismology and stratigraphy of the Yucca Mountain area, Nevada: U.S. Geological Survey Professional Paper 1689.
- Langenheim, V.E., and Ponce, D.A., 1994, Gravity and magnetic investigations of Yucca Wash, southwest Nevada, *in* High Level Radioactive Waste Management: American Nuclear Society Annual International Conference, 5<sup>th</sup>, Las Vegas, Nev., 1994 Proceedings, v. 4, p. 2272-2278.
- Levy, S.S., and O'Neil, J.R., 1989, Moderate-temperature zeolitic alteration in a cooling pyroclastic deposit: *Chemical Geology*, v. 76, Amsterdam, The Netherlands, Elsevier, p. 321–326.
- Lipman, P.W., Christiansen, R.L., and O'Connor, J.T., 1966, A compositionally zoned ash-flow sheet in southern Nevada: U.S. Geological Survey Professional Paper 524-F.

Lipman, P.W., and McKay, E.J., 1965, Geologic map of the Topopah Spring SW quadrangle, Nye County, Nevada: U.S. Geological Survey Geologic Quadrangle Map GQ-439, scale 1:24,000.

Lundstrom, S.C., Paces, J.B., and Mahan, S.A., 1996, Late Quaternary history of Fortymile Wash, southern Nevada: a record of geomorphic response to climate change in the Yucca Mountain region: Geological Society of America Abstracts with Programs, v. 28, p. A-552.

Lundstrom, S.C., Paces, J.B., and Mahan, S.A., 1998, Late Quaternary History of Fortymile Wash in the area near the H-Road crossing, *in* Taylor, E.M., ed., Quaternary geology of the Yucca Mountain area, southern Nevada: Field Trip Guide, Annual Meeting of the Friends of the Pleistocene, Pacific Cell, October 9-11, 1998, p. 63-76.

Lundstrom, S.C., and Warren, R.G., 1994, Late Cenozoic evolution of Fortymile Wash: Major change in drainage pattern in the Yucca Mountain, Nevada region during late Miocene volcanism, *in* High Level Radioactive Waste Management: Proceedings of the Fifth Annual International Conference, Las Vegas, Nevada, May 22-26, 1994, American Nuclear Society, La Grange, Illinois, v. 4, p. 2121-2130.

Majer, E.L., Feighner, M., Johnson, L., Daley, T., Karageorgi, E., Lee, K., Williams, K., and McEvelly, T., 1996, Surface geophysics: Volume I of synthesis of borehole and surface



geophysical studies at Yucca Mountain, Nevada and vicinity: Lawrence Berkeley National Laboratory, Berkeley, California, Report UCID-39319

Maldonado, F., and Koether, S.L., 1983, Stratigraphy, structure, and some petrographic features of volcanic rocks at the USW G-2 drill hole, Yucca Mountain, Nye County, Nevada: U.S. Geological Survey Open-File Report 83-732.

Martin, R.J., Price, R.H., Boyd, P.J., and Noel, J.S., 1994, Bulk and mechanical properties of the Paintbrush Tuff recovered from borehole USW NRG-6: Data report: Sandia National Laboratories SAND93-4020.

Martin, R.J., Price, R.H., Boyd, P.J., and Noel, J.S., 1995, Bulk and mechanical properties of the Paintbrush Tuff recovered from borehole USW NRG 7/7A: Data report: Sandia National Laboratories SAND94-1996.

McDonald, E., and McFadden, L.D., 1994, Quaternary stratigraphy of the Providence Mountains piedmont and preliminary age estimates and regional stratigraphic correlations of Quaternary deposits in the eastern Mojave Desert, California, *in* McGill, S.F., and Ross, T.M., eds., Geological investigations of an active margin: Geological Society of America, Cordilleran Section, Fieldtrip Guidebook 8, p. 205–213.

- McFadden, L.D., and Weldon, R.J., III, 1987, Rates and processes of soil development on Quaternary terraces in Cajon Pass, California: *Geological Society of America Bulletin*, v. 98, p. 280–293.
- McFadden, L.D., Wells, S.G., and Jercinovich, M.J., 1987, Influences of eolian and pedogenic processes on the origin and evolution of desert pavements: *Geological Society of America, Geology*, v. 15, p. 504–508.
- McGovern, T.F., 1983, An evaluation of seismic reflection studies in the Yucca Mountain area, Nevada Test Site: U.S. Geological Survey Open-File Report 83-912.
- Menges, C.M., Taylor, E.M., Vadurro, G., Oswald, J.A., Cress, R., Murray, M., Lundstrom, S.C., Paces, J.B., and Mahan, S.A., 1997, Logs and paleoseismic interpretations from trenches 14C and 14D on the Bow Ridge fault, northeastern Yucca Mountain, Nye County, Nevada: U.S. Geological Survey Miscellaneous Field Studies Map 2311.
- Menges, C.M., Taylor, E.M., Wesling, J.R., Swan, F.H., Coe, J.A., Ponti, D.J., and Whitney, J.W., 2004, Summary of Quaternary faulting on the Paintbrush Canyon, Stagecoach Road, and Bow Ridge faults, *in* Keefer, W.R., Whitney, J.W., and Taylor, E.M., eds., *Quaternary paleoseismology and stratigraphy of the Yucca Mountain area, Nevada*: U.S. Geological Survey Professional Paper 1689, p. 41–69.

Menges, C.M., Wesling, J.R., Whitney, J.W., Swan, F.H., Coe, J.A., Thomas, A.P., and Oswald, J.A., 1994, Preliminary results of paleoseismic investigations of Quaternary faults on eastern Yucca Mountain, Nye County, Nevada, *in* High Level Radioactive Waste Management: Proceedings of the Fifth Annual International Conference, Las Vegas, Nevada, May 22-26, 1994, American Nuclear Society, La Grange, Illinois, v. 4, p. 2373–2390.

Menges, C.M., and Whitney, J.W., 2004, Distribution of Quaternary faults at Yucca Mountain, *in* Keefer, W.R., Whitney, J.W., and Taylor, E.M., eds., Quaternary paleoseismology and stratigraphy of the Yucca Mountain area, Nevada: U.S. Geological Survey Professional Paper 1689, p. 23–31.

Minor, S.A., 1995, Superposed local and regional paleostresses: Fault-slip analysis of Neogene extensional faulting near coeval caldera complexes, Yucca Flat, Nevada: *Journal of Geophysical Research*, v. 100, p. 10507–10528.

Minor, S.A., Hudson, M.R., and Fridrich, C.J., 1996, Fault-slip data bearing on the Miocene tectonic development of northern Crater Flat basin, southern Nevada: *Geological Society of America Abstracts with Programs*, v. 28, p. A-192.

Minor, S.A., Sawyer, D.A., Wahl, R.R., Frizzell, V.A., Jr., Schilling, S.P., Warren, R.G., Orkild, P.P., Coe, J.A., Hudson, M.R., Fleck, R.J., Lanphere, M.A., Swadley, WC, and Cole,

- J.C., 1993, Preliminary geologic map of the Pahute Mesa 30' X 60' quadrangle: U.S. Geological Survey Open-File Report 93-299.
- Mongano, G.S., Singleton, W.L., Moyer, T.C., Beason, S.C., Eatman, G.L.W., Albin, A.L., and Lang, R.C., 1999, Geology of the ECRB Cross Drift — Exploratory Studies Facility, Yucca Mountain Project, Yucca Mountain, Nevada: Summary Report by the U.S. Bureau of Reclamation to the U.S. Department of Energy, Yucca Mountain Project Data Tracking Number GS990908314224.010, 46 p., 4 plates.
- Monsen, S.A., Carr, M.D., Reheis, M.C., and Orkild, P.P., 1992, Geologic map of Bare Mountain, Nye County, Nevada: U.S. Geological Survey Miscellaneous Investigations Map I-2201, scale 1:24,000.
- Montazer, P., and Wilson, W.E., 1984, Conceptual hydrologic model of flow in the unsaturated zone, Yucca Mountain, Nevada: U.S. Geological Survey Water-Resources Investigations Report 84-4345.
- Morrison, R.B., 1991, Introduction, *in* Morrison, R.B., ed., Quaternary nonglacial geology — conterminous U.S.: Geological Society of America, The Geology of North America, v. K-2, p. 1–12.

Moyer, T.C., and Geslin, J.K., 1995, Lithostratigraphy of the Calico Hills Formation and Prow Pass Tuff (Crater Flat Group) at Yucca Mountain, Nevada: U.S. Geological Survey Open-File Report 94-460.

Moyer, T.C., Geslin, J.K., and Buesch, D.C., 1995, Summary of lithologic logging of new and existing boreholes at Yucca Mountain, Nevada, July 1994 to November, 1994: U.S. Geological Survey Open-File Report 95-102.

Moyer, T.C., Geslin, J.K., and Flint, L.E., 1996, Stratigraphic relations and hydrologic properties of the Paintbrush Tuff nonwelded (PTn) hydrologic unit, Yucca Mountain, Nevada: U.S. Geological Survey Open-File Report 95-397.

Muller, D.C., and Kibler, J.E., 1984, Preliminary analysis of geophysical logs from drill hole UE-25p#1, Yucca Mountain, Nye County, Nevada: U.S. Geological Survey Open-File Report 84-649, 14 p.

Munsell Color Company, Inc., 1988, Munsell soil color charts: Baltimore, Maryland.

Nelson, P.H., 1993, Estimation of water-filled and air-filled porosity in the unsaturated zone, Yucca Mountain, Nevada, *in* High Level Radioactive Waste Management: Proceedings of the Fourth Annual International Conference, Las Vegas, Nevada, April 26-30, 1993, American Nuclear Society, La Grange, Illinois, v. 1, p. 949-954.

Nelson, P.H., 1994, Saturation levels and trends in the unsaturated zone, Yucca Mountain, Nevada, *in* High Level Radioactive Waste Management: Proceedings of the Fifth Annual International Conference, Las Vegas, Nevada, May 22-26, 1994, American Nuclear Society, La Grange, Illinois, v. 4, p. 2774–2781.

Nelson, P.H., 1996, Computation of porosity and water content from geophysical logs, Yucca Mountain, Nevada: U.S. Geological Survey Open-File Report 96-078.

Nelson, P.H., Muller, D.C., Schimschal, U., and Kibler, J.E., 1991, Geophysical logs and core measurements from forty boreholes at Yucca Mountain, Nevada: U.S. Geological Survey Geophysical Investigations Map GP-1001.

Nevada Bureau of Mines and Geology, 1997, The Nevada mineral industry 1996: Nevada Bureau of Mines and Geology Special Publication MI-1996.

Nichols, K.K., Bierman, P.R., Foniri, W.R., Gillespie, A.R., Caffee, M. and Finkel, R., 2006, Dates and rates of arid region geomorphic processes: *GSA Today*, v. 16, p. 4-10.

Noble, D.C., and Hedge, C.E., 1969, Sr87/Sr86 variations within individual ash-flow sheets: U.S. Geological Survey Professional Paper 650-C, p. C133–C139.

- Ortiz, T.S., Williams, R.L., Nimick, F.B., Whittet, B.C., and South, D.L., 1985, A three-dimensional model of reference thermal/mechanical and hydrological stratigraphy at Yucca Mountain, southern Nevada: Sandia National Laboratories SAND84-1076.
- Osterkamp, W.R., Lane, L.J., and Savard, C.S., 1994, Recharge estimates using a geomorphic/distributed-parameter simulation approach, Amargosa River Basin: Water Resources Association Water Resources Bulletin, v. 30, p. 493–506.
- Pabst, M.E., Beck, D.A., Glancy, P.A., and Johnson, J.A., 1993, Streamflow and selected precipitation data for Yucca Mountain and vicinity, Nye County, Nevada, water years 1983-85: U.S. Geological Survey Open-File Report 93-438.
- Pankratz, L.W., 1982, Reconnaissance seismic refraction studies at Calico Hills, Wahmonie, and Yucca Mountain, southwest Nevada Test Site, Nye County, Nevada: U.S. Geological Survey Open-File Report 82-478.
- Peterman, Z.E., and Futa, K., 1996, Geochemistry of core samples of the Tiva Canyon Tuff from drill hole UE-25 NRG#3, Yucca Mountain, Nevada: U.S. Geological Survey Open-File Report 95-325.
- Peterman, Z.E., Spengler, R.W., Singer, F.R., and Dickerson, R.P., 1993, Isotopic and trace element variability in altered and unaltered tuffs at Yucca Mountain, Nevada, *in* High Level Radioactive Waste Management: Proceedings of the Fourth Annual International

Conference, Las Vegas, Nevada, April 26-30, 1993, American Nuclear Society, La Grange, Illinois, v. 2, p. 1940–1947.

Ponce, D.A., 1993, Geophysical investigations of concealed faults near Yucca Mountain, southwest Nevada, *in* High Level Radioactive Waste Management: Proceedings of the Fourth Annual International Conference, Las Vegas, Nevada, April 26-30, 1993, American Nuclear Society, La Grange, Illinois, v. 1, p. 168–174.

Ponce, D.A., and Langenheim, V.E., 1994, Preliminary gravity and magnetic models across Midway Valley and Yucca Wash, Yucca Mountain, Nevada: U.S. Geological Survey Open-File Report 94-572.

Potter, C.J., Day W.C., Sweetkind, D.S., and Dickerson, R.P., 2004, Structural geology of the proposed site area for a high-level radioactive waste repository, Yucca Mountain, Nevada: Geological Society of America Bulletin, v. 116, no. 7/8, p. 858–879.

Potter, C.J., Dickerson, R.P., and Day, W.C., 1999, Nature and continuity of the Sundance fault, Yucca Mountain, Nevada: U.S. Geological Survey Open-File Report 98-266.

Potter, C.J., Dickerson, R.P., Sweetkind, D.S., Drake, R.M., II, Taylor, E.M., Fridrich, C.J., San Juan, C.A., and Day, W.C., 2002a, Geologic map of the Yucca Mountain region, Nye County, Nevada: U.S. Geological Survey Geologic Investigations Series I-2755, scale 1:50,000.



Potter, C.J., Sweetkind, D.S., Dickerson, R.P., and Kilgore, M.L., 2002b, Hydrostructural maps of the Death Valley regional flow system, Nevada and California: U.S. Geological Survey Miscellaneous Field Studies Map MF-2372, scale 1:350,000.

Ramelli, A.R., Oswald, J.A., Vadurro, G., Menges, C.M., and Paces, J.B., 2004, Quaternary faulting on the Solitario Canyon fault, *in* Keefer, W.R., Whitney, J.W., and Taylor, E.M., eds., Quaternary paleoseismology and stratigraphy of the Yucca Mountain area: U.S. Geological Survey Professional Paper 1689, p. 89–109.

Reheis, M.C., and Kihl, R., 1995, Dust deposition in southern Nevada and California, 1984-1989: Relations to climate, source area, and source lithology: American Geophysical Union Journal of Geophysical Research, v. 100, p. 8893–8918.

Reheis, M.C., Sowers, J.M., Taylor, E.M., McFadden, L.D., and Harden, J.W., 1992, Morphology and genesis of carbonate soils on the Kyle Canyon fan, Nevada, U.S.A.: Geoderma, v. 52, p. 303–342.

Reynolds and Associates, 1985, Final report, 1985 repository surface facility seismic survey, Yucca Mountain area, NTS, Nye County, Nevada: Charles B. Reynolds and Associates, Albuquerque, New Mexico, Report # MOL.19970415.0158.

- Robinson, G.D., 1985, Structure of pre-Cenozoic rocks in the vicinity of Yucca Mountain, Nye County, Nevada – a potential nuclear-waste disposal site: U.S. Geological Survey Bulletin 1647.
- Rosenbaum, J.G., Hudson, M.R., and Scott, R.B., 1991, Paleomagnetic constraints on the geometry and timing of deformation at Yucca Mountain, Nevada: American Geophysical Union Journal of Geophysical Research, v. 96, p. 1963–1979.
- Rush, F.E., Thordarson, W., and Pyles, D.G., 1984, Geohydrology of test well USW H-1, Yucca Mountain, Nye County, Nevada: U.S. Geological Survey Water-Resources Investigations Report 84-4032.
- Sarna-Wojcicki, A.M., Meyer, C.E., Wau, E., and Soles, S., 1993, Age and correlation of tephra layers in Owens Lake drill core OL-92-1 and -2: U.S. Geological Survey Open-File Report 93-683.
- Sawyer, D.A., Fleck, R.J., Lanphere, M.A., Warren, R.G., Broxton, D.E., and Hudson, M.R., 1994, Episodic caldera volcanism in the Miocene southwestern Nevada volcanic field: revised stratigraphic framework,  $^{40}\text{Ar}/^{39}\text{Ar}$  geochronology, and implications for magmatism and extension: Geological Society of America Bulletin 106, p. 1304–1318.

Schenker, A.R., Guerin, D.C., Robey, T.H., Rautman, C.A., and Barnard, R.W., 1995, Stochastic hydrogeologic units and hydrogeologic properties development for total-system performance assessments: Sandia National Laboratories SAND94-0244.

Scott, R.B., 1990, Tectonic setting of Yucca Mountain, southwest Nevada, *in* Wernicke, B.P., ed., Basin and Range extensional tectonics near the latitude of Las Vegas, Nevada: Geological Society of America Memoir 176, p. 251–282.

Scott, R.B., 1992, Preliminary geologic map of southern Yucca Mountain, Nye County, Nevada: U.S. Geological Survey Open-File Report 92-266, scale 1:12,000.

Scott, R.B., Bath, G.D., Flanigan, V.J., Hoover, D.B., Rosenbaum, J.G., and Spengler, R.W., 1984, Geological and geophysical evidence of structures in northwest-trending washes, Yucca Mountain, southern Nevada, and their possible significance to a nuclear waste repository in the unsaturated zone: U.S. Geological Survey Open-File Report 84-567.

Scott, R.B., and Bonk, Jerry, 1984, Preliminary geologic map of Yucca Mountain, Nye County, Nevada, with geologic sections: U.S. Geological Survey Open-File Report 84-494, scale 1:12,000.

Senterfit, R.M., Hoover, D.B., and Chornack, M.P., 1982, Resistivity sounding investigation by the Schlumberger method in the Yucca Mountain and Jackass Flats area, Nevada Test Site, Nevada: U.S. Geological Survey Open-File Report 82-1043.

Simonds, F.W., Whitney, J.W., Fox, K.F., Ramelli, A.R., Yount, J.C., Carr, M.D., Menges, C.M., Dickerson, R.P., and Scott, R.B., 1995, Map showing fault activity in the Yucca Mountain area, Nye County, Nevada: U.S. Geological Survey Miscellaneous Investigations Map I-2520, 1:24,000 scale.

Smith, C., and Ross, H.P., 1982, Interpretation of resistivity and induced polarization profiles with severe topographic effects, Yucca Mountain area, Nevada Test Site, Nevada: U.S. Geological Survey Open-File Report 82-182, 82 p.

Smith, R.L., 1960a, Ash flows: Geological Society of America Bulletin, v. 71, p. 795–842.

Smith, R.L., 1960b, Zones and zonal variations in welded ash flows: U.S. Geological Survey Professional Paper 354-F, p. 149–159.

Spengler, R.W., Byers, F.M., Jr., and Warner, J.B., 1981, Stratigraphy and structure in volcanic rocks in drill hole USW-G1, Yucca Mountain, Nye County, Nevada: U.S. Geological Survey Open-File Report 81-1349.

Spengler, R.W., and Chornack, M.P., 1984, Stratigraphic and structural characteristics of volcanic rocks in corehole USW-G4, Yucca Mountain, Nevada, with a section on geophysical logs by D.C. Muller and J.E. Kibler: U.S. Geological Survey Open-File Report 84-789.

Spengler, R.W., and Peterman, Z.E., 1991, Distribution of rubidium, strontium, and zirconium in tuff from two deep coreholes at Yucca Mountain, Nevada, *in* High Level Radioactive Waste Management: Proceedings of the Second Annual International Conference, Las Vegas, Nevada, April 28-May 3, 1991, American Nuclear Society, La Grange, Illinois, v. 2, p. 1416–1422.

Squires, R.R., and Young, R.L., 1984, Flood potential of Fortymile Wash and its principal southwestern tributaries, Nevada Test Site, southern Nevada: U.S. Geological Survey Water-Resources Investigations Report 83-4001.

Stamatakos, J.A., and Ferrill, D.A., 1998, Strike-slip fault system in Amargosa Valley and Yucca Mountain, Nevada—comment: *Tectonophysics* 294, p. 151–160.

Stewart, J.H., 1988, Tectonics of the Walker Lane belt, western Great Basin: Mesozoic and Cenozoic deformation in a zone of shear, *in* Ernst, W.G., ed., *Metamorphism and crustal evolution of the Western United States*: Prentice-Hall, Englewood Cliffs, New Jersey, Rubey Volume 7, p. 683–713.

Stuckless, J.S., Marshall, B.D., Vaniman, D.T., Dudley, W.W., Peterman, Z.E., Paces, J.B., Whelan, J.F., Taylor, E.M., Forester, R.M., and O’Leary, D.W., 1998, Comments on “Overview of calcite/opal deposits at or near the proposed high-level nuclear waste site, Yucca Mountain, Nevada, USA: pedogenic, hypogene, or both,” by C.A. Hill, Y.V.

Dublyansky, R.S. Harmon, and C.M. Schluter: *Environmental Geology*, v. 34, no. 1, p. 70–78.

Swadley, WC, Hoover, D.L., and Rosholt, J.N., 1984, Preliminary report on late Cenozoic faulting and stratigraphy in the vicinity of Yucca Mountain, Nye County, Nevada: U.S. Geological Survey Open-File Report 84-788.

Swan, F.W., Wesling, J.R., Angell, M.M., Thomas, A.P., Whitney, J.W., and Gibson, J.D., 2001, Evaluation of the location and recency of faulting near prospective surface facilities in Midway Valley, Nye County, Nevada: U.S. Geological Survey Open-File Report 01-55.

Sweetkind, D.S., Anna, L.O., Williams-Stroud, S.C., and Coe, J.A., 1997, Characterizing the fracture network at Yucca Mountain, Nevada: Part 1, Integration of field data with simulations, *in* Hoak, T.E., Klawitter, A.L., and Bloomquist, P.K., eds., *Fractured reservoirs: Characterization and modeling*: Rocky Mountain Association of Geologists, *Characterization and Modeling Guidebook* — 1997, p. 185–196.

Sweetkind, D.S., Dickerson, R.P., Blakely, R.J., and Denning, P.D., 2001, Interpretive geologic cross section for the Death Valley regional flow system and surrounding areas, Nevada and California: U.S. Geological Survey Miscellaneous Field Studies Map MF-2370.

Tanko, D.J., and Glancy, P.A., 2001, Flooding in the Amargosa River drainage basin, February 23-24, 1998, southern Nevada and eastern California, including the Nevada Test Site: U.S. Geological Survey Fact Sheet 036-01.

Taylor, E.M., 1986, Impact of time and climate on Quaternary soils in the Yucca Mountain area of the Nevada Test Site [M.S. thesis]: Boulder, Colorado, University of Colorado.

Taylor, E.M., 2004, Quaternary faulting on the Southern Crater Flat fault, *in* Keefer, W.R., Whitney, J.W., and Taylor, G.M., eds., Quaternary paleoseismology and stratigraphy of the Yucca Mountain area, Nevada: U.S. Geological Survey Professional Paper 1689, p. 135–144.

Taylor, E.M., Menges, C.M., and Beason, S.C., 1998, Characteristics of the Ghost Dance fault at Yucca Mountain, Nevada, *in* High Level Radioactive Waste Management: Proceedings of the Eighth Annual International Conference, Las Vegas, Nevada, May 11-14, 1998, American Nuclear Society, La Grange, Illinois, p. 279–282.

Taylor, E.M., Menges, C.M., and Buesch, D.C., 2004, Results of paleoseismic investigations on the Ghost Dance fault, *in* Keefer, W.R., Whitney, J.W., and Taylor, E.M., eds., Quaternary paleoseismology and stratigraphy of the Yucca Mountain area, Nevada: U.S. Geological Survey Professional Paper 1689, p. 71–88.

- Trexler, J.H., Jr., Cole, J.C., and Cashman, P.H., 1996, Middle Devonian-Mississippian stratigraphy on and near the Nevada Test Site: Implications for hydrocarbon potential: American Association of Petroleum Geologists Bulletin, v. 80, p. 1736–1762.
- U.S. Department of Energy, 1988, Site characterization plan: DOE/RW-0199, Office of Civilian Radioactive Waste Management, Washington, D.C.
- U.S. Department of Energy, 1993, Evaluation of the potential adverse condition “Evidence of extreme erosion during the Quaternary Period” at Yucca Mountain, Nevada: U.S. Department of Energy Topical Report YMP/92-41-TPR, 71 p.
- U.S. Geological Survey, 1984, A Summary of geologic studies through January 1, 1983, of a potential high-level radioactive waste repository site at Yucca Mountain, southern Nye County, Nevada: U.S. Geological Survey Open-File Report 44-792.
- Vaniman, D., Bish, D., Broxton, D., Byers, F., Heiken, G., Carlos, B., Semarge, E., Caporuscio, F., and Gooley, R., 1984, Variations in authigenic mineralogy and sorptive zeolite abundance at Yucca Mountain, Nevada, based on studies of drill cores USW GU-3 and G-3: Los Alamos National Laboratory LA-9707-MS.
- Warren, R.G., Sawyer, D.A., and Covington, H.R., 1989, Revised volcanic stratigraphy of the southwestern Nevada volcanic field, *in* Olsen, C.W., and Carter, J.A., eds., Proceedings of the fifth symposium on containment of underground nuclear explosions, Santa



Barbara, California, September 19-21, 1989: Mission Research Corporation CONF-8909163, v. 2, p. 387.

Wesling, J.R., Bullard, T.F., Swan, F.H., Perman, R.C., Angell, M.M., and Gibson, J.D., 1992, Preliminary mapping of surficial geology of Midway Valley, Yucca Mountain, Nye County, Nevada: Sandia National Laboratories Report SAND91-0607, 55 p., scale 1:6,000.

Whitney, J.W., and Harrington, C.D., 1993, Relict colluvial boulder deposits as paleoclimate indicators in the Yucca Mountain region, southern Nevada: Geological Society of America Bulletin, v. 105, p. 1008–1018.

Whitney, J.W., Simonds, F.W., Shroba, R.R., and Murray, Michele, 2004a, Quaternary faulting on the Windy Wash fault, *in* Keefer, W.R., Whitney, J.W., and Taylor, E.M., eds., Quaternary paleoseismology and stratigraphy of the Yucca Mountain area, Nevada: U.S. Geological Survey Professional Paper 1689, p. 125–134.

Whitney, J.W., Swadley, WC, and Shroba, R.R., 1985, Middle Quaternary sand ramps in the southern Great Basin, California and Nevada: Geological Society of America Abstracts with Programs, v. 17, p. 750.

Whitney, J.W., Taylor, E.M., and Menges, C.M., 2004b, Introduction to Quaternary paleoseismology and stratigraphy of the Yucca Mountain area, Nevada, *in* Keefer, W.R.,

Whitney, J.W., and Taylor, E.M., eds., Quaternary seismology and stratigraphy of the Yucca Mountain area, Nevada: U.S. Geological Survey Professional Paper 1689, p. 1–10.

Whitney, J.S., Taylor, E.M., and Wesling, J.R., 2004c, Quaternary mapping and stratigraphy, *in* Keefer, W.R., Whitney, J.R., and Taylor, E.M., Quaternary paleoseismology and stratigraphy of the Yucca Mountain area, Nevada: U.S. Geological Survey Professional Paper 1689, p. 11–21.

Winograd, I.J., and Thordarson, W., 1975, Hydrogeology and hydrochemical framework, south-central Great Basin, Nevada-California, with special reference to the Nevada Test Site: U.S. Geological Survey Professional Paper 712-C.

Winograd, I.J., Szabo, B.J., Copen, T.B., and Riggs, A.C., 1988, A 250,000-year climate record from Great Basin vein calcite: Implications for Milankovitch theory: American Association for the Advancement of Science, *Science*, v. 242, p. 1275–1280.

## FIGURES

Figure 1. Generalized geologic map showing distribution of major lithostratigraphic units in the Yucca Mountain site area and vicinity. Claim Canyon caldera is in southern part of the southwestern Nevada volcanic field. Modified from Potter et al. (2002a).

Figure 2. Map of Yucca Mountain site area showing distribution of principal stratigraphic units, major faults, and locations of geographic features named in text. Faults shown with solid lines, although some segments are concealed or inferred beneath Quaternary deposits. Labeled faults: BR, Bow Ridge; FW, Fatigue Wash; IR, Iron Ridge; PC, Paintbrush Canyon; SC, Solitario Canyon; WW, Windy Wash. Generalized from Day et al. (1998a).

Figure 3. Low-oblique aerial photograph looking southeast across Yucca Mountain, with floor of Solitario Canyon in foreground. Note scarp-like nature of west slope of Yucca Mountain and the dissected terrain across the gently sloping east side. Light-colored band toward top of west slope is the Paintbrush Tuff nonwelded hydrogeologic unit (PTn), which here is about 30 meters (100 feet) thick, and underlying ledge is top of densely welded subzone of the vitric zone of the crystal-rich member of the Topopah Spring Tuff. Crest of Yucca Mountain is about 215 meters (700 feet) above floor of Solitario Canyon. Photo courtesy of D.W. Wehner, Bechtel-SAIC Corp. Ltd.

Figure 4. View looking south along west-facing scarp of the Windy Wash fault. Photograph courtesy of C.J. Potter, U.S. Geological Survey.

Figure 5. Lithostratigraphic zones in the Tiva Canyon and Topopah Spring Tuffs at Yucca Mountain. Adapted from Buesch et al. (1996a). Not to scale.

Figure 6. Photomicrograph of vitric (A) and densely welded (B) rocks in the crystal-poor member of the Tiva Canyon Tuff. Figure 6A is about 6x8 millimeters and shows vitric, nonwelded colorless bubblewall shards in a matrix of glass dust; matrix porosity is approximately 25-35 volume percent. Figure 6B is about 12x12 millimeters, and shows vitric, densely welded tuff with no microscopic porosity; interstitial dust is fused. Photomicrograph courtesy of F.R. Singer, Epsilon Systems Solutions, Inc.

Figure 7. Graph showing concentrations, with depth, of titanium (Ti) and zirconium (Zr) for core samples from borehole UE-25a#1. Location of borehole shown in Figure 8. Stratigraphic units: Tpc, Tiva Canyon Tuff; Tp, Yucca Mountain and Pah Canyon Tuffs; Tpt, Topopah Spring Tuff; Tac, Calico Hills Formation; Tcp, Prow Pass Tuff; Tcb, Bullfrog Tuff. From Peterman et al. (1993).

Figure 8. Map of Yucca Mountain site area showing locations of stratigraphic cross sections (Figs. 10, 11), boreholes mentioned in text, and cross sections across Fortymile Wash (Fig. 14). (Note: borehole numbers not shown with prefixes UE-25 or USW.) Bedrock areas shown in gray, Quaternary deposits are white. Coordinates in UTM, Zone 11)

Figure 9. Lithostratigraphy and porosity from cores and geophysical logs and quantitative mineralogy from x-ray diffraction on rock samples from borehole UE-25 UZ#16. Location of borehole shown in Figure 8. Stratigraphic units: Qal, Quaternary alluvium; Tpc, Tiva Canyon Tuff; Tp, bedded tuffs and upper part of the crystal-rich member of Topopah Spring Tuff; Tpt, Topopah Spring Tuff; Tac, Calico Hills Formation, lowermost part of Topopah Spring Tuff, and bedded tuff; Tcp, Prow Pass Tuff. Abbreviations: ft, feet; cm<sup>3</sup>, cubic centimeter; 105, sample oven-dried at 105°Celsius; RH, relative humidity. Note that values for minor minerals in right-hand column are given on a reverse scale (zero to right). Modified from Chipera et al. (1995).

Figure 10. East-west stratigraphic cross section. Datum is top of Topopah Spring Tuff; structure not shown. Abbreviations: Qa, Quaternary alluvium; El., ground elevation; T.D., total depth. Based on formation tops identified in the plotted boreholes by R.W. Spengler and D.C. Buesch (U.S. Geological Survey, unpublished data). Bedded tuff units are included at the base of overlying formation. Location of section shown in Figure 8.

Figure 11. North-south stratigraphic cross section. Datum is top of Topopah Spring Tuff; structure not shown. Abbreviations: Qa, Quaternary alluvium; El., ground elevation; T.D., total depth. Based on formation tops identified in plotted boreholes by R.W. Spengler and D.C. Buesch (U.S. Geological Survey, unpublished data). Bedded tuff units are included at base of overlying formation. Location of section shown in Figure 8.

Figure 12. Generalized surficial geologic map of the Yucca Mountain site area. Modified from Potter et al. (2002a).

Figure 13. Plot showing age distribution of mapped Quaternary units Qa2-Qa5 in Midway Valley and Fortymile Wash. Shaded areas represent the main periods of deposition and (or) soil development. Each of the horizontal axes is a relative scale for each probability density function expressed in percent probability per thousand years. Footnotes: a, Matuyama-Brunhes chronozone boundary (Morrison, 1991); b, astronomical age of marine oxygen-isotope substage 5e boundary (Imbrie et al., 1984); c, arbitrary age suggested for Pleistocene-Holocene boundary (Hopkins, 1975). Ages given in thousands of years; note scale change at 100,000 years. From Whitney et al. (2004c; unit ages determined by J.D. Paces and S.A. Mahan, U.S. Geological Survey).

Figure 14. Generalized cross sections showing evolution of Fortymile Wash. Locations of sections shown in Figure 8. Based on CRWMS M&O (2000, Figure 7.4-4).

Figure 15. View looking north toward south slope of Jake Ridge (location shown in Fig. 2), showing debris flows and flow tracks (light-colored strips) resulting from intense storm activity on July 21-22, 1984. Photograph courtesy of J.A. Coe, U.S. Geological Survey.

Figure 16. Map showing distribution of faults in Yucca Mountain site area and adjacent areas to south and west. Fault names in bold print indicate faults with demonstrable Quaternary movement; all faults are shown with solid lines although many segments are concealed or

inferred. Symbols and abbreviations: bar and bell, downthrown side of fault; arrows, relative direction of strike-slip movement; ESF, Exploratory Studies Facility; CD, Cross Drift. Rectangle defines site area. Based on Potter et al. (2002a).

Figure 17. East-west structure section across Yucca Mountain site area. Line of section shown in Figure 16. Not all faults shown are plotted in Figure 16. Datum is mean sea level. ESF, position of Exploratory Studies Facility at intersection with line of section. Simplified from Day et al. (1998a, cross section B-B').

Figure 18. Exposure of Paintbrush Canyon fault displacing surficial deposits (west side down) on west side of Busted Butte. View is south-southwest, with the Lathrop Wells volcanic center on skyline to right (location shown in Fig. 1). Photograph courtesy of J.A. Coe, U.S. Geological Survey.

Figure 19. Map showing location of geophysical surveys in the Yucca Mountain site area. Shaded areas are exposed volcanic bedrock. Seismic reflection data were collected along all lines labeled "REG" and "YMP". REG-2 and REG-3 are regional reflection lines (Brocher et al., 1998) and HR-I and HR-2 are very high-resolution seismic reflection lines (station spacings 1-2 meters); all others are standard high-resolution seismic reflection lines (station spacing 6-12 meters; Feighner et al., 1996). Ground-based gravity data were collected along all lines, except YMP-3 top, YMP-4 top, YMP-7, HR-I, HR-2, and Line-1. Ground magnetic data were collected along all lines except YMP-3 top, YMP-3 ext, YMP-4 top, YMP-4 ext, HR-2, and Line-1. Magnetelluric data were

collected only along YMP-3. Lines G1, G2, and G4 are gravity and magnetic surveys of Ponce and Langenheim (1994). Adapted from Swan et al. (2001).



## **TABLES**

Table 1. Generalized stratigraphic column of Tertiary volcanic rocks in the Yucca Mountain site area.

Table 2. Summary of diagnostic surface and soil properties of Quaternary map units at Yucca Mountain.

Table 3. Maximum bedrock erosion rates on Yucca Mountain.

Table 4. Varnish cation ratio age estimates from boulder deposits around Yucca Mountain.

Table 5. Ages of four boulder deposits around Yucca Mountain.

**TABLE 1. GENERALIZED STRATIGRAPHIC COLUMN OF TERTIARY VOLCANIC ROCKS IN THE YUCCA MOUNTAIN SITE AREA**

Group	Formation/Unit	Thickness in Site Area <sup>1</sup> (meters)	General Lithology	Correlative Units				
				Hydro-Geologic <sup>2</sup>	Thermal-Mechanical <sup>3</sup>			
Timber Mountain	Ammonia Tanks Tuff	Not present in site area	Welded to nonwelded rhyolite tuff	Unconsolidated surficial material	Undifferentiated overburden			
	Rainier Mesa Tuff	Generally <30	High-silica rhyolite and quartz latite tuffs					
	Pre-Rainier Mesa Tuff bedded tuff	17 <sup>4</sup>	Nonlithified pyroclastic-flow deposits					
Paintbrush	Rhyolite of Comb Peak	≤130	Rhyolite lava flows and related tephra; pyroclastic-flow deposits					
	Tuff Unit "X"	6–23 <sup>5</sup>						
	Rhyolite of Vent Pass	0–150						
	Post Tiva Canyon Tuff bedded tuff	<2–4.5	Pyroclastic-flow and fallout tephra deposits					
	Tiva Canyon Tuff	Crystal-rich member	<50–175			Compositionally zoned (rhyolite to quartz latite) tuff sequence; each member divided into several zones and subzones <sup>6</sup>	_____ a _____	_____ a _____
		Crystal-poor member					_____ b _____	_____ b _____
	Pre-Tiva Canyon Tuff bedded tuff	<1–3 <sup>7</sup>	Pyroclastic fallout tephra deposits with thin weathered zones					
	Yucca Mountain Tuff	0–55	Nonwelded to densely welded pyroclastic-flow deposit	Paintbrush Tuff nonwelded (PTn)	Paintbrush Tuff nonwelded (PTn)			
	Rhyolite of Black Glass Canyon	2–14	Rhyolite lava flows and related tephra					
	Rhyolite of Delirium Canyon	≤250 (lava) ≤100 (ash flows)						
	Rhyolite of Zig Zag Hill	≤10						
Pre-Yucca Mountain Tuff bedded tuff	<1–46 <sup>7</sup>	Nonwelded pyroclastic-flow deposits						
Pah Canyon Tuff	0–79	Pyroclastic-flow deposits; abundant large pumice clasts						
Pre-Pah Canyon Tuff bedded tuff	3–10 <sup>7</sup>	Vitric to devitrified and altered fallout tephra and ash-flow tuff						

**TABLE 1. GENERALIZED STRATIGRAPHIC COLUMN OF TERTIARY VOLCANIC ROCKS IN THE YUCCA MOUNTAIN SITE AREA (Continued)**

Group	Formation/Unit		Thickness in Site Area <sup>1</sup> (meters)	General Lithology	Correlative Units	
					Hydro-Geologic <sup>2</sup>	Thermal-Mechanical <sup>3</sup>
Paintbrush (continued)	Topopah Spring Tuff	Crystal-rich member	0-381	Compositionally zoned (rhyolite to quartz latite) tuff sequence; each member divided into several zones and subzones <sup>6</sup> . Potential repository host rock is within crystal-poor member <sup>8</sup>	_____ c _____ Topopah Spring welded	_____ c _____ Topopah Spring welded <sup>9</sup>
		Crystal-poor member				
	Pre-Topopah Spring Tuff bedded tuff		0-17 <sup>7</sup>	Bedded tuffaceous deposits	_____ d _____	_____ d _____
	Calico Hills Formation		15-457	Rhyolite tuffs and lavas; contains five pyroclastic units	Calico Hills nonwelded	Calico Hills and lower Paintbrush nonwelded
	Pre-Calico Hills Formation bedded tuff		9-39 <sup>7</sup>	Pyroclastic-flow and coarse-grained fallout deposits		
Crater Flat	Prow Pass Tuff		15-194	Includes four variably welded pyroclastic-flow deposits	Calico Hills nonwelded or Crater Flat unit	_____ e _____ Prow Pass welded <sup>10</sup>
	Pre-Prow Pass Tuff bedded tuff		<1-3.5 <sup>7</sup>	Pumiceous tuffs and pyroclastic-flow deposits		Upper Crater Flat nonwelded <sup>11</sup>
	Bullfrog Tuff		15-366	Includes two pyroclastic-flow deposits separated by a pumiceous fallout unit		Bullfrog welded <sup>12</sup>
	Pre-Bullfrog Tuff bedded tuff		6-11 <sup>7</sup>	Pyroclastic-flow deposits with thin zones of fallout tephra		Middle Crater Flat nonwelded <sup>13</sup>
	Tram Tuff		0-370	Pyroclastic-flow deposits and bedded tuffs		Tram welded <sup>14</sup>
	Pre-Tram Tuff bedded tuff		0-21 <sup>7</sup>	Pyroclastic-flow and fallout deposits		
		Dacitic lava and flow breccia		111-249 <sup>15</sup>		Dacitic lavas and flow breccia; bedded tuff at base
Lithic Ridge Tuff		185-304 <sup>16</sup>	Pyroclastic-flow deposit			
Pre-Lithic Ridge Tuff volcanic rocks		45-350+ <sup>17</sup>	Pyroclastic-flow deposits and bedded tuffs			

NOTES: <sup>1</sup> Thickness based on identification of formation tops in some 50 boreholes by R.W. Spengler and D.C. Buesch (unpublished data, U.S. Geological Survey), unless otherwise indicated.

<sup>2</sup> Arnold et al. (1995); Flint (1998).

<sup>3</sup> Ortiz et al. 1985.

<sup>4</sup> Thickness in boreholes UE-25 NRG-#2C and UE-25 NRG-42D

<sup>5</sup> Thicknesses in boreholes near Exile Hill

<sup>6</sup> Member subdivisions described in Table 4.5.2 of CRWMS M&O 2000, based principally on Buesch et al. 1996a.

<sup>7</sup> Thicknesses in the seven boreholes shown in Figures 10 and 11.

<sup>8</sup> Potential repository host rock includes upper lithophysal (lower part), middle nonlithophysal, lower lithophysal, and lower nonlithophysal zones of crystal-poor member of the Topopah Spring Tuff.

<sup>9</sup> Thermal-mechanical Topopah Spring welded unit is divided into lithophysae-rich (upper), lithophysae-poor (middle) and vitrophyre (base) units.

<sup>10</sup> Thermal-mechanical Prow Pass welded unit includes upper part of welded pyroclastic-flow deposit of the Prow Pass Tuff.

<sup>11</sup> Thermal-mechanical Upper Crater Flat nonwelded unit includes the lower part of the welded pyroclastic-flow deposit and underlying units of the Prow Pass Tuff, the pre-Prow Pass bedded tuff, and the upper pyroclastic-flow deposit of the Bullfrog Tuff.

<sup>12</sup> Thermal-mechanical Bullfrog welded unit includes pumiceous fallout unit and upper part of lower pyroclastic-flow deposit of the Bullfrog Tuff.

<sup>13</sup> Thermal-mechanical Middle Crater Flat nonwelded unit includes the lower part of the lower pyroclastic-flow deposit of the Bullfrog Tuff, the pre-Bullfrog Tuff bedded tuff, and the upper part of the lithic-poor unit of the Tram Tuff.

<sup>14</sup> Thermal-mechanical Tram welded unit includes lower part of the lithic-poor unit and underlying units of the Tram Tuff.

<sup>15</sup> Thickness in borehole USW H-6

<sup>16</sup> Thickness in borehole USW G-3

<sup>17</sup> Thickness in borehole USW G-2

**Labeled Stratigraphic Horizons:**

<sup>a</sup> Contact between moderately welded (above) and densely welded (below) subzones of the vitric zone of the crystal-rich member of the Tiva Canyon Tuff.

<sup>b</sup> Contact between lower nonlithophysal (above) and vitric (below) zones of the crystal-poor member of the Tiva Canyon Tuff.

<sup>c</sup> Contact between moderately welded (above) and densely welded (below) subzones of the vitric zone of the crystal-rich member of the Topopah Spring Tuff.

<sup>d</sup> Contact between densely welded (above) and moderately welded (below) subzones of the vitric zone of the crystal-poor member of the Topopah Spring Tuff; coincides closely with "vitric-zeolitic" boundary mentioned in text.

<sup>e</sup> Contact between pyroxene-rich (above) and welded pyroclastic-flow deposits (below) in upper part of Prow Pass Tuff

**TABLE 2. SUMMARY OF DIAGNOSTIC SURFACE AND SOIL CHARACTERISTICS OF QUATERNARY MAP UNITS AT YUCCA MOUNTAIN**

Map Unit	Surface Characteristics <sup>1</sup>				Soil Characteristics				
	Desert Pavement <sup>2</sup>	Desert Varnish <sup>3</sup>	Rubification <sup>4</sup>	Depositional-bar Relief <sup>5</sup>	Horizon Sequence <sup>6</sup>	Structure <sup>7</sup>	Clay Films <sup>8</sup>	Maximum Reddening <sup>9</sup>	Maximum CaCO <sub>3</sub> Stage Morphology <sup>10</sup>
Qa7	None	1±2 12	4	High, unaltered	Cu	sg	n.p.	10YR	n.p.
Qa6	None	0±0 0	0	do	A-Ck	sg	n.p.	10YR	n.p.
Qa5	Weak to moderate	1±1 28	33	Moderately high, slightly altered.	A- Bwk/Btjk- Bk-Ck	1 vf-f sbk	n.p.-1 n co	10YR	I
Qa4	Moderate to strong	62±27 97	87	Low	Av-Btkq- Bkq-Ck	2-3 f-m sbk	3 n-mk pf	7.5YR	I-II
Qa3	Strong	43±28 94	54	do	Av-BA- Btkq- Kq/Bkq-Ck	3 m sbk	3 n-mk pf	7.5YR	II+ -III
Qa2	Strong	80 (est.) 100 (est.)	100 est.	do	Av-Btq- Btkq-Kq- Bkq-Ck	3 m sbk	3 mk pf	7.5-5YR	IV
Qa1	Locally strong	20±21 84	80	None	Av-BA- Btkq-Kqm- Bkq-Ck	m-3 m pl	2 n pf	10-7.5YR	IV
QT0		Degraded					Erod		

Notes:

<sup>1</sup> See Wesling et al. (1992) for detailed definitions of surface parameters.

<sup>2</sup> Describes the relative degree of interlocking of surface clasts; based on qualitative estimate.

<sup>3</sup> First number is the average varnish cover (percent ± 1σ); second number refers to the percent of varnished clasts; from Wesling et al. (1992).

<sup>4</sup> Percent rubified clasts; from Wesling et al. (1992).

<sup>5</sup> The relative height of depositional bars from the top of the bar to the trough of the adjacent swale.

<sup>6</sup> Refers to the sequence of soil horizons that is representative of each map unit. Abbreviations for master horizons: A-surface horizon characterized by accumulation of organic matter and typically as a zone of illuviation of clay, sesquioxides, silica, gypsum, carbonate, and/or salts; B-subsurface horizon characterized by a redder color, stronger structure development, and/or accumulation of secondary illuvial materials (clay, sesquioxide, silica, gypsum, and salts); C-subsurface horizon that may appear similar to the parent material and includes unaltered material and material in various stages of weathering; K-subsurface horizon engulfed with carbonate to the extent that its morphology is determined by the carbonate. Abbreviations for master horizon modifiers; j-used in conjunction with other modifiers to denote incipient development of that particular feature or property; k-accumulation of carbonates; m-strong cementation; q-accumulation of silica; t-accumulation of clay; u-soil properties undifferentiated; v-vesicular structure; w-color of structural B horizon.

<sup>7</sup> Abbreviations: sg, single grained; m, massive; 1, weak; 2, moderate; 3, strong; vf, very fine; f, fine; m, medium; pl, platy; sbk, subangular blocky.

<sup>8</sup> Abbreviations: N.P., not present; 1, few; 2, common; 3, many; n, thin; mk, moderately thick; pf, ped face; co, colloidal stains.

<sup>9</sup> Hue determined with Munsell Soil Color Chart, Munsell Color Co., Inc. (1988).

<sup>10</sup> Terminology of Gile et al. (1966) and Birkeland (1984).

Source: Whitney et al. (2004b)

**TABLE 3. MAXIMUM BEDROCK EROSION RATES ON YUCCA MOUNTAIN**

Sample Number	<sup>10</sup> Be Conc. (atoms/g)	Max Erosion Rate	
		cm/k.y.	Uncertainty (cm/k.y.)
CDH-AR-1*	4.71	0.041	(0.028-0.064)
CDH-AR-5	2.33	0.11	(0.083-0.16)
CDH-AR-6	1.95	0.14	(0.10-0.19)
CDH-WR-1*	3.23	0.071	(0.052-0.10)
CDH-WR-2	1.08	0.27	(0.21-0.37)
CDH-WR-5	1.16	0.25	(0.20-0.35)
CDH-WR-6	2.80	0.090	(0.067-0.13)

Notes: Samples partially processed by the University of Arizona, Tucson, Arizona, and analyzed at the University of Pennsylvania, Philadelphia, Pennsylvania.

\* Samples partially processed by the University of Arizona, and analyzed at PRIME Lab, Purdue University, Lafayette, Indiana.

Abbreviations: g, gram; cm/k.y., centimeter/thousand years

Source: CRWMS M&O (1998, Table 3.4-6)

**TABLE 4. VARNISH CATION RATIO AGE ESTIMATES FROM BOULDER DEPOSITS AROUND YUCCA MOUNTAIN**

Sample	Age (k.y.)
YME-1	440 (320-590)
YME-2	100 (80-140)
YMW-1	310 (230-420)
YMW-2	440 (330-600)
YMW-3	480 (360-660)
YMN-1	530 (390-720)
LSM-1	680 (500-930)
SKM-1	550 (400-750)
SKM-2	580 (430-800)
SKM-3	850 (600-1180)
SKM-3A	700 (510-960)
BM-1	1020 (730-1430)

Note: Error  $\pm 1\sigma$

Abbreviation: k.y., thousand years

Source: Modified from CRWMS M&O (1998, Table 3.4-7).

**TABLE 5. AGES OF FOUR BOULDER DEPOSITS AROUND YUCCA MOUNTAIN**

<b>Boulder Deposit Location</b>	<b>Calculated Cation Ratio Age (k.y.)</b>	<b>Calculated Cosmogenic Nuclide Age (k.y.)</b>
Buckboard Mesa	730-1430	460-765
Skull Mountain Pass	500-930	620-1,030
East Side Yucca	320-590	480-805
West Side Yucca	360-660	660-1,100

NOTES: The uncertainties in the cation ratio ages are the 95 percent confidence limits of the curve regression line.

The cosmogenic age 1 $\sigma$  uncertainties are 25 percent of the mean age.

Abbreviation: k.y., thousand years

Source: CRWMS M&O (2000, Table 7.4-2).

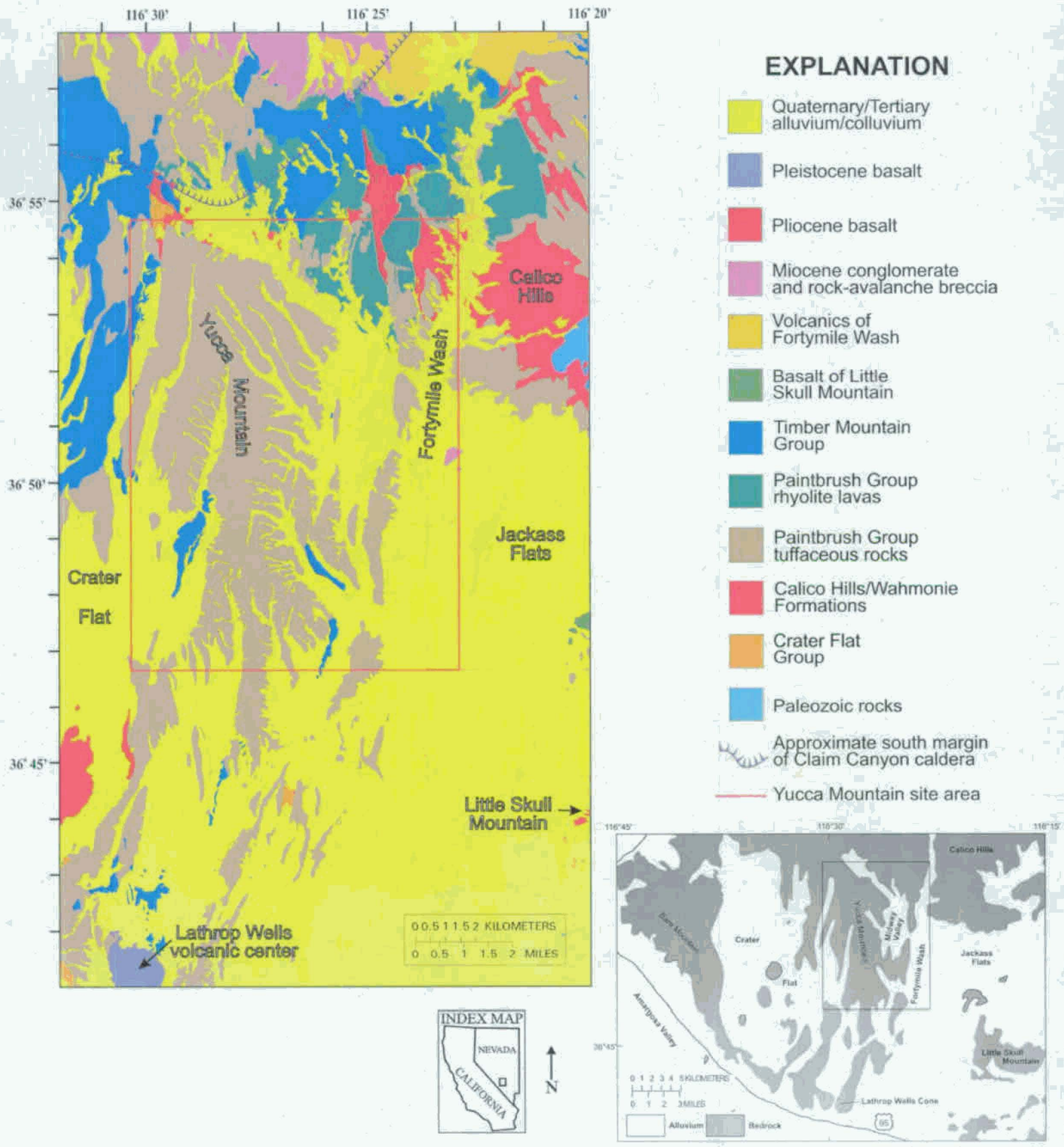


Figure 1



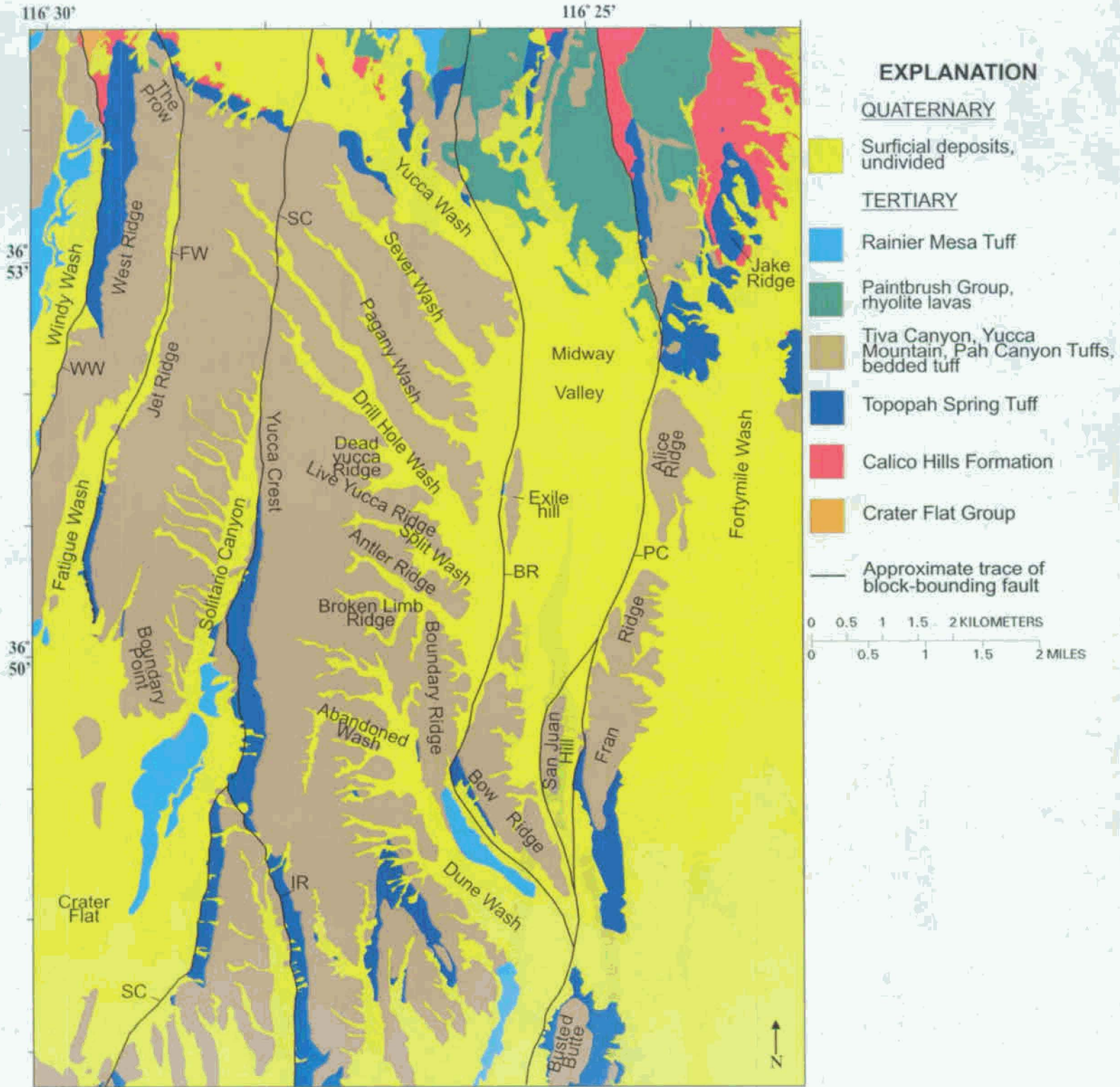


Figure 2





Skull Mountain

Little Skull Mountain

Jackass Flats

Fortymile Wash

Fran Ridge

Busted Butte

Midway Valley

Yucca

Mountain

Solitario Canyon

Figure 3



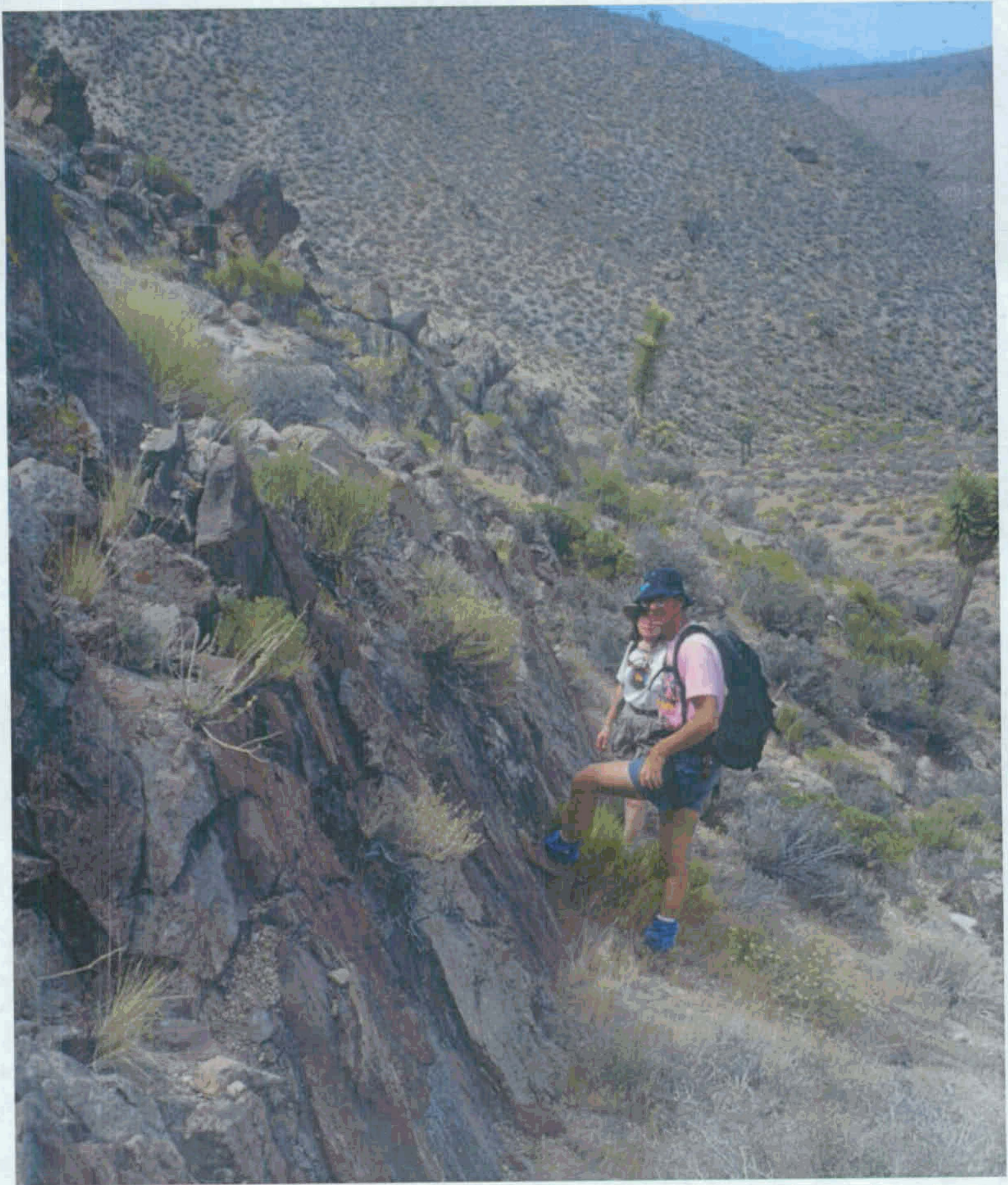
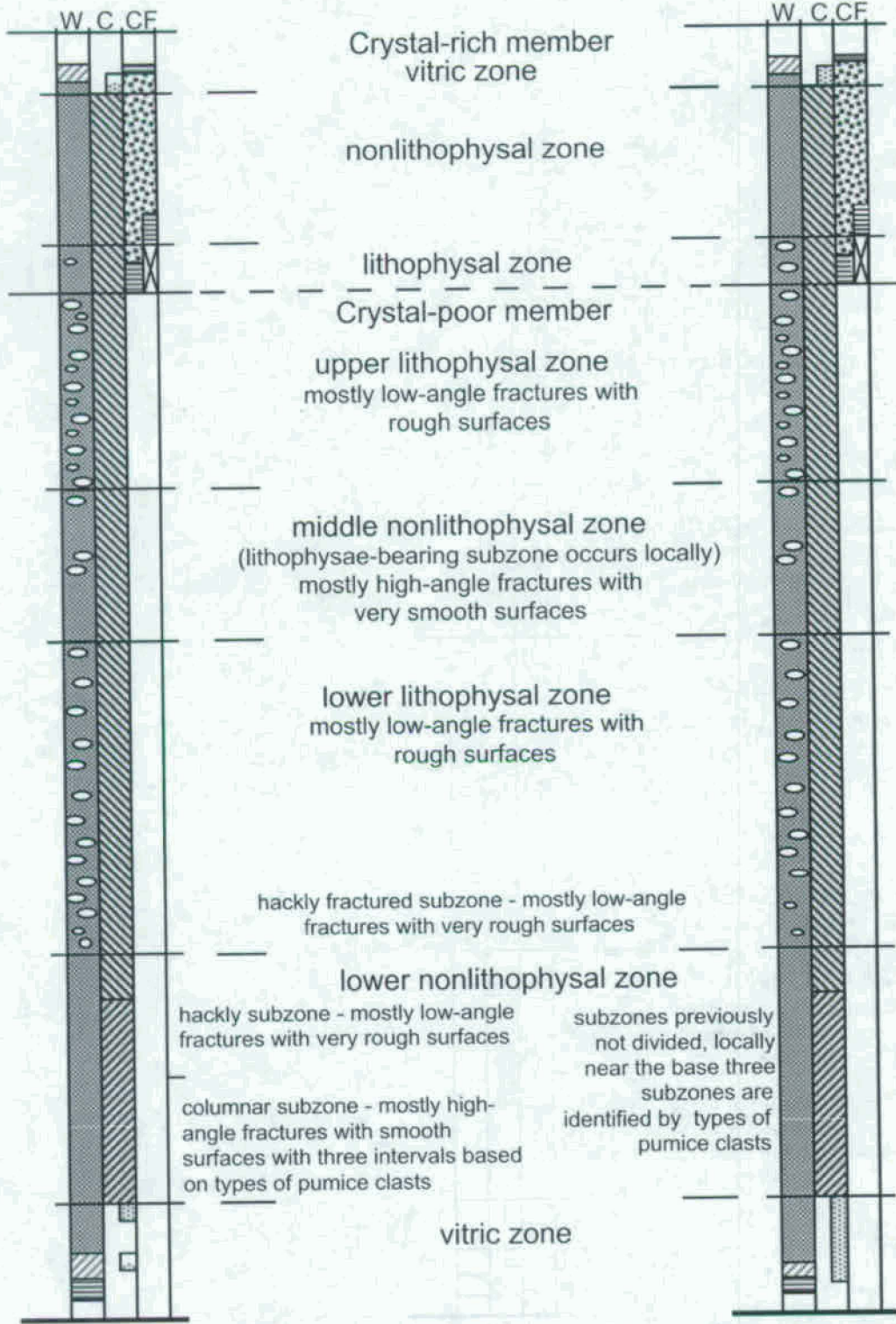


Figure 4



Tiva Canyon Tuff

Topopah Spring Tuff



Zones of welding (W)

- Densely (○ lithophysae)
- Moderately
- Partially
- Nonwelded

Zones of crystallization (C)

- Crystallized
- Crystallized + vapor-phase minerals
- Vitric / Vitric + vapor-phase or moderate temperature alteration minerals

Crystal fragments (CF)

- Greater than 10 percent
- 5 to 10 percent
- Less than 5 percent
- Unit locally absent

Figure 5



**A**



**B**

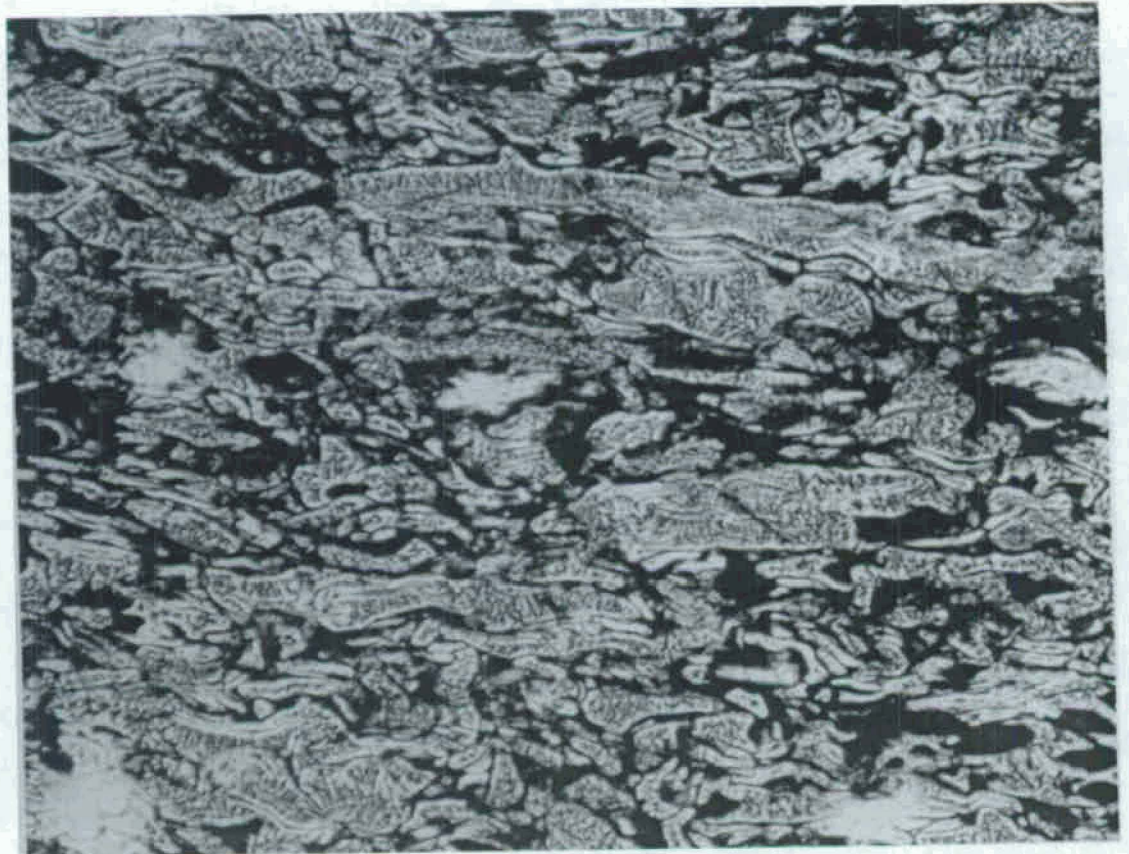


Figure 6

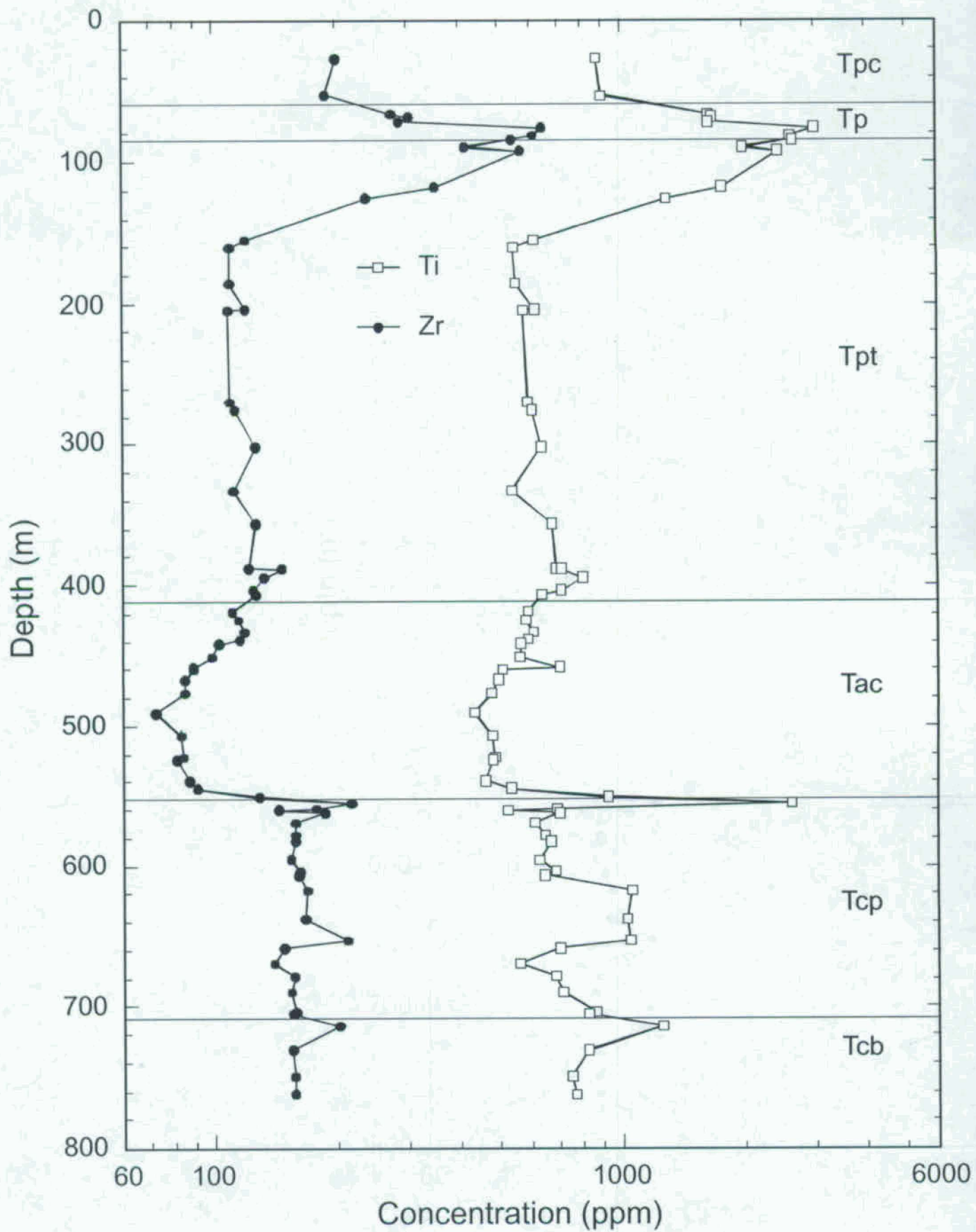


Figure 7





# EXPLANATION

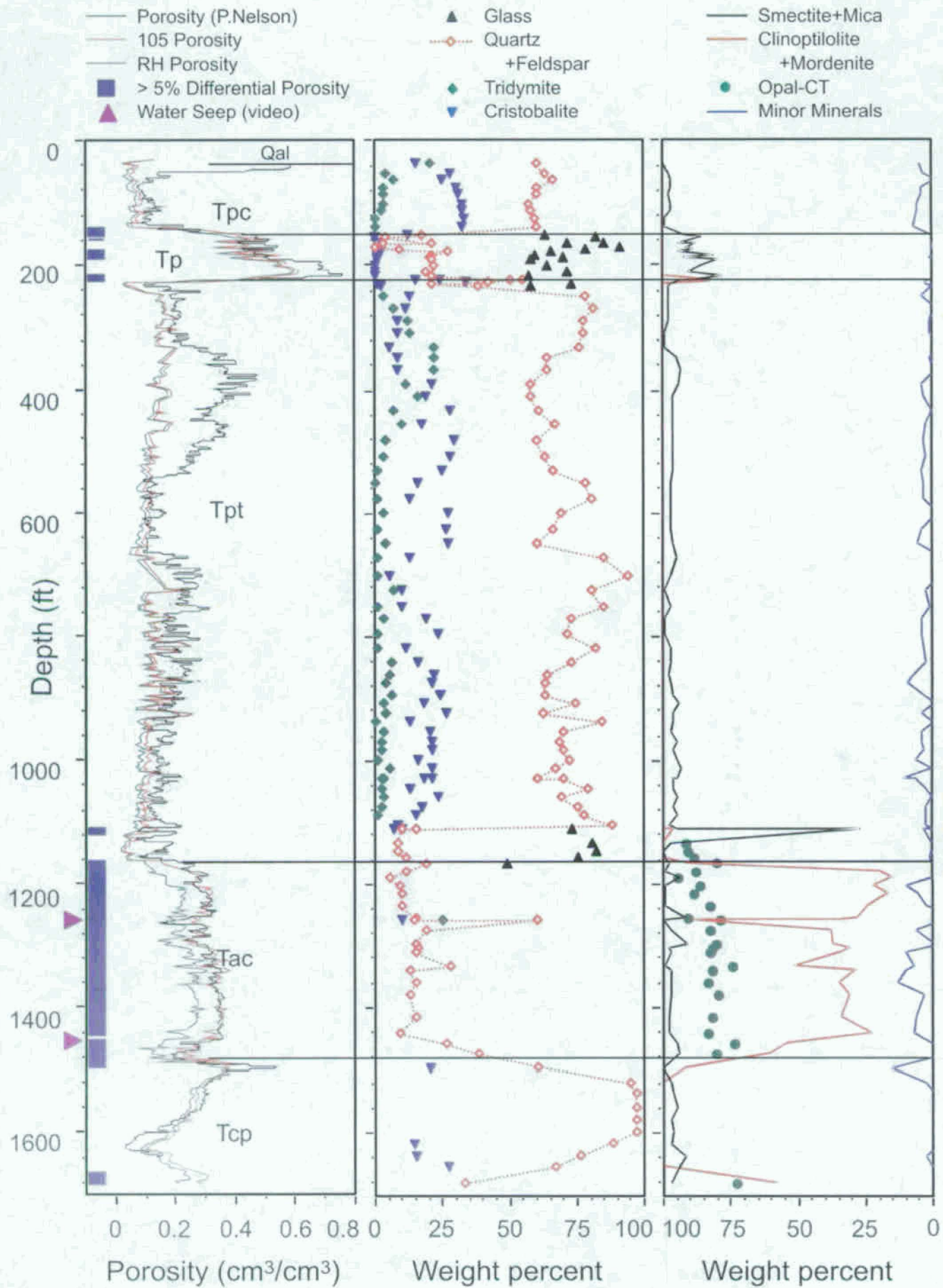


Figure 9



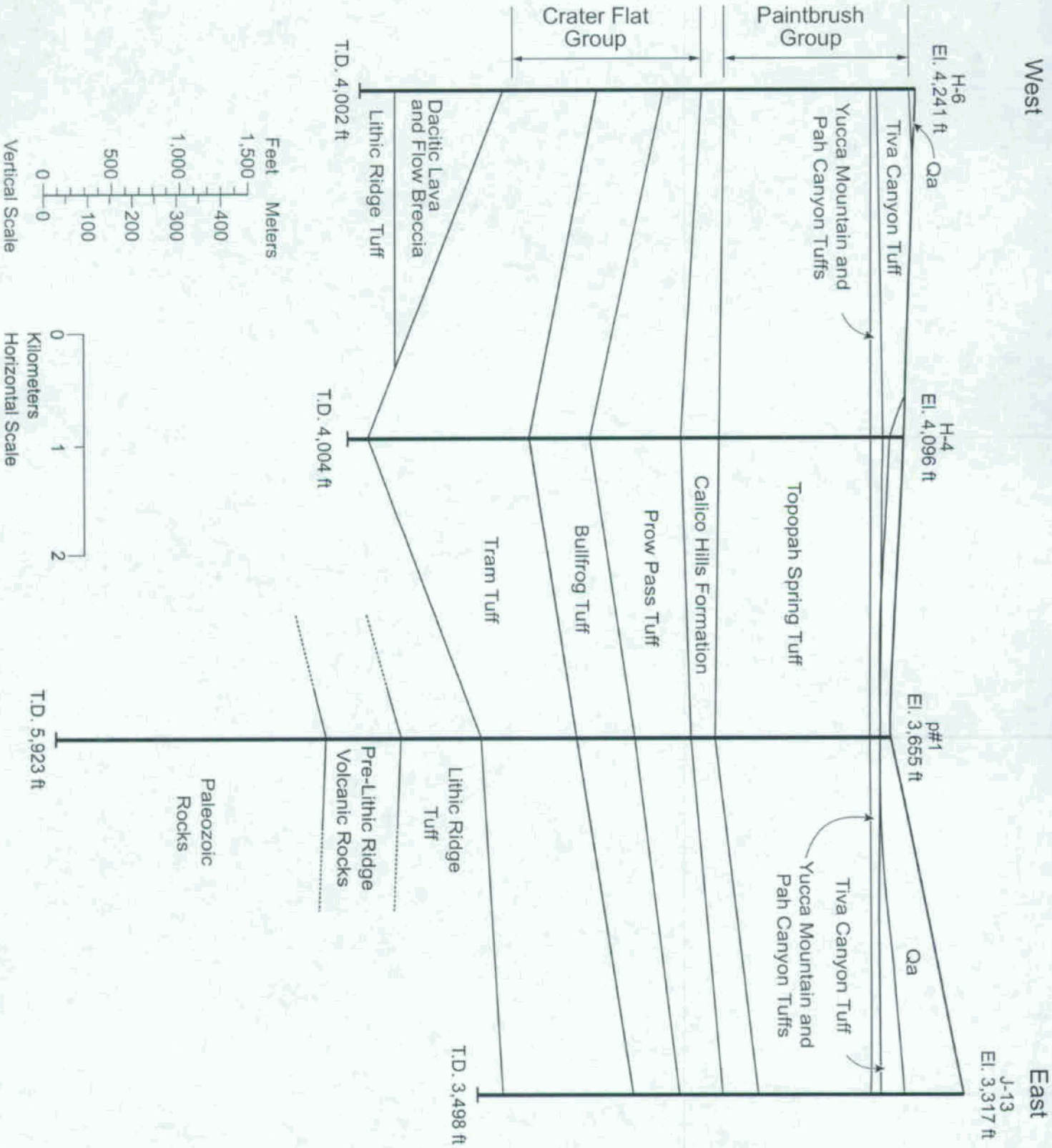


Figure 10

South

North

G-2  
El. 5,097 ft

G-3  
El. 4,856 ft

H-4  
El. 4,096 ft  
Qa

G-1  
El. 4,350 ft  
Qa

Paintbrush Group

Crater Flat Group

Tiva Canyon Tuff  
Yucca Mountain Tuff  
Pah Canyon Tuff

Tiva Canyon Tuff

Yucca Mountain and  
Pah Canyon Tuffs

Topopah Spring Tuff

Calico Hills Formation

Prow Pass Tuff

Bullfrog Tuff

Tram Tuff

Dacitic Lava and  
Flow Breccia

Lithic Ridge Tuff

T.D. 4,004 ft

Lithic Ridge Tuff

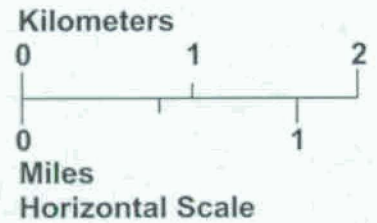
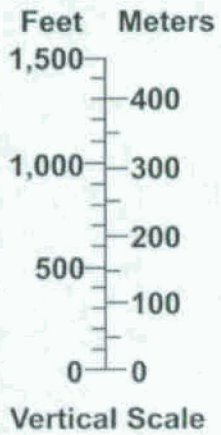
T.D. 5,030 ft

Pre-Lithic Ridge Volcanic Rocks

Pre-Lithic Ridge Volcanic Rocks

T.D. 6,006 ft

T.D. 6,000 ft



South

North

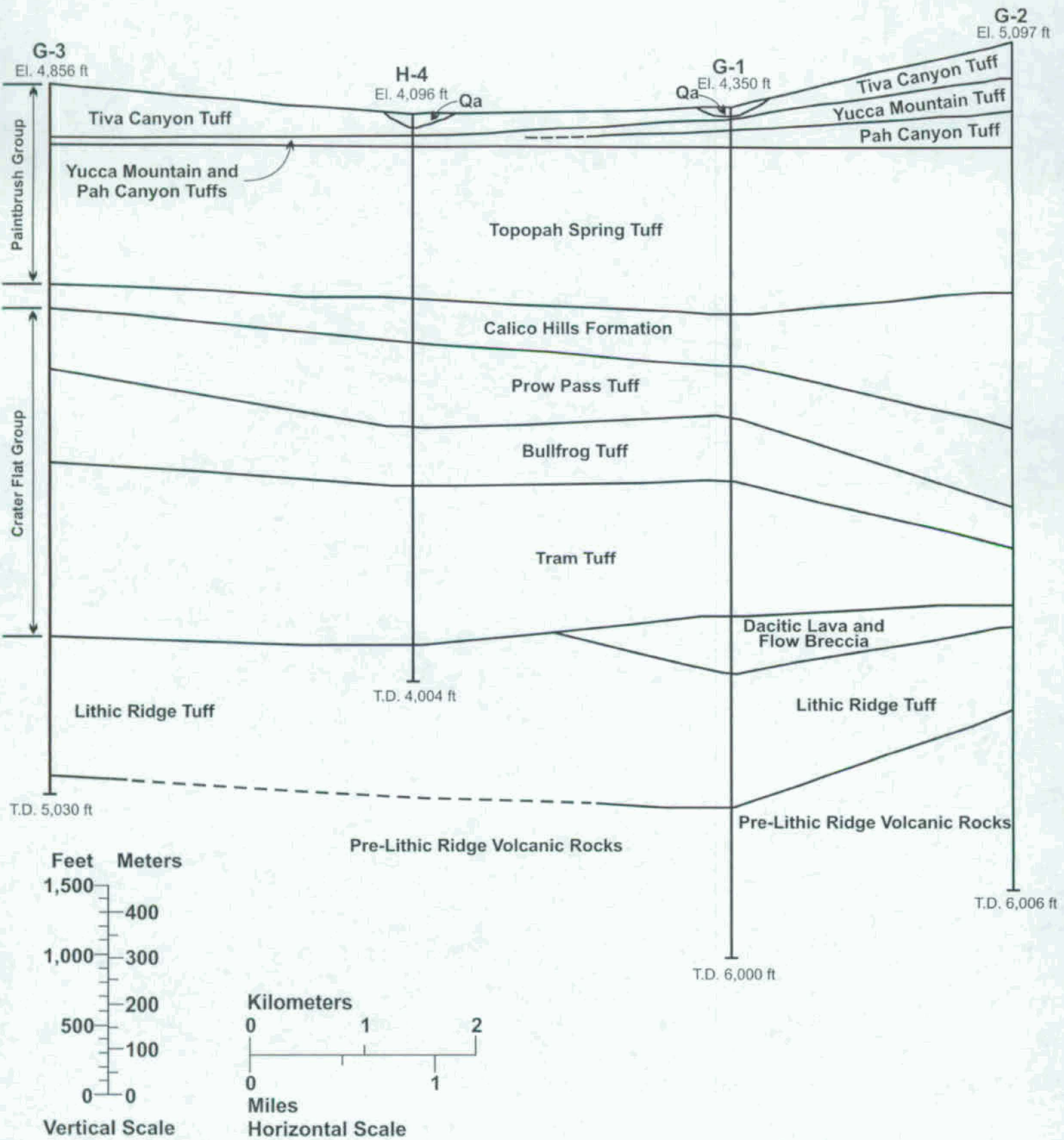
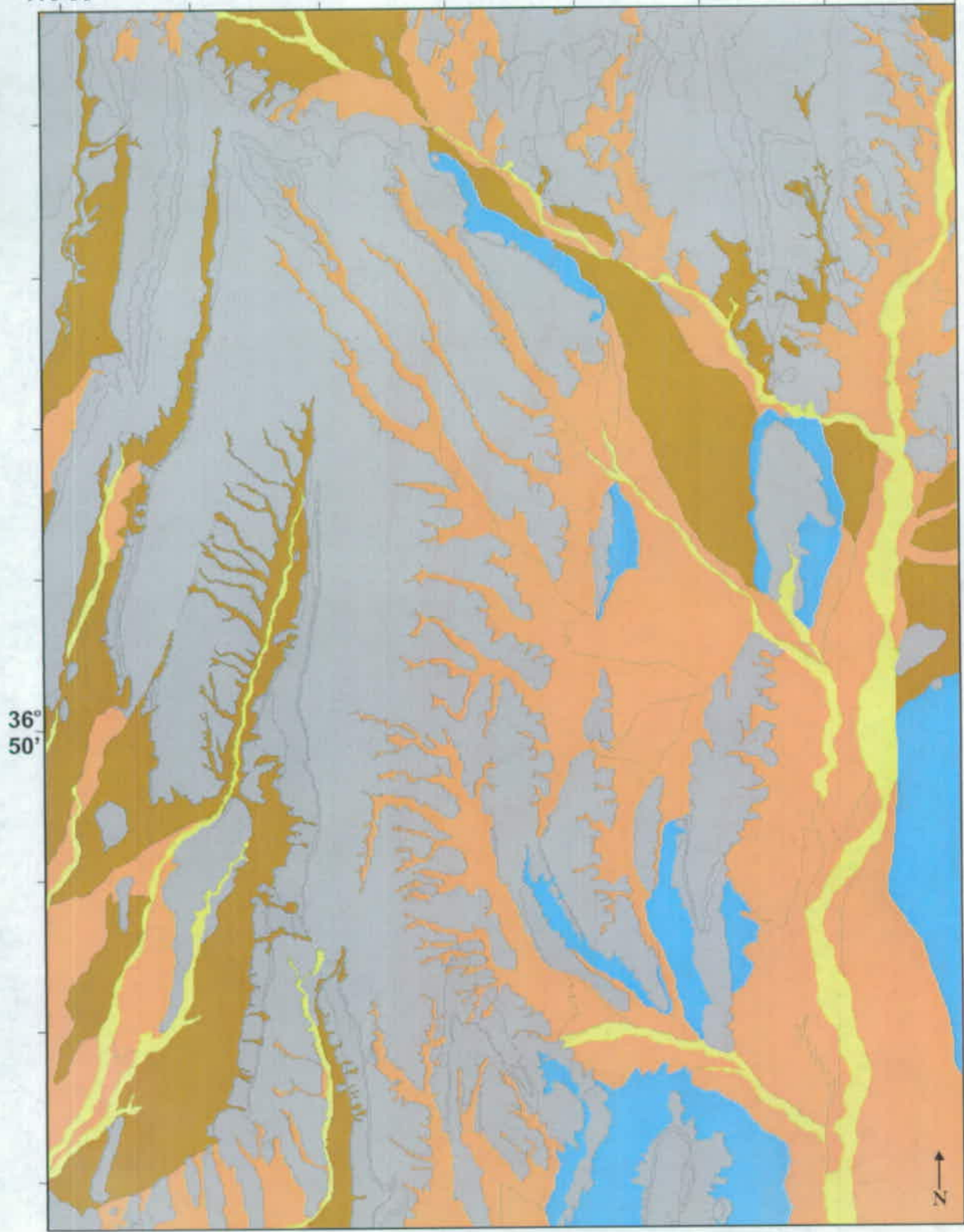


Figure 11.

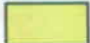






116°30'

116°25'



### MAP UNITS

-  Holocene alluvium (Units Qa5-Qa7)
-  Middle Pleistocene to Holocene alluvium (Units Qa2-Qa4)
-  Early to middle Pleistocene alluvium (Units Qa0-Qa1)
-  Early Pleistocene to Holocene eolian deposits
-  Tertiary bedrock

36°  
50'

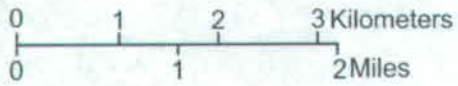


Figure 12

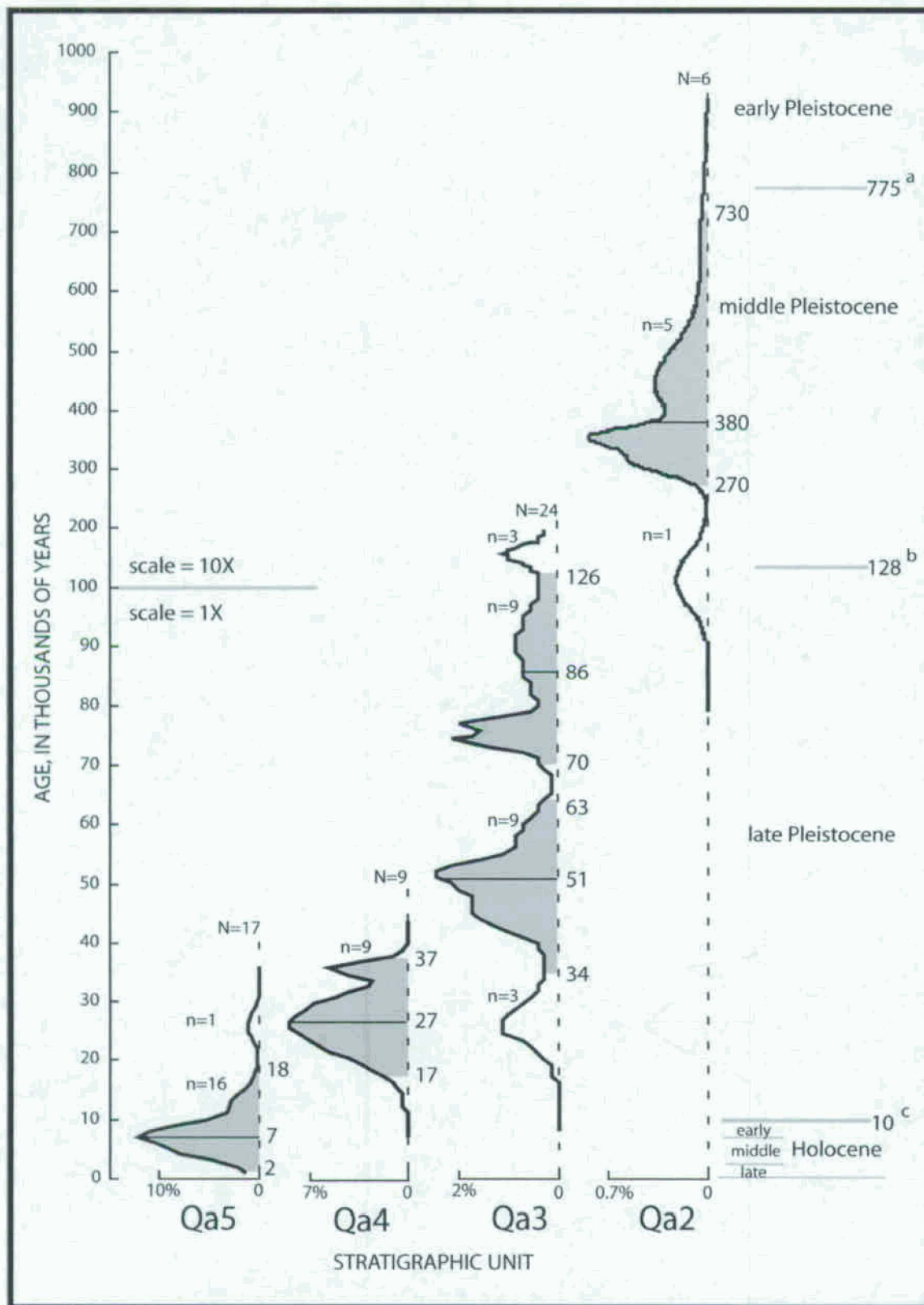
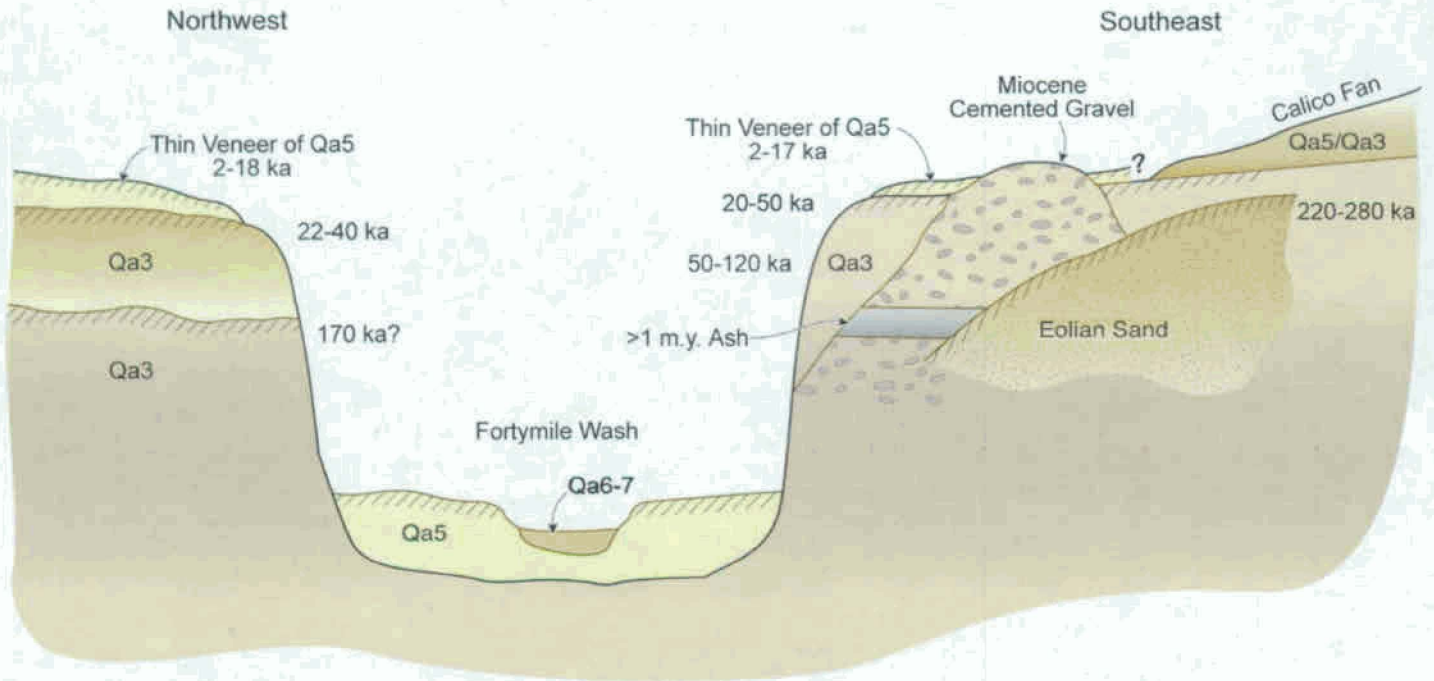


Figure 13

### Calico Fan Site

(a)



### Yucca Mountain Road Crossing

(b)

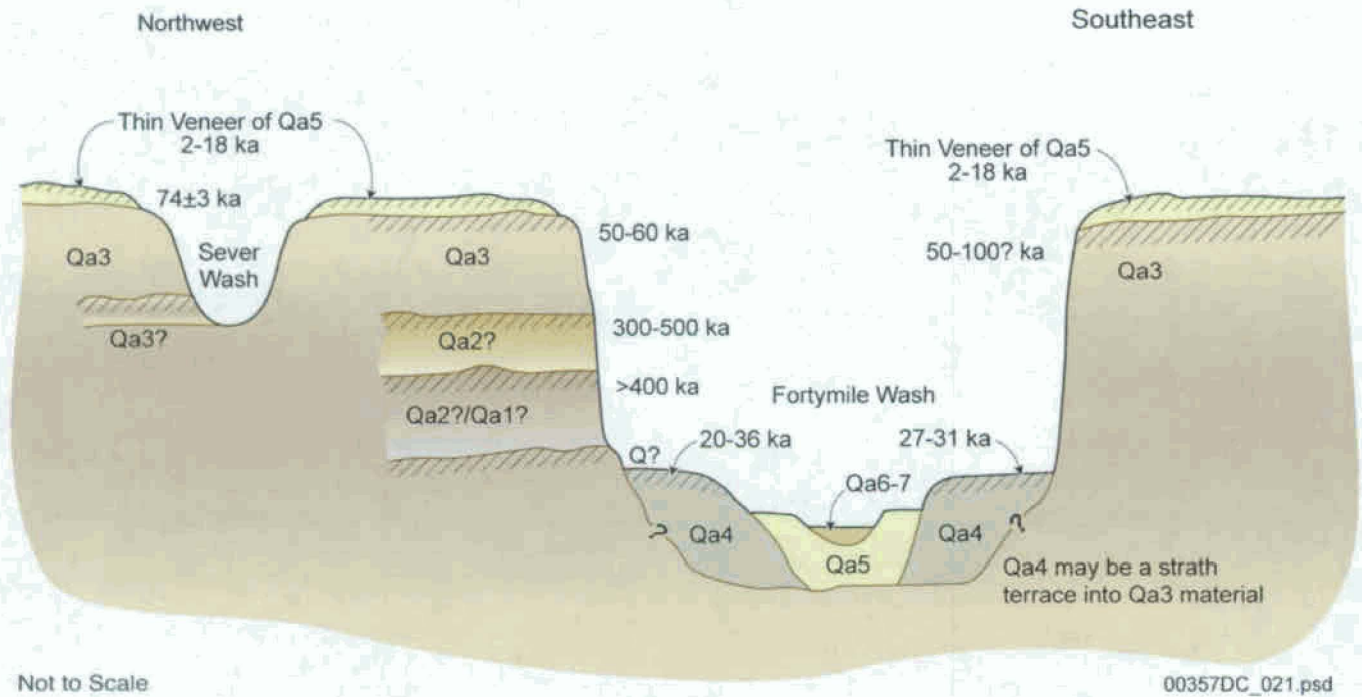


Figure 14





Figure 15



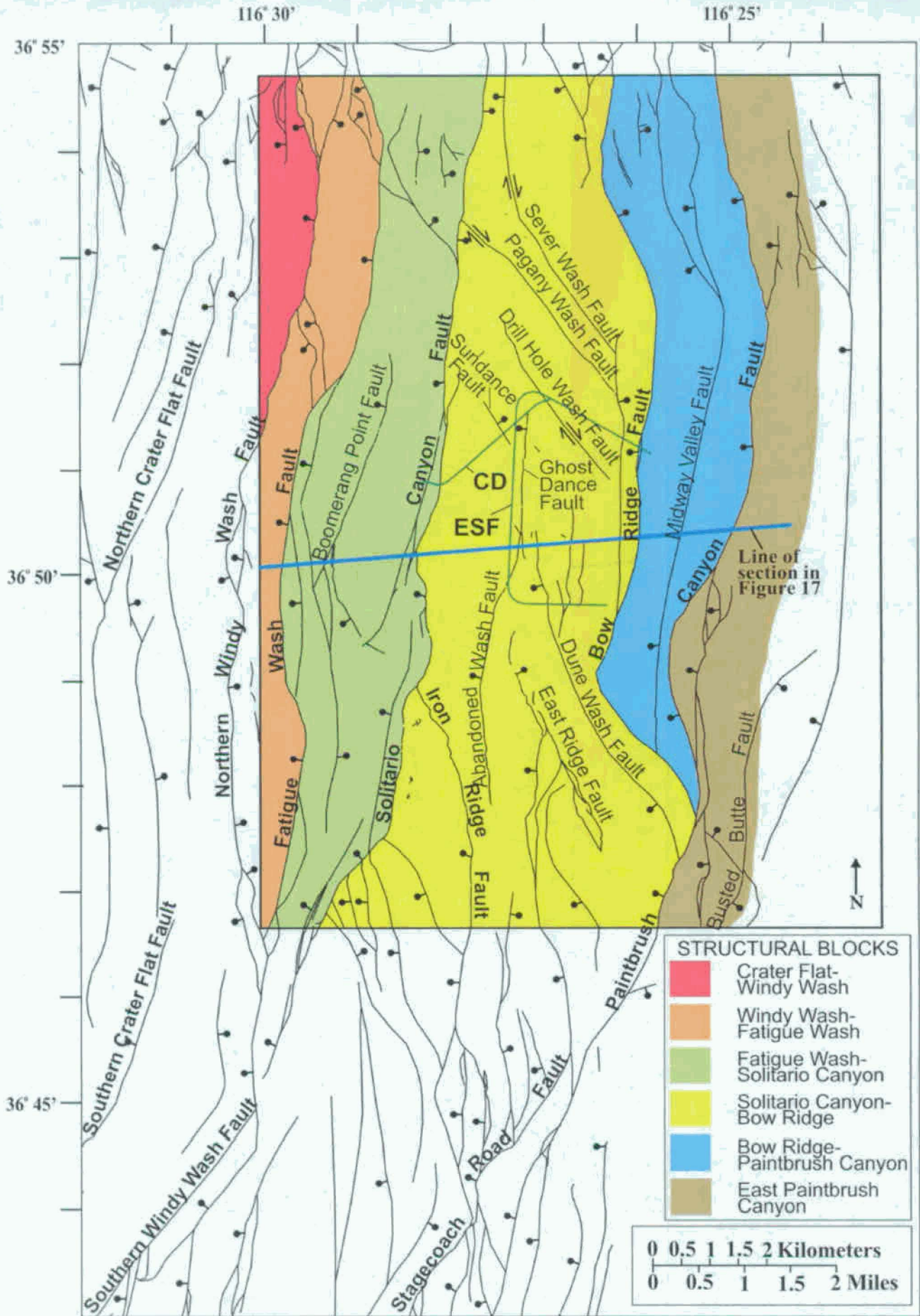


Figure 16



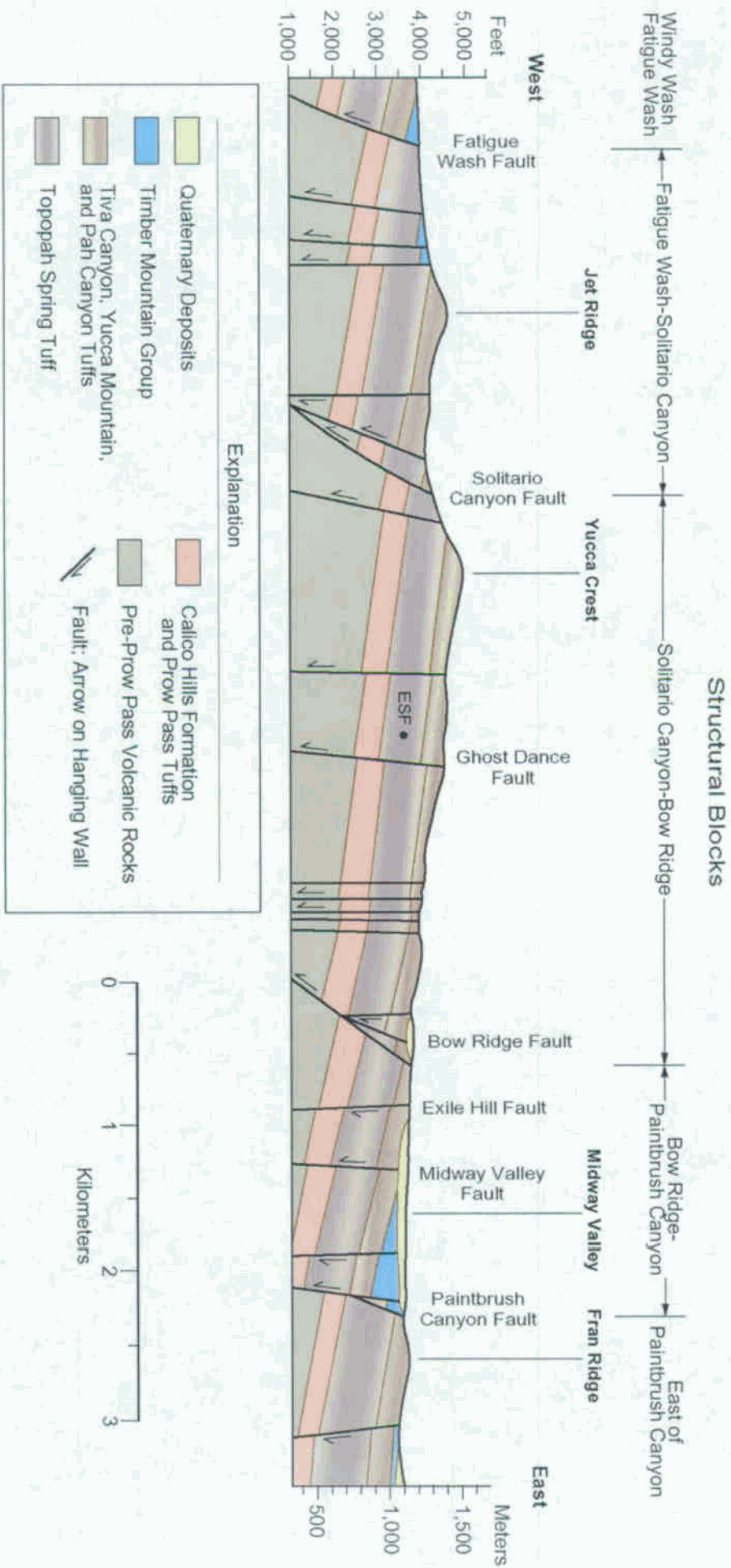


Figure 17

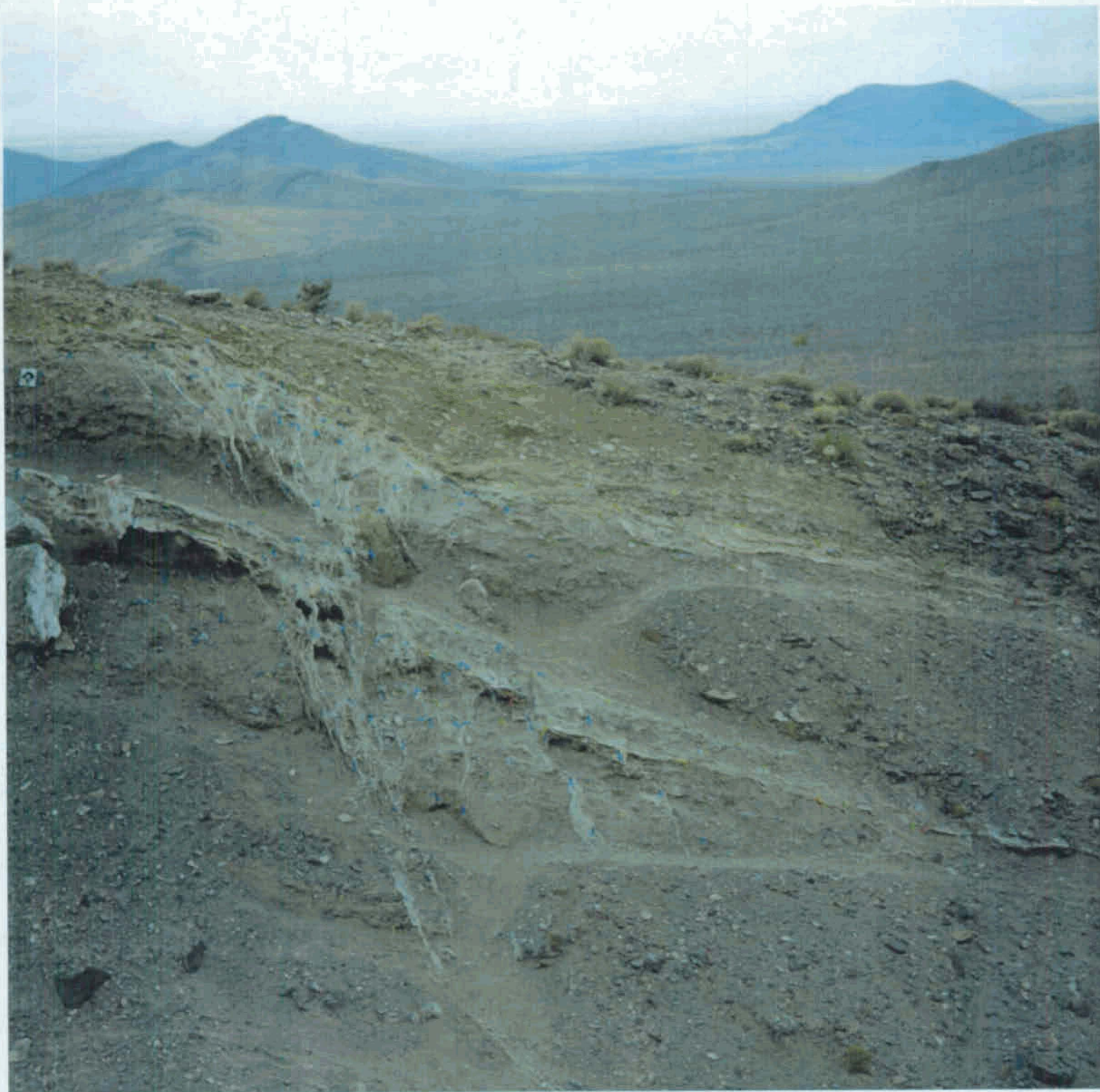


Figure 18



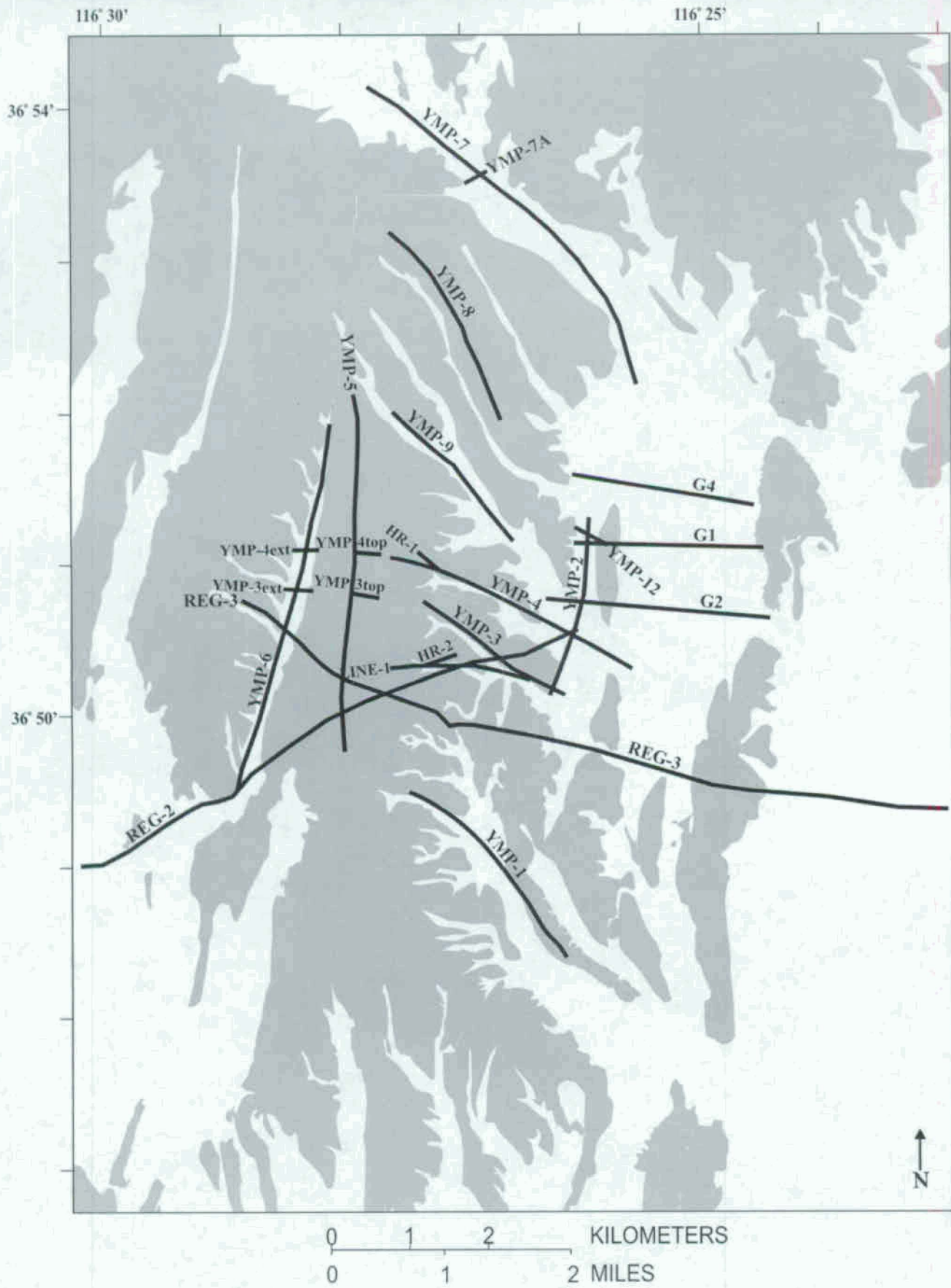


Figure 19